Response to comments on "GOLUM-CNP v1.0: a data-driven modeling of carbon, nitrogen and phosphorus cycles in major terrestrial biomes" by Y. Wang et al.

We thank the referee for reviewing our manuscript. Please find attached a point-by point reply to each of the comments raised by the referee with legible text and figures organized along the text.

Overall this is an interesting and detailed summary of an improvement to an existing model. Though not the first to put in a N cycle, the P cycle is relatively novel and there is clearly diligent work done by the authors to ensure values are appropriately backed up by data where possible. There are a few points that I think need clarifying and some aspects of the model that seem to me a bit odd, and therefore need provisos about the appropriate (or inappropriate) use of the model. Some of the conclusions about openness are a bit of a stretch given the model setup. But with some extra information discussing the limitations, this will be a worthwhile model description.

Response:

We would like to thank the referee for the valuable comments and suggestions for improving our manuscript. Following the reviewer's comments, we carefully revised our manuscript. Please find below the point-to-point responses (in black) to all referee comments (in blue). For your convenience, changes in the revised manuscript are highlighted with dark red. All the pages and line numbers correspond to the original version of text. Of note GOLUM-CNP is not an improvement to an existing model, but an independent model that uses the outputs from CARDAMOM and incorporate the data-driven estimates of N and P cycles (see detailed response to Comment 3).

Major points

1. The issue of this being an equilibrium model for the present day/recent past is a concern to me. It isn't sufficiently explained how an equilibrium estimate (including anthropogenic N deposition) is valid in equilibrium. I can see the justification if it's preindustrial (excluding anthropogenic N deposition), but it doesn't make sense to me as it is. In particular, the openness of the system seems to me to be almost completely determined by the assumption of equilibrium. If the outputs and inputs are balanced (i.e. the equations are solved to 0, as is stated on P7 L32), then surely the store size is at least partly determined by something we know to be wrong. Given that the equilibrium assumption should increase the carbon storage, it's odd that in Table 2 (assuming these are present-day values), the NPP and the soil and vegetation pools are all smaller than many other models and global estimates suggest.

Response:

We develop a steady-state model as a first attempt of a CNP data-driven diagnostic model. The objective of this study is not to reproduce the present day state, but to provide a steady-state estimates of C, N and P cycle with current input of C, N and P, stoichiometry of

N:C and P:C ratios, and residence times of different pools, because there is a lack of data to constraint a transient state (see point 1). As a result, we choose to constrain an equilibrium state. Although it does not correspond in some aspects to the present day state, it is still useful for evaluating global models as these model are able to simulate a equilibrium state for present day conditions and a direct comparison is possible (see point 2 and point 3).

1) Although we described processes in the C, N and P cycles by a set of differential equations (Eqs. A1-A5, B1-B7, C1-C7), only few global long-term observations associated with N and P were available to constrain a transient simulation. For example, the synthesis of stoichiometries in different pools are based on published literature during the last four decades, and almost no data are available for preindustrial period; field-scale manipulation experiments have shown that warming, elevated atmospheric CO_2, and N and P fertilization can drive changes in stoichiometries and nutrient resorption in terrestrial ecosystems (Sistla and Schimel, 2012; Sardans et al., 2012; Sardans and Peñuelas, 2012; Mayor et al., 2014; Yang et al., 2014; Yuan and Chen, 2015; Sardans et al., 2016; Sardans et al., 2017), but these data are insufficient to infer these changes in terrestrial ecosystems during the past years. As a result, for a data-driven model framework, we computed the equilibrium estimates and this equilibrium corresponds to the state where the inputs of C, N and P (e.g. NPP for C cycle, N deposition and fixation for N cycle, P deposition and release of P by rock weathering for P cycle) and residence times equal to the estimates under present-day conditions.
2) Some previous studies that have investigated the changes in C, N stocks between pre-industrial period and present day. Thornton et al. (2007) investigated the C stock changes from pre-industrial times and present day (1976-2000) using CLM-CN model. They found the C stocks in vegetation, litter and SOM increased by 35, 1 and 10 Pg, which equal to only 5%, 6% and 3% of the respective initial C stocks in 1850. Zaehle et al. (2010) estimated the C stock changes and N stock changes in vegetation and SOM, using the O-CN terrestrial biosphere model. By excluding the impact by land use change, that vegetation C stocks increased by 62 Pg and soil C stocks increased by 39 Pg from 1860 to 2002, being 13% and 3% of initial C stocks for vegetation and SOM respectively. The N stocks increased by 376 Tg and 2836 Tg in vegetation and SOM, being 11% and 3% of initial N stocks. Zaehle et al. (2013) further accounted for the effect of land use change on the global C and N cycles. The results also showed that the cumulative effect of anthropogenic disturbance from preindustrial times are small (<5%) on the natural C and N cycles. The evidences for the change of global P cycling from pre-industrial times are quite limited and highly uncertain (Goll et al., 2012). At local scales, some places are experiencing significant anthropogenic disturbances, mostly through deposition and fertilizer (Jornard et al., 2015). However, the extent to which natural ecosystems are affected by these disturbances are not clear (Wang et al., 2017). Given these state-of-the-art estimates about the magnitude of anthropogenic disturbance on natural C, N and P cycles and large uncertainties, it is still useful to take steady-state estimates as a diagnostic to evaluate DGVMs in simulating global C, N and P cycling (Wang et al., 2010; Xu-ri et al., 2008; Yang et al., 2009; Lawrence et al., 2011). The estimates based on steady state assumptions listed above match well with a wide range of *in-situ* observations in recent years.

3) CARDAMOM is the only spatially explicit data-driven product of C cycle, which does not rely on a steady-state assumption. In this study, our aim is to develop a steady-state model (see point 1) in which a consistency between different datasets are achieved (which is a novelty). We chose to use the variables in the CARDAMOM products: NPP, residence times and fire fractions, which were constrained by global long-term observations of MODIS LAI and MODIS burned area. For other C variables whose direct constraints do not have a global coverage in CARDAMOM (such as biomass), we recalculated them based on the equilibrium assumption. With this steady state C cycle, we compute the associated N and P pools and fluxes. For example, the N and P in SOM pool equal to the product of N:C/P:C ratios and equilibrated C content.

In summary, given the three concerns mentioned above, we computed an equilibrium estimate of C, N and P cycle, where the inputs of C, N and P into the terrestrial ecosystems (NPP, N and P deposition, N fixation and release of P by rock weathering), stoichiometries of N:C and P:C ratios, the residence times of different pools and the land cover are held constant as the period 2001-2010. Although this steady-state estimates deviate from the actual state of present-day disturbed cycles, we compare the GOLUM-CNP with the original CARDAMOM to show that the steady-state estimates in GOLUM-CNP are still within the range of such large uncertainties from data on the present day state.

To address the referee's concern about steady-state assumption in a quantitative way, we compare the recomputed pool sizes for C with the original CARDAMOM estimates (Fig. S1 in the revised supporting information). The steady-state transformed pool sizes are within the [25, 75th] percentile range of the original CARDAMOM results at more than 90% forest grid cells. The major part of the deviation comes from the treatment of grassland in GOLUM and are not associated to the steady-state assumption: In GOLUM-CNP grasslands are considered as a distinct biome, while the original CARDAMOM did not use land cover information and provided some woody biomass pools for grassland dominated regions. As GOLUM does not consider woody biomass for grass, we transfer wood growth from CARDAMOM into non-woody tissue for grasslands. This makes our C pools more different from the original CARDAMOM at grassland-dominated pixels than at forest-dominated pixels. However, although the biomass at grassland grid cells in GOLUM-CNP are much lower than the biomass in CARDAMOM, the litter and SOM pool sizes at grassland grid cells in GOLUM-CNP are still within the [5, 95th] percentile range of the original CARDAMOM results (Fig. S1b and S1c in the revised supporting information). In addition, we also mention in the revised manuscript: although GOLUM-CNP is presented for steady state in this study, the methods and equations used to compute fluxes and pools are generic and could be extended to non-steady state. In the future, when more data will become available, a transient version of GOLUM-CNP will incorporate the new data and improved understandings in C, N and P cycles.

We outline in the revised paper that some variables like the *openness* do not strongly rely on the equilibrium assumption. The openness is defined as:

$$XO = \frac{I_x}{F_x + RSB_x} \quad (1)$$

where I_x ($X \in \{N,P\}$) is the new nutrient inputs, i.e. deposition (N_d) and biological fixation (N_{fix}) for N cycle and deposition (P_d) and rock weathering (P_w) for P cycle. These variables are in fact the nutrient inputs to the system, which are derived from observations and are not estimated from equilibrium assumption. F_x+RSB_X represent the total uptake of nutrients by plant, which are determined by NPP, allocation fractions of NPP to different vegetation pools and stoichiometries in different vegetation pools. These variables are also the inputs to GOLUM-CNP and represent the non-steady state situation under current climate condition from original CARDAMOM without equilibrium assumption (as discussed above, only the C store sizes are computed based on equilibrium assumption). In consequence, this computation is actually based on a mass-balance framework and driven by fluxes as observed in present day transient state. However, we do assume that the stoichiometries of N:C and P:C ratios do not change significantly during the period considered (2001-2010), although small changes in stoichiometry in fast-turnover plant tissue is being observed on such a time scale (Jonard et al. 2015). Such an approach is common and is similar to that of Cleveland et al. (2013). In Cleveland et al. (2015), they computed NPP_{new} and $NPP_{recycle}$ where N:C and P:C ratios are the same in these two types of NPP. In our study, we use new nutrient input (i.e. I_x) and total nutrient uptake (i.e. F_x+RSB_X) rather than two types of NPP.

Under the equilibrium assumption, conceptually, the pool sizes do not represent the current stock. However, our estimates under equilibrium assumption are very close to observation-based estimates of NPP and C stocks (Table R1) and are all within the range of other estimates. In fact, our estimates of biomass and SOM stocks are a little bit larger than the state-of-the-art estimates listed in Table R1. In addition, the C stocks are not necessarily larger than the dynamic state. For example, Jones et al. (2009) showed that when the climate forcing was held constant after 2050, the equilibrated forest cover in a region of Amazon forest will be smaller than the dynamic state in 2050, resulting less equilibrated biomass than the dynamic biomass in this region. Given these evidences, we do not think that our results about the steady state are significantly underestimated.

Table R1 Computed NPP and C stocks under equilibrium assumption compared with published estimates.

variable	This study	Other
NPP (Pg yr^{-1})	52.5	54 (Zhao et al., 2005)
Terrestrial biomass (Pg)	493	450 [380-536] (Erb et al., 2018)
		450 [375-540] (Bar-on et al., 2018)
SOM (Pg)	1421	1408±154[1] (Batjes et al., 2016)

[1] This value represent the C stock between the depth 0-100 cm, generally correspond to the biologically active depth

To address all the points raised by the referee, in the revised manuscript, we revised the manuscript:

- Page 2 line 37 – page 3 line 6: "We present a new global data-driven diagnostic of C, N and P pools and fluxes, called GOLUM-CNP (Global Observation-based Land-ecosystems Utilization Model of Carbon, Nitrogen and Phosphorus) which is based on

the assumption that these cycles are equilibrated with present day conditions (see below for limitations of this approach). The goals of this study are to: 1) establish a global data-driven diagnostics of C, N and P fluxes and pools in order to compare nutrient use efficiencies, nutrient turnover rates and other relevant indicators across biomes; and 2) provide a new dataset that can be used to evaluate the results of global terrestrial biosphere models with consistent state of C, N and P cycles. In GOLUM-CNP, the C, N and P cycles are estimated for different biomes assuming steady state with present-day input of carbon (NPP), nitrogen (N deposition and N fixation) and phosphorus (P deposition and release from rock weathering) (see Sect. 3.2). The reason for this steady-state computation lies in the fact that only few global long-term observations associated with N and P cycles are available and are insufficient to constrain a transient simulation under the model framework. For example, field-scale manipulation experiments have shown that warming, elevated atmospheric CO_2, and N and P fertilization can drive changes in stoichiometries and nutrient resorption (Sistla and Schimel, 2012; Mayor et al., 2014; Yang et al., 2014; Yuan and Chen, 2015) in terrestrial ecosystems, but these data are insufficient to infer these changes in terrestrial ecosystems during the past decades. As more data becomes available the model framework can be adjusted to simulate a transient present day state. Although, the steady-state assumption hampers the comparison of stocks with present day observations, a direct comparison with simulated steady states of DGVM is possible as these model can simulate the steady-state for present day conditions.

Starting from a CARbon DAta MOdel fraMework (CARDAMOM) …we incorporated observed stoichiometric ratios (C:N:P) in each pool, N and P external input fluxes, transformations and losses in ecosystems and ~~losses and observation based information for~~ the fraction of gaseous losses of N to total (gaseous and leaching) losses of N from a global dataset of ^{15}N measurements in soils. Although the diagnostics is presented for steady state, the methods used to compute fluxes and pools are generic and could be extended to non-steady state (see Sect. 2 and equations in Appendix A-C) when more data will become available in the future (see Sect. 5.3)."

- Sect. 5.3 page 12 lines 35-37: "… Our results are a first step for evaluating global biogeochemical cycles. Although our steady-state C pool sizes (given the NPP and residence time at the condition of current climate) were within the [25, 75th] percentile range of the original non-steady-state CARDAMOM results (Fig. S1) at most grid cells, the biomass C stocks at 5%-10% of forest grid cells exceed the uncertainty range of CARDAMOM. In addition, independent remote-sensing estimates for 30 ℃N to 80 ℃N were 4.76 ±1.78 kg C m-2 for mean forest C density and 79.8 ±29.9 Pg C for total forest C (Thurner et al., 2014), which were lower than the GOLUM-CNP estimates (6.51 kg C m-2 for mean forest C density across pixels defined as forest in Fig. 2, and 181 Pg C for total forest C) for this region. This inconsistency was largely due to the fact that northern temperate and boreal forests may deviate substantially from their equilibrium for the current NPP (Pan et al., 2011), because of climate change and elevated CO2. Residual overestimation could be also due to the fact that biomass removal by harvesting and from disturbance other than fires was not explicitly constrained in CARDAMOM and thus not represented in GOLUM-CNP. A transient simulation of N and P cycling

will be needed in future studies…"

- We also specify the computation method for the output variables, to indicate whether these variables depend or not on the equilibrium assumption (Table 1 in the revised manuscript).

2. Reading between the lines, it seems that the N fixation is about 120Tg/year. How does this square with other estimates, e.g. Vitousek et al. 2013 (44Tg/year)? Since it's not discussed where this N fixation number came from (and the reference isn't available), or where the N deposition number came from, it makes it difficult to give much credibility to the openness discussions which rely on these.

Response:

The estimates of global BNF from synthesis and extrapolation are highly uncertain. Cleveland et al. (1999) estimated of biome- and global-level BNF based on scaling up of *in situ* measurements of BNF. They applied average plot-level BNF rates measured within each biome to the biome as a whole, assuming empirical range of values for the cover of plants with potential N-fixing symbioses. They estimated that global BNF by natural ecosystems was ~195 Tg N yr^{-1} (with a range 100-290 Tg N yr^{-1}) during pre-industrial. The estimates by Cleveland et al. (1999) were criticized by Galloway et al. (2004) and later Sullivan et al. (2014) as too high, in particular for tropical regions. Galloway et al. (2004) suggested a lower global BNF to be 128 Tg N yr^{-1}; Wang et al. (2007) made the estimate of BNF using the principle of resource optimization, and their global estimate for the year 1900 was 125 Tg N yr^{-1} (Wang and Houlton, 2009). Vitousek et al. (2013) incorporated information on N fluxes with ^{15}N relative abundance data and estimated pre-industrial N fixation was 44 TgN yr^{-1}. The large range (44-290 TgN yr^{-1}) in the estimates of BNF mentioned above reflects both a paucity of measurements of N fixation, as well as an incomplete understanding of the biophysical and biochemical controls on BNF.

In this study, we used estimates of biological N fixation from the CABLE model simulation by Peng et al. with a N fixation model developed by Wang et al. (2007), and used by Wang and Houlton (2009). This work by Peng et al. still is under review for Global Biogeochemical Cycles. We agree that there are considerable uncertainties about the magnitude of BNF. Vitousek (2013) estimated the total global N fixation from ranges from 40 to 100 Tg N yr^{-1} for the preindustrial time. Our estimated rate of 116 Tg N/yr^{-1} for the present days is still close to the upper limit of Vitouske (2013). Much of the difference may result from much higher rates used in this study for tropical forests than the recent estimate by Sullivan et al. (2014) that was based on the measurements at sites in southwest Costa Rica. However, estimates of BNF from Vitousek et al. (2013) are only available at global scale. BNF from CABLE, a process-based model validated for observations for diverse terrestrial biomes (Wang et al., 2007; Houlton et al., 2008) is to our best knowledge the only available global spatially explicit estimates of BNF besides the heavily criticized estimates by Cleveland et al. (1999), and is therefore used in this study. We discussed the uncertainties of BNF in the revised manuscript on page 5 line 7: "We used the spatially explicit estimates of N deposition (Wang et al., 2017) for 2001-2010, which were evaluated with globally distributed *in-situ* measurements. The spatially explicit N fixation was taken from the CABLE model simulation for 2001-2010 (Peng et al., submitted) with a N fixation model developed by

Wang et al. (2007). The simulation result matches the relative abundance of N_2-fixing legumes in different ecosystems. Globally, the N fixation was 116 Tg N yr^{-1}, within the range of empirical data (100-290 Tg N yr^{-1}; Cleveland et al., 1999; Galloway et al., 2004), but was larger than the estimate of 44 Tg N yr^{-1} by Vitousek et al. (2013) for pre-industrial. The large range (44-290 TgN yr^{-1}) in the estimates of nitrogen fixation reflects both a paucity of measurements of N fixation, as well as incomplete understanding of the biophysical and biochemical controls on N fixation. However, as mentioned in Sect. 2.2, our estimates of total N inputs (N deposition + N fixation) are consistent with the estimate from Houlton et al. (2018). And to our knowledge, CABLE simulation is the only product that has spatially explicit and processed-based estimates of N fixation, and is therefore used in this study. The resorption coefficients of leaves…"

3. The relationship between GOLUM-CNP and CARDOMON is opaque and needs to be clarified. It is particularly unclear with regard to what the relationship between the code provided and CARDOMON is. For example, does this code work independently? Or does it need CARDOMON to run? If CARDOMON is part of the code provided, which parts are new and which are CARDOMON?

Response:

The code of GOLUM-CNP is not just an extension of CARDAMOM, but a new model that used the outputs of CARDAMOM, i.e. data-driven C variables. The relationship between GOLUM-CNP and CARDAMOM are: 1) the C pools and fluxes in GOLUM-CNP follows that of CARDAMOM after steady state transformation, except that we group foliar and vegetation labile C into a single pool because labile C is not a measurable pool and no observation data were available to separate it from foliar in terms of stoichiometry. The N and P cycles in GOLUM-CNP were added on top of this C cycle model by adding two pools (soil inorganic N and P) and associated N and P fluxes; 2) GOLUM-CNP used some of the CARDAMOM results as inputs which are listed and explained in Table 1. These variables are the key parameters that describe the C cycle and influence the estimates of status of nutrient cycles. For instance, the residence time of C pools were used in the calculation of N and P fluxes (Eqs. E15, E16, E26 and E27).

To precise the relationship between GOLUM-CNP and CARDAMOM in the manuscript, we made the following revisions:

- We added on page 3 line 8: "~~The~~ GOLUM-CNP ~~framework~~ describes the C, N and P cycles in natural (i.e. non-agricultural) terrestrial ecosystems (Fig. 1). We used the same C pools and fluxes as in ~~The C cycle follows the model structure of~~ the CARDAMOM diagnostic (see Sect. 2.1 for details) to describe the C cycle and we computed associated N and P pools and fluxes. Biomass is divided into three pools: foliage, fine roots and wood…"
- We revised the sentence on page 4 line 35: "…the N and P contents in soil control the decomposition of soil C and thus the soil C pool observed (Manzoni et al., 2010). In this sense, it is appropriate to use C cycle from CARDAMOM as inputs to estimate the pool and fluxes of N and P."

The code must be run with variables from CARDAMOM (and also other required datasets, see "Inputs" in Table 1). Following the referee's suggestion, we comment the code

thoroughly. Please refer to the code resubmitted for detail.

4. It's not explained what the intended use of this model is. It's essential early on in the paper to have some examples of use, as well as specific limits on what it shouldn't be used for, (particularly given the limitation of it being an equilibrium model). This is slightly covered right at the end of the paper, but needs to be earlier and more extensive.

Response:

Thank you for this suggestion to improve the manuscript. We agree with the referee this information is quite important for the readers. In the revised manuscript, we explained the objects of this study in the introduction and discussed the equilibrium assumption in Sect. 5.3 (see answer to Major comment 1).

We remind the readers that current GOLUM-CNP results are steady-state estimates, when comparing our results with other DGVMs, it is better to run the DGVMs to steady state with present-day inputs of C, N and P. We revised the manuscript by:

- Adding a paragraph in Sect. 5.3 about this point: "The model structure of GOLUM-CNP is mainly described by the inputs (NPP for C cycle, N deposition and fixation for N cycle, P deposition and release from rock weathering for P cycle) and residence times. Most DGVMs (e.g. Goll et al., 2012, 2017a; Medvigy et al., 2009; Parton et al., 2010; Thornton et al., 2007; Wang et al., 2010; Weng and Luo, 2008; Xu-Ri and Prentice, 2008; Yang et al., 2009; Zaehle et al., 2014; Zaehle and Friend, 2010) can be summarized by these two components, although these models have more processes and use complex equations to describe the dynamics controlling carbon and nutrient distribution among pools and the turnover of each pool. In this context, the output of the GOLUM-CNP provides a traceable tool that can be used in the future to compare the results between GOLUM-CNP and different DGVMs. As DGVMs are capable of computing the steady state of the biogeochemical cycles for present conditions, a direct comparison between GOLUM-CNP estimate and DGVMs' estimates is possible."
- Revising page 12 line 38 to page 13 line 3: "At last, ~~The~~the sensitivity matrix presented in Sect. 4.4 provides a useful tool for assessing the uncertainties in model outputs by propagating the uncertainties in the model inputs. We applied this method to quantitatively assess the sources of uncertainties in the estimated nutrient-use efficiencies (Sect. 5.1 and Fig. 8), but we also found that the uncertainties for some other quantities were currently difficult to obtain, because the estimates of uncertainties were not available for all spatially explicit input data. This sensitivity analysis can be used in future studies to quantify the contribution of each input data set to the uncertainty in other model outputs, to characterize the dominant sources of uncertainties in the estimated C, N and P processes, to identify the major differences between different models (e.g. GOLUM-CNP versus DGVMs) and thus to identify priorities for future data syntheses to fill the largest gaps in uncertainty. Future studies that provide global data sets will need to include systematic evaluations and spatially explicit estimates of uncertainties in their data sets."
- Revising the conclusion on page 13 lines 10-17: "… The structure of GOLUM-CNP is analogous to most other process-based ~~LSMs~~ DGVMs describing carbon and nutrient interactions ~~(e.g. Goll et al., 2012, 2017a; Medvigy et al., 2009; Parton et al., 2010;~~

~~Thornton et al., 2007; Wang et al., 2010; Weng and Luo, 2008; Xu-Ri and Prentice, 2008; Yang et al., 2009; Zaehle et al., 2014; Zaehle and Friend, 2010), although these models have more processes and use complex equations to describe the dynamics controlling carbon and nutrient distribution among pools and the turnover of each pool.~~ The output of the GOLUM-CNP provides a traceable tool and~~, in which a consistency between different datasets of global C, N and P cycles has been achieved. Such a framework~~ can ~~thus~~ be used in the future to test the performance of ~~these~~ complex ~~LSMs~~ DGVMs in the simulation of interactions between C, N and P cycling."

5. The code is very dense, making it very difficult to read. Code should have comments every 1 - 10 lines, depending on how interpreted/dense, etc. the code is. Ideally, code should be commented so that, if you stripped out the actual code or if you didn't know python at all, you could re-write it in another language just from the comments. I was also a bit surprised not to see any functions used.

Response:

We write detailed comments in the new code. In fact, we have the main code "Globe_ss_Anal.py" and another two files incorporating three modules: 1) ncload.py, in which the module "ncload" reads the netcdf4 files and associated variables very efficiently; 2) ss_Anal.py, which make the computation at each grid cell. In ss_Anal.py, two functions ("tree" and "grass") making the computation for forest and grassland are defined separately. In the main code Globe_ss_Anal.py, "ncload" are called at the beginning of the code to read all the variables; "tree" and "grass" are called according to the dominant biomes of each grid cell.

Minor points

1. P.2 L6-7. Yes, but also water, light etc. are essential controls - if there's no light and water it doesn't matter how much N or P there is, nothing will grow.

Response:

Thank you for noting this inappropriate expression. We revised the sentence as: "…in terrestrial ecosystems. N and P availability affects vegetation productivity, growth and other processes (Norby et al., 2010; Sutton et al., 2008; Vitousek and Howarth, 1991)."

2. P.2 L17 - 30. This seems to mix up P and N fertiliser. It would be better to keep the two issues separate wherever possible.

Response:

Thank you for the suggestion. We rephrase this paragraph: "… Many of the underlying processes are not fully understood, and comprehensive data for evaluation are lacking to constrain the representation of some key processes (Zaehle et al., 2014), so model structure, the processes included and the prescribed parameters differ widely among DGVMs (Zaehle and Dalmonech, 2011). For example, some models assume constant stoichiometry (N:C and P:C ratios) in plant tissues (Thornton et al., 2007; Weng and Luo, 2008), but others have a flexible stoichiometry (Wang et al., 2010; Xu-Ri and Prentice, 2008; Yang et al., 2009; Zaehle and Friend, 2010). For the N cycle, for instance, some models do not include losses of gaseous N ~~due to~~ from denitrification (Medvigy et al., 2009), some use the "hole-in-the-pipe" approach to simulate the denitrification flux (Thornton et al., 2007; Wang et al., 2010),

assuming it is proportional to net N mineralization, and others calculate this flux as a function of soil N-pool size and soil conditions (temperature, moisture, pH, etc.) (Parton et al., 2010; Xu-Ri and Prentice, 2008; Zaehle and Friend, 2010). For models of the terrestrial P cycle, for instance, Jahnke (2000) estimated a global amount of soil P of 200 Pg and that P contained in plants was 3 Pg, based on empirical P content of soils (0.1%) and soil thickness (60 cm). These estimates were questioned by Wang et al. (2010) and Goll et al. (2012), who estimated that P in plants ranged between 0.23 and 0.39 Pg and that P in soil was only 26.5 Pg based on P:C ratios derived from more comprehensive stoichiometric data sets. Furthermore, ~~these models~~ terrestrial ecosystem models are usually only evaluated for specific ecosystems or at a limited number of sites (Goll et al., 2017a; Yang et al., 2014). The application of these models for simulations with global coverage is thus highly uncertain (Goll et al., 2012; Wang et al., 2010; Zhang et al., 2011)."

3. P18. L28. Reference to Peng missing.

Response:

Please see the response to the 2nd major point. And we added the reference accordingly.

4. P21. Table 2. When is this table referring to? (Pre-industrial? Present day?) It needs to be specified.

Response:

We revised the caption of Table 2 into: "Global annual mean C-pool sizes, NPP and heterotrophic-respiration fluxes in the C-cycle model assuming steady states under the climate conditions of 2001-2010." We also revised the text in the manuscript on page 8 line 3: "Table 2 shows the global C-pool sizes and main fluxes of the steady-state C cycle transformed from CARDAMOM under the climate conditions of 2001-2010, which are compared with the means and percentile ranges from the original non-steady-state CARDAMOM results during 2001-2010. The differences between the steady-state transformed pool sizes…"

5. P22. Figure 1. The caption would be more useful if the terms at the top of the figure were defined first, and then worked downwards.

Response:

Thank you for the suggestion. We reorganized the sentences in the caption: "**Figure 1** Schematic representation of the pools and fluxes in the C, N and P cycles within GOLUM-CNP. The gray, blue and red arrows represent C, N and P fluxes, respectively. Plants are divided into foliar, fine root and wood pools, where the wood pool includes woody stems and coarse roots. Litter and soil are two separate pools. The inorganic pool represents the nutrient sources in the soil that are available for plant uptake. Arrows between the pools represent the directions of C, N and P flow between pools. External inputs of N are atmospheric deposition (N_d) and biological N fixation (N_{fix}). External inputs of P are atmospheric deposition (P_d) and P released by rock weathering (P_w). F_C is net primary production (NPP). F_N and F_P are plant uptake of N and P from the inorganic N and labile soil P pools, respectively. R_h is release of C due to heterotrophic respiration. Mineralization of N and P is modeled along with litter and SOM decomposition, and N and P immobilization is modeled by a flux from the inorganic pool to SOM. External losses of N occur by fire, leaching and denitrification. External losses

of P occur by fire, leaching and transfer to occluded P in the soil."

6. P24. Figure 3. This is a very difficult to read. A table or a series of bar plots would be much better.

Response:

We tried to use tables or bar plots (Fig. R1) as the referee suggested. There are many variables involved, and we want to separate the seven biomes to see their major differences in the C, N and P cycle. As shown in Fig. R1, such figures will need 6 y-axis, and a very long space to put 6 figures. Even though we tried to optimize the spacing between figures, it is hard to put it on one A4 page and the texts are small. In addition, with the original plots, we depict the full C, N and P cycles including the pool sizes, residence times of different pools and fluxes. But with bar plots, only a small subset of the variables could be shown in limited space so that the readers will lose the whole pictures of the C, N and P cycles when reading these bar plots only. It is the same case to use a series of tables, because readers would need to link the variables from the tables in their own mind. At last, we decide to use the same figure, but rearrange them. We put the figures in a 3 by 3 grid so that all figures and numbers in the figures are larger and more easily to be read (please see the revised manuscript). And for readers who are more interested in reading bar plots, we also provide these bar plots in the supplementary material.

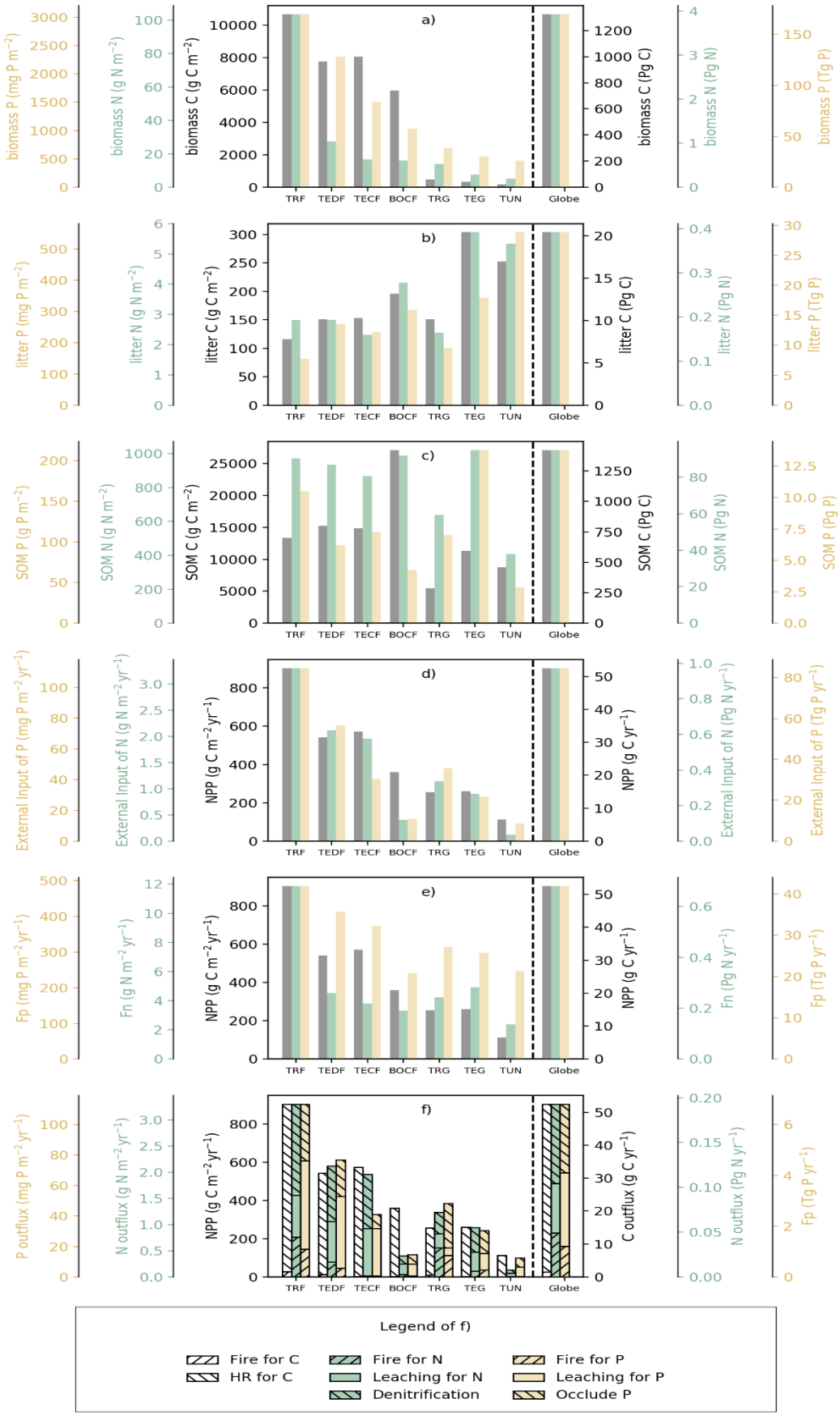

Figure R2 Pool sizes and fluxes of C (black), N (green) and P (yellow) computed from

GOLUM-CNP. The targeted biomes are tropical rainforests (TRF, a), temperate deciduous forests (TEDF, b), temperate coniferous forests (TECF, c), boreal coniferous forests (BOCF, d), tropical/C4 grasslands (TRG, e), temperate/C3 grasslands (TEG, f) and tundra (TUN, g).

7. P28. Figure 7. Two points need to be addressed for this figure. First that the text is so small that it is impossible to read printed A4. That's true of the ones in the SI too. Second that it's ironic that a red-green color scheme is used, despite one of the authors being color-blind. I just… Other color schemes are available.

Response:

Following the referee's suggestion, we revise this figure and the corresponding figures in the SI. The two plots are placed up and down, so that the circles and texts are enlarged. We also changed the color schemes for all the figures in the paper. With these modifications, we also want to mention that the color in these figures are indicative enough to show the different order of magnitude in the sensitivity. The numbers in each grid cell gives the same information as the colors but gives the precise values corresponding to the colors.

8. P29. Figure 8. It would be a courtesy to your readers to include in the key what YC1, etc. are. It could literally just go beneath the current labels.

Response:

Thank you for your comments. We revised the figure accordingly.

References:

Bar-On, Y. M., Phillips, R. and Milo, R.: The biomass distribution on Earth, PNAS, 201711842, doi:10.1073/pnas.1711842115, 2018.

Batjes, N. H.: Harmonized soil property values for broad-scale modelling (WISE30sec) with estimates of global soil carbon stocks, Geoderma, 269, 61–68, doi:10.1016/j.geoderma.2016.01.034, 2016.

Cleveland, C. C., Townsend, A. R., Schimel, D. S., Fisher, H., Howarth, R. W., Hedin, L. O., Perakis, S. S., Latty, E. F., Von Fischer, J. C., Elseroad, A. and Wasson, M. F.: Global patterns of terrestrial biological nitrogen (N2) fixation in natural ecosystems, Global Biogeochem. Cycles, 13(2), 623–645, doi:10.1029/1999GB900014, 1999.

Cleveland, C. C., Houlton, B. Z., Smith, W. K., Marklein, A. R., Reed, S. C., Parton, W., Grosso, S. J. D. and Running, S. W.: Patterns of new versus recycled primary production in the terrestrial biosphere, Proc. Natl. Acad. Sci., 110(31), 12733–12737, doi:10.1073/pnas.1302768110, 2013.

Erb, K.-H., Kastner, T., Plutzar, C., Bais, A. L. S., Carvalhais, N., Fetzel, T., Gingrich, S., Haberl, H., Lauk, C., Niedertscheider, M., Pongratz, J., Thurner, M. and Luyssaert, S.: Unexpectedly large impact of forest management and grazing on global vegetation biomass, Nature, 553(7686), 73–76, doi:10.1038/nature25138, 2018.

Galloway, J. N., Dentener, F. J., Capone, D. G., Boyer, E. W., Howarth, R. W., Seitzinger, S. P., Asner, G. P., Cleveland, C. C., Green, P. A., Holland, E. A., Karl, D. M., Michaels, A. F., Porter, J. H., Townsend, A. R. and V öosmarty, C. J.: Nitrogen Cycles: Past, Present, and Future, Biogeochemistry, 70(2), 153–226, doi:10.1007/s10533-004-0370-0, 2004.

Goll, D. S., Brovkin, V., Parida, B. R., Reick, C. H., Kattge, J., Reich, P. B., van Bodegom, P. M. and Niinemets, Ü.: Nutrient limitation reduces land carbon uptake in simulations with a model of combined carbon, nitrogen and phosphorus cycling, Biogeosciences, 9, 3547–3569, doi:10.5194/bg-9-3547-2012, 2012.

Jonard, M., Fürst, A., Verstraeten, A., Thimonier, A., Timmermann, V., Potočić, N., Waldner, P., Benham, S., Hansen, K., Meril ä, P., Ponette, Q., Cruz, A. C. de la, Roskams, P., Nicolas, M., Crois é, L., Ingerslev, M., Matteucci, G., Decinti, B., Bascietto, M. and Rautio, P.: Tree mineral nutrition is deteriorating in Europe, Global Change Biology, 21(1), 418–430, doi:10.1111/gcb.12657, 2015.

Jones, C., Lowe, J., Liddicoat, S. and Betts, R.: Committed terrestrial ecosystem changes due to climate

change, Nature Geoscience, 2(7), 484, 2009.
Lawrence, D. M., Oleson, K. W., Flanner, M. G., Thornton, P. E., Swenson, S. C., Lawrence, P. J., Zeng, X., Yang, Z.-L., Levis, S., Sakaguchi, K., Bonan, G. B. and Slater, A. G.: Parameterization improvements and functional and structural advances in Version 4 of the Community Land Model, Journal of Advances in Modeling Earth Systems, 3(1), doi:10.1029/2011MS00045, 2011.
Mayor, J. R., Wright, S. J. and Turner, B. L.: Species-specific responses of foliar nutrients to long-term nitrogen and phosphorus additions in a lowland tropical forest, Journal of Ecology, 102(1), 36–44, doi:10.1111/1365-2745.12190, 2014.
Peng, J, Wang Y-P and Houlton B.Z. Estimates of biological nitrogen fixation and implication of land carbon uptake from 1901 to 2100. under review in Global Biogeochemical Cycles.
Sardans, J. and Peñuelas, J.: The role of plants in the effects of global change on nutrient availability and stoichiometry in the plant-soil system, Plant Physiology, pp.112.208785, doi:10.1104/pp.112.208785, 2012.
Sardans, J., Rivas-Ubach, A. and Peñuelas, J.: The C:N:P stoichiometry of organisms and ecosystems in a changing world: A review and perspectives, Perspectives in Plant Ecology, Evolution and Systematics, 14(1), 33–47, doi:10.1016/j.ppees.2011.08.002, 2012.
Sardans, J., Alonso, R., Janssens, I. A., Carnicer, J., Vereseglou, S., Rillig, M. C., Fernández‐Martínez, M., Sanders, T. G. M. and Peñuelas, J.: Foliar and soil concentrations and stoichiometry of nitrogen and phosphorous across European Pinus sylvestris forests: relationships with climate, N deposition and tree growth, Functional Ecology, 30(5), 676–689, doi:10.1111/1365-2435.12541, 2016.
Sardans, J., Grau, O., Chen, H. Y. H., Janssens, I. A., Ciais, P., Piao, S. and Peñuelas, J.: Changes in nutrient concentrations of leaves and roots in response to global change factors, Global Change Biology, 23(9), 3849–3856, doi:10.1111/gcb.13721, 2017.
Sistla, S. A. and Schimel, J. P.: Stoichiometric flexibility as a regulator of carbon and nutrient cycling in terrestrial ecosystems under change, New Phytologist, 196(1), 68–78, doi:10.1111/j.1469-8137.2012.04234.x, 2012.
Thornton, P. E., Lamarque, J.-F., Rosenbloom, N. A. and Mahowald, N. M.: Influence of carbon-nitrogen cycle coupling on land model response to CO2 fertilization and climate variability, Glob. Biogeochem. Cycles, 21(4), GB4018, doi:10.1029/2006GB002868, 2007.
Vitousek, P. M., Menge, D. N. L., Reed, S. C. and Cleveland, C. C.: Biological nitrogen fixation: rates, patterns and ecological controls in terrestrial ecosystems, Philos Trans R Soc Lond B Biol Sci, 368(1621), doi:10.1098/rstb.2013.0119, 2013.
Wang, Y. P., Law, R. M. and Pak, B.: A global model of carbon, nitrogen and phosphorus cycles for the terrestrial biosphere, Biogeosciences, 7(7), 2010.
Xu-Ri and Prentice, I. C.: Terrestrial nitrogen cycle simulation with a dynamic global vegetation model, Glob. Change Biol., 14(8), 1745–1764, doi:10.1111/j.1365-2486.2008.01625.x, 2008.
Yang, X., Wittig, V., Jain, A. K. and Post, W.: Integration of nitrogen cycle dynamics into the Integrated Science Assessment Model for the study of terrestrial ecosystem responses to global change, Glob. Biogeochem. Cycles, 23(4), 2009.
Yang, Y., Fang, J., Ji, C., Datta, A., Li, P., Ma, W., Mohammat, A., Shen, H., Hu, H., Knapp, B. O. and Smith, P.: Stoichiometric shifts in surface soils over broad geographical scales: evidence from China's grasslands, Global Ecology and Biogeography, 23(8), 947–955, doi:10.1111/geb.12175, 2014.
Yuan, Z. Y. and Chen, H. Y. H.: Decoupling of nitrogen and phosphorus in terrestrial plants associated with global changes, Nature Climate Change, 5(5), 465–469, doi:10.1038/nclimate2549, 2015.
Zaehle, S., Friend, A. D., Friedlingstein, P., Dentener, F., Peylin, P. and Schulz, M.: Carbon and nitrogen cycle dynamics in the O-CN land surface model: 2. Role of the nitrogen cycle in the historical terrestrial carbon balance, Global Biogeochemical Cycles, 24(1), doi:10.1029/2009GB003522, 2010.
Zaehle, S.: Terrestrial nitrogen–carbon cycle interactions at the global scale, Philos. Trans. R. Soc. Lond. B Biol. Sci., 368(1621), 20130125, doi:10.1098/rstb.2013.0125, 2013.
Zhao, M., Heinsch, F. A., Nemani, R. R. and Running, S. W.: Improvements of the MODIS terrestrial gross and net primary production global data set, Remote Sensing of Environment, 95(2), 164–176, doi:10.1016/j.rse.2004.12.011, 2005.

Response to comments on "GOLUM-CNP v1.0: a data-driven modeling of carbon, nitrogen and phosphorus cycles in major terrestrial biomes" by Y. Wang et al.

We thank the referee for reviewing our manuscript. Please find attached a point-by point reply to each of the comments raised by the referee with legible text and figures organized along the text.

This manuscript presented a simple model for coupled terrestrial carbon-nitrogen-phosphorus cycles. A model-data fusion approach was applied to estimate steady-state values for selected model state variables, fluxes, and parameters. In particular, the estimated quantities allowed for computation of carbon, nitrogen, and phosphorus pool sizes, the openness of the N and P cycles, characteristic turnover times, and nutrient use efficiencies.
In principle, I think that estimation of these quantities using model-data fusion is a worthwhile and interesting idea. However, I think there is substantial room for improvement in both the presentation and the approaches used. Here are a few general comments:

Response:

We would like to thank the referee for the valuable comments and suggestions for improving our manuscript. Following the reviewer's comments, we carefully revised our manuscript. Please find below the point-to-point responses (in black) to all referee comments (in blue). For your convenience, changes in the revised manuscript are highlighted with dark red. All the pages and line numbers correspond to the original version of text.

1. The paper contains no statement of objectives, questions, or hypotheses. Including any or all of these features would help to orient the reader. But without them, the paper is difficult to evaluate because the goals of the paper are unstated.

Response:

Thank you for the suggestion. We revise the paragraph in the introduction (page 2 line 37 – page 3 line 6):

"We present a new global data-driven diagnostic of C, N and P pools and fluxes, called GOLUM-CNP (Global Observation-based Land-ecosystems Utilization Model of Carbon, Nitrogen and Phosphorus) which is based on the assumption that these cycles are equilibrated with present day conditions (see below for limitations of this approach). The goals of this study are to: 1) establish a global data-driven diagnostics of C, N and P fluxes and pools in order to compare nutrient use efficiencies, nutrient turnover rates and other relevant indicators across biomes; and 2) provide a new dataset that can be used to evaluate the results of global terrestrial biosphere models with consistent state of C, N and P cycles. In GOLUM-CNP, the C, N and P cycles are estimated for different biomes assuming steady state with present-day input of carbon (NPP), nitrogen (N deposition and N fixation) and phosphorus (P deposition and release from rock weathering) (see Sect. 3.2). The reason for this steady-state computation lies in the fact that only few global long-term observations associated with N and

P cycles are available and are insufficient to constrain a transient simulation under the model framework. For example, field-scale manipulation experiments have shown that warming, elevated atmospheric CO_2, and N and P fertilization can drive changes in stoichiometries and nutrient resorption (Sistla and Schimel, 2012; Mayor et al., 2014; Yang et al., 2014b; Yuan and Chen, 2015) in terrestrial ecosystems, but these data are insufficient to infer these changes in terrestrial ecosystems during the past decades. As more data becomes available the model framework can be adjusted to simulate a transient present day state. Although, the steady-state assumption hampers the comparison of stocks with present day observations, a direct comparison with simulated steady states of DGVM is possible as these model can simulate the steady-state for present day conditions.

Starting from a CARbon DAta MOdel fraMework (CARDAMOM) …we incorporated observed stoichiometric ratios (C:N:P) in each pool, N and P external input fluxes, transformations and losses in ecosystems and ~~losses and observation-based information for~~ the fraction of gaseous losses of N to total (gaseous and leaching) losses of N from a global dataset of ^{15}N measurements in soils. Although the diagnostics is presented for steady state, the methods used to compute fluxes and pools are generic and could be extended to non-steady state (see Sect. 2 and equations in Appendix A-C) when more data will become available in the future (see Sect. 5.3).

We first present the model structure (Sect. 2) and the data sets used to derive its outputs consisting of pools…"

2. The model is meant to be applied to natural ecosystems, and so the model-data fusion approach should be valid in grid cells that are dominated by nature ecosystems. However, the problem is that very few such grid cells remain (Ellis and Ramankutty 2008). I would therefore expect biases to emerge when the natural ecosystem model is applied to grid cells that are biogeochemically influenced by humans. I am bothered that anthropogenic effects are not accounted for in the global and (natural) biome scale averages computed by the authors.

Response:

We agree with the reviewer that current terrestrial ecosystem are largely influenced by anthropogenic activities. Here, however, "natural ecosystem" refers to non-agricultural ecosystems. The inputs of C, N and P to these natural system in our framework account for anthropogenic influences. For example, the estimates of NPP from CARDAMOM represent NPP under current level of atmospheric CO_2 concentration and climate change. The estimate of atmospheric N and P deposition (Wang et al., 2017) includes anthropogenic emissions of reactive N and of P from fuel combustion. Our definition of "natural ecosystems" follows the terminology used in previous studies, such as Cleveland et al. (2013).

In the revised manuscript, we specify this point on page 3 line 14: "The GOLUM-CNP framework describes the C, N and P cycles in natural (i.e. non-agricultural) terrestrial ecosystems (Fig. 1). We follow the model structure …" We change "natural vegetation" to "non-agricultural vegetation" and "natural biomes" to "non-agricultural biomes" all through the manuscript.

3. In a way, not enough information is presented. I would be interested in seeing spatial maps of at least some quantities and some confirmation that the model-data fusion approach is

satisfactory on the grid cell level. I am skeptical of the biome- and global-level results without having a better idea of the grid cell level information used to construct them.

Response:

Thanks for the suggestion. We add the global gridded map of N deposition (input data, Fig. S3a), N fixation (input data, Fig. S3b), P deposition (input data, Fig. S4a), release of P from weathering (input data, Fig. S4b), openness of N (output of GOLUM-CNP, Fig. S5a), openness of P (output of GOLUM-CNP, Fig. S5b), $\tau_{N,eco}$ (output of GOLUM-CNP, Fig. S6a), $\tau_{P,eco}$ (output of GOLUM-CNP, Fig. S6b), NUE (output of GOLUM-CNP, Fig. S7a) and PUE (output of GOLUM-CNP, Fig. S7b) in the supplementary materials and remind the readers of these spatial maps in the main text when necessary.

4. In another way, too much information is presented, making the paper confusing (see Figs. 3, 7). It would help to have a better-defined narrative arc. While many numbers were presented, I think the authors could do a better job in drawing attention to new, qualitative insights.

Response:

We think Fig. 3 depict the full C, N and P cycles including the pool sizes, residence times of different pools and fluxes. We prefer these plots rather than some bar plots which may be easier to read but only show specific aspects of the C, N and P cycling. Following thre reviewer's comments, we revise Sect. 4.2:

- In Sect. 4.2, we first compare the C, N and P cycles in different biomes. Such comparisons include the plant uptake, stocks in vegetation, litter and SOM, and the loss fluxes from the ecosystems.
- We then compare our estimates of global N and P stocks with previous studies, showing that our estimates are close to the estimates from previous studies.
- At last, we compare the global estimates of total nutrient inputs and losses with previous studies. We highlight that the loss of N by fire accounted for 26% of total N loss, while less fraction of P is lost through fire.

Fig. 7 shows the sensitivity of the selected output variables to all input variables. Sensitivities (dy/dx), not like the attribution of which input variable contribute the most to the overall uncertainties in the output (for example, Fig. 8), have no priority for different variables but they show how output change as a result of change in the input. The colors in these figures give qualitative information about the sensitivities' magnitude. The numbers in each grid cell give the quantitative information with precise values for readers interested in the exact numbers. As suggested by the reviewer, we improve the texts in Sect. 4.4.

5. I would like to know approximately what level of bias the steady-state assumption incurs. These ecosystems are unlikely to be at steady state for many reasons (CO2 fertilization, changes in nutrient deposition, climate extremes such as droughts, etc.).

Response:

The reviewer mentions several processes that related to both short-term (climate extremes) and long-term (e.g. CO_2 fertilization, changes in nutrient deposition) disequilibrium. Firstly, short-term disturbance causes temporal changes in the C sink and source at yearly to decadal scales, but has no impact on long-term C fluxes and pools unless the disturbance change its regime (e.g. become more frequent) (Luo and Weng, 2011).

Regarding the long-term effect, some previous studies have investigated the changes in C, N stocks between pre-industrial times and present day. Thornton et al. (2007) investigated the C stock changes from 1850 to present day (1976-2000) using CLM-CN model. They found that the C stocks in vegetation, litter and SOM increased by 35, 1 and 10 Pg, which equalled to only 5%, 6% and 3% of the respective initial C stocks in 1850. Zaehle et al. (2010) estimated the C and N stock changes in vegetation and SOM, using the O-CN terrestrial biosphere model. By excluding the impact of land use change, vegetation C stocks increased by 62 Pg and soil C stocks increased by 39 Pg from 1860 to 2002, being 13% and 3% of initial C stocks for vegetation and SOM respectively. The N stocks increased by 376 Tg and 2836 Tg in vegetation and SOM, being 11% and 3% of initial N stocks. Zaehle et al. (2013) further accounted for the effect of land use change on the global C and N cycles. The results also showed that the cumulative effect of anthropogenic disturbance from preindustrial times are small (<5%) on the natural C and N cycles. These evidences indicate that anthropogenic disturbance on the natural C, N and P cycles are not so significant at global scale. However, at local scales, some places are experiencing significant anthropogenic disturbances, mostly through deposition and fertilizer (Jornard et al., 2015). However, the extent to which natural ecosystems are affected by these disturbances are not clear (Wang et al., 2017). To check the long-term effect, we compare the recomputed pool sizes for C with the original CARDAMOM estimates (Fig. S1 in the revised supporting information). The steady-state transformed pool sizes are within the [25, 75th] percentile range of the original CARDAMOM results at more than 90% forest grid cells. The major part of the deviation comes from the treatment of grassland in GOLUM and are not associated to the steady-state assumption: In GOLUM-CNP grasslands are considered as a distinct biome, while the original CARDAMOM did not use land cover information and provided some woody biomass pools for grassland dominated regions. As GOLUM does not consider woody biomass for grass, we transfer wood growth from CARDAMOM into non-woody tissue for grasslands. This makes our C pools more different from the original CARDAMOM at grassland-dominated pixels than at forest-dominated pixels. However, although the biomass at grassland grid cells in GOLUM-CNP are much lower than the biomass in CARDAMOM, the litter and SOM pool sizes at grassland grid cells in GOLUM-CNP are still within the [5, 95th] percentile range of the original CARDAMOM results (Fig. S1b and S1c in the revised supporting information).

Here, we also remind that we develop a steady-state model as a first attempt of a CNP data-driven diagnostic model. The objective of this study is not to reproduce the present day state, but to provide a steady-state estimates of C, N and P cycle with current input of C, N and P, stoichiometry of N:C and P:C ratios, and residence times of different pools, because there is a lack of data to constraint a transient state (see point 1). As a result, we choose to constrain an equilibrium state. Although it does not correspond in some aspects to the present day state, it is still useful for evaluating global models as these model are able to simulate a equilibrium state for present day conditions and a direct comparison is possible (see point 2 and point 3).

1) Although we described processes in the C, N and P cycles by a set of differential equations (Eqs. A1-A5, B1-B7, C1-C7), only few global long-term observations associated with N and P were available to constrain a transient simulation. For example, the synthesis of stoichiometries in different pools are based on published literature during

the last four decades, and almost no data are available for preindustrial period; field-scale manipulation experiments have shown that warming, elevated atmospheric CO_2, and N and P fertilization can drive changes in stoichiometries and nutrient resorption in terrestrial ecosystems (Sistla and Schimel, 2012; Sardans et al., 2012; Sardans and Peñuelas, 2012; Li et al., 2013; Mayor et al., 2014; Yang et al., 2014; Yuan and Chen, 2015; Sardans et al., 2016; Sardans et al., 2017), but these data are insufficient to infer these changes in terrestrial ecosystems during the past years. As a result, for a data-driven model framework, we computed the equilibrium estimates and this equilibrium corresponds to the state where the inputs of C, N and P (e.g. NPP for C cycle, N deposition and fixation for N cycle, P deposition and release of P by rock weathering for P cycle) and residence times equal to the estimates under present-day conditions.

2) Given the state-of-the-art estimates about the magnitude of anthropogenic disturbance on natural C, N and P cycles and large uncertainties as mentioned above, it is still useful to take steady-state estimates as a diagnostic to evaluate DGVMs in simulating global C, N and P cycling (Wang et al., 2010; Xu-ri et al., 2008; Yang et al., 2009; Lawrence et al., 2011). The estimates based on steady state assumptions listed above match well with a wide range of *in-situ* observations in recent years.
3) CARDAMOM is the only spatially explicit data-driven product of C cycle, which does not rely on a steady-state assumption. In this study, our aim is to develop a steady-state model (see point 1) in which a consistency between different datasets are achieved (which is a novelty). We chose to use the variables in the CARDAMOM products: NPP, residence times and fire fractions, which were constrained by global long-term observations of MODIS LAI and MODIS burned area. For other C variables whose direct constraints do not have a global coverage in CARDAMOM (such as biomass), we recalculated them based on the equilibrium assumption. With this steady state C cycle, we compute the associated N and P pools and fluxes. For example, the N and P in SOM pool equal to the product of N:C/P:C ratios and equilibrated C content.

In summary, given the three concerns mentioned above, we computed an equilibrium estimate of C, N and P cycle, where the inputs of C, N and P into the terrestrial ecosystems (NPP, N and P deposition, N fixation and release of P by rock weathering), stoichiometries of N:C and P:C ratios, the residence times of different pools and the land cover are held constant as the period 2001-2010. Although this steady-state estimates deviate from the actual state of present-day disturbed cycles, we compare the GOLUM-CNP with the original CARDAMOM to show that the steady-state estimates in GOLUM-CNP are still within the range of such large uncertainties from data on the present day state.

6. The model is simple, which is okay for a first attempt. But there does not seem to be any substantial discussion of how to make the model more realistic by including other known fluxes and feedbacks (especially appropriate in 5.3, Future research and data needs).

Response:

Thanks for the suggestion. We substantially extended the discussion about future development for GOLUM-CNP towards a more realistic / complex diagnostic.

7. The manuscript needs a careful proofreading by a fluent English speaker. Starting with the title, "model" would make more sense than "modeling".

Response:

Thank you for your suggestion. We have requested several fluent English speakers to play a more active role in the re-writing and editing of the whole manuscript. We hope that the revised manuscript could satisfactorily address all of your concerns.

Specific comments:

8. Page 2, lines 17-21: Not clear if you are talking about N cycling, P cycling, or both

Response:

We revise this paragraph: "… Many of the underlying processes are not fully understood, and comprehensive data for evaluation are lacking to constrain the representation of some key processes (Zaehle et al., 2014), so model structure, the processes included and the prescribed parameters differ widely among LSMs (Zaehle and Dalmonech, 2011). For example, some models assume constant stoichiometry (N:C and P:C ratios) in plant tissues (Thornton et al., 2007; Weng and Luo, 2008), but others have a flexible stoichiometry (Wang et al., 2010; Xu-Ri and Prentice, 2008; Yang et al., 2009; Zaehle and Friend, 2010). For the N cycle, for instance, some models do not include losses of gaseous N ~~due to~~ from denitrification (Medvigy et al., 2009), some use the "hole-in-the-pipe" approach to simulate the denitrification flux (Thornton et al., 2007; Wang et al., 2010), assuming it is proportional to net N mineralization, and others calculate this flux as a function of soil N-pool size and soil conditions (temperature, moisture, pH, etc.) (Parton et al., 2010; Xu-Ri and Prentice, 2008; Zaehle and Friend, 2010). For models of the terrestrial P cycle, for instance, Jahnke (2000) estimated a global amount of soil P of 200 Pg and that P contained in plants was 3 Pg, based on empirical P content of soils (0.1%) and soil thickness (60 cm). These estimates were questioned by Wang et al. (2010) and Goll et al. (2012), who estimated that P in plants ranged between 0.23 and 0.39 Pg and that P in soil was only 26.5 Pg based on P:C ratios derived from more comprehensive stoichiometric data sets. Furthermore, ~~these models~~ terrestrial ecosystem models are usually only evaluated for specific ecosystems or at a limited number of sites (Goll et al., 2017a; Yang et al., 2014). The application of these models for simulations with global coverage is thus highly uncertain (Goll et al., 2012; Wang et al., 2010; Zhang et al., 2011)."

9. Page 2, lines 28-30: Too bad that this is not discussed further

Response:

We add some discussions about the different quantities of P pool sizes. Please refer to the response to Comment 8.

10. Page 3, lines 17-19, state that an inorganic P pool was added to the model, and it is assumed that this P is accessible to plants. However, in reality, very little inorganic P is accessible to plants.

Response:

P exists in various forms in soil with different accessibilities to plants (Yang and Post, 2011). P may enter the solution through desorption or dissolution of inorganic P, or by

mineralization of organic P, and then is utilized by plants.

In the original manuscript, we referred only to "inorganic P that are accessible by plants" for an integration of all the forms that can be easily used by plants. In the model developed by Wang et al. (2007) they defined four P pools (labile P, sorbed P, strongly sorbed P and occluded P) in soil and argued that the time for reaching equilibrium between labile inorganic P and sorbed inorganic P in soil is less than one hour. In this context, although the inorganic P that is directly accessible to plants is very small, there are still considerable amount of other forms of P that can be fast transformed to inorganic P that can be utilized by plants. A recent synthesis of a database of soil P fractions by Yang and Post (2011) also confirmed that the amount of labile P in soils (defined as the sum of resin Pi, bicarbonate Pi and Po using Hedley fractionation method) is generally much higher than vegetation demand, even in highly weathered soils commonly considered as P limited. They argued that P uptake by microbial (immobilization) competing with plant uptake strongly controls the P availability of plants, citing evidence by Cole et al. (1977) "…two grassland sites…, root uptake of P vs. microbial uptake of P was 5.26 kg P ha^{-1} yr^{-1} vs. 24.57 kg P ha^{-1} yr^{-1} and 12.00 kg P ha^{-1} yr^{-1} vs. 31.60 kg P ha^{-1} yr^{-1} respectively". These evidences all show that although some P in soils is not readily accessible to plants, a large amount of this P can be transformed quickly into a form that can be used by plants, and that this transformation is usually faster than the time scale (one year) of our computation. In consequence, it is possible to define a single pool to represent labile soil P available for plants. And our results (original Fig. 3) about the immobilization fluxes and plant uptake in most biomes are supported by Yang and Post (2011) indeed.

To address the comments by the referee, we use "labile soil P" instead of "inorganic P" all through the manuscript and revised the text: "…Two additional pools not present in CARDAMOM are added, representing soil inorganic N and labile soil P. These two N and P pools are assumed to represent nutrients accessible by plants (see Sect. 2.1 and 2.2). Of note is that these inorganic N and labile P pools represent an integration of various forms of N and P. For example, P has various forms in soil and can be transformed between those forms (Wang et al., 2007; Yang and Post, 2011). Some forms of organic P (e.g. bicarbonate Po in Hedley method) can also be easily mineralized and thus were implicitly included in our labile soil P pool. Other forms of P that are not easily accessible to plants are referred to as "occluded P" and labile soil P can become occluded P (Wang et al., 2010; Goll et al., 2017a). Fluxes connecting the pools are described by the differential equations …"

11. Page 3, line 31: What do you think about N from rock weathering (Houlton et al. 2018)?

Response:

Thank you for pointing out this newly published paper. The paper of Houlton et al. (2018) pointed out that about 19 to 31 Tg N yr^{-1} are mineralized from near-surface rocks. Their results also suggested that rock N inputs are particularly important in montane and high-latitude ecosystems. However, they also discussed the fact that at some places where rock weathering occurs deep beneath the soil, N from rocks may be released to groundwater and transported to fluvial systems. The ability of plants to use weathered N in deep soils depends on the depth of their roots and how much of the rock N inputs are actually used by plants was not quantified in their study. In another synthesis mentioned by the referee

(Augusto et al., 2017) in Comment 14, soil N availability was shown not significantly dependent on soil parent material or soil weathering stage. Augusto et al., (2017) argued that soil parent material and weathering stage only have indirect effects on soil N availability through its influence on edaphic factors such as soil pH. These evidences together show that rock weathering may contribute a significant amount of N to the soil, but the amount of these N are accessible to plants are still unknown and needed to be assessed.

Computationally, in our modelling framework, if fluxes of rock N inputs are taken into account, they should act as an input of N to non-agricultural ecosystems. Qualitatively, considering the computation of the model outputs (Appendix E) only the size of inorganic N is related to the total input of N to non-agricultural ecosystems (Eq. E17). Quantitatively, our estimate of the total input of N to non-agricultural ecosystems (188 Tg yr^{-1}) is at the higher end of the estimate by Houlton et al. (2018) even when they considered the rock N inputs (mean 147 Tg yr^{-1}, and range between 99.1 and 185.1 Tg yr^{-1}). Compared with estimates from Houlton et al. (2018), the fluxes from rock N inputs ignored in GOLUM-CNP are compensated by the larger estimate of N fixation and atmospheric N deposition used by GOLUM-CNP. In consequence, our estimates of total N inputs, and thus the associated model output (inorganic N) cover the uncertainty related to missing N inputs from rocks.

In the revised manuscript, we mention the recent paper by Houlton et al. (2018) on page 3 line 35: "… The N cycle includes a specific soil inorganic-N pool in addition to the five pools of the C cycle. The inputs of N to ecosystems include atmospheric N deposition and N fixation (Nd+Nfix in Fig. 1), both of which are assumed to enter the inorganic-N pool. We did not consider the flux of N mobilized from near-surface rocks, although a recent paper by Houlton et al. (2018) pointed out this flux may be an important N sources in montane and high-latitude ecosystems. The total N-fixation flux in this study includes both symbiotic and asymbiotic fixation…" In the discussion section on page 12 line 37, we add more discussions about it: "In addition, some processes, such as the N inputs from rock weathering (Houlton et al., 2018) were not considered in this study, because 1) as stated in Houlton et al. (2018), it is still unknown how much of rock-released N can be used by plants when rock weathering happens deep beneath the soils; 2) in GOLUM-CNP, adding rock N inputs has the same effect than N fixation and N deposition (Eqs. B6 and E17); and 3) the estimate of total input of N to ecosystems (188 Tg N yr-1) in this study are already at the higher end of the estimate (mean 147 Tg yr-1, and range between 99.1 and 185.1 Tg yr-1) of Houlton et al. (2018), even if rock N inputs are not accounted for, due to our larger estimates of N fixation and N deposition than Houlton et al. (2018). In the future, the rock N inputs and the fraction of these N inputs are accessible to plants should be further quantified and the quantity of total N inputs to the ecosystems should be reconciled between different studies. With these improvements, the future development of data-driven GOLUM-CNP should take into all these processes and fluxes."

12. Page 3, lines 37-38: N fixation is not entirely controlled by plants. In fact, the authors mentioned asymbiotic fixation a few lines above.

Response:

We agree with the referee. Biological N fixation occur in two ways: symbiotic and asymbiotic (or free-living). However, there are a diversity of the relationship between the

N_2-fixing organisms and plants and these is no clear line separating symbiotic and asymbiotic N fixiation and how these N can be used by plants and microbes (Reed et al., 2011). In this study, we do not separate the two and this is not a problem under steady state, since the inputs of N fixation are either used by plants, used by microbes (e.g. through immobilization) or even lost through leaching.

To address the concerns by the referee, we revised the manuscript: "The total N-fixation flux in this study includes both symbiotic and asymbiotic fixation, separately estimated from a previous study (see Sect. 3.1). We do not separate the two fixation processes and assume that they together contribute to the inorganic-N pool, although these two pathways of N fixation are differed in terms of the relationships between N_2-fixing microorganisms and plants. We did not consider the flux of N mobilized from near-surface rocks, although a recent paper by Houlton et al. (2018) pointed out this flux may be an important N sources in montane and high-latitude ecosystems. N uptake (F_N) by plants is assumed…"

13. Page 4, lines 21-22: much inorganic P is neither strongly sorbed, nor immediately available to plants. See, for example, Yang et al. (2013).

Response:

We agree with the referee. Please refer to revision of the manuscript in the response to Comment 10.

14. Page 5, lines 2-6: why the biome-scale analysis? Soil parent material is perhaps the most important factor governing nutrient limitation (Augusto et al. 2017) and has substantial sub-biome scale variability.

Response:

Firstly, Augusto et al. (2017) grouped their database into four climate classes (tropical, dry, temperate and cold) rather than different ecosystems/biomes, because "… generally low number of values per climate–ecosystem combination" in their database. And because of the limited number of data, "For a given climate class (e.g., temperate class), we found no statistical difference of nutrient limitation among ecosystem types (e.g., forests vs. grasslands)" – their analyses were only made for different ecosystems within their climate classes, but were not made for ecosystem across the globe.

In Augusto et al. (2017), they used three independent approaches and defined three indexes to address nutrient limitation: 1) plant growth response to nutrient addition (fertilization) (index 1 hereafter); 2) leaf chemistry including N:P ratios and nutrient resorption efficiency based on a leaf database containing values of N content and/or P content for green leaves and senescent leaves (index 2 hereafter); and 3) a model framework quantifying soil N and P in soils that are available to plants (index 3 hereafter). Of note is that the former two indices are defined from a vegetation perspective, while the third index is defined from a perspective of soil properties.

Augusto et al. (2017) found that N limitation (all three indexes) was best explained by climate (Fig. 3d-f and Sect. 3.2 in Augusto et al., 2017) and not directly linked to soil parent materials (Fig. S10g in Augusto et al., 2017) and weathering stage (Fig. S10a in Augusto et al., 2017). They found P-limited plant growth (index 1) was not directly linked to climate or latitude (Fig. 3h, j, k in Augusto et al., 2017) but partly related to P atmospheric deposition

(Sect 3.3 in Augusto et al., 2017). They found that soil P availability (index 3) could be "*partly*" explained by soil types and soil parent materials. Of note is that only one of the three indexes, and only for P, was attributed to soil properties in Augusto et al. (2017). In addition, even grouped into different classes of soil parent materials, there are substantial sub-classes variability related to soil properties (Fig. S10b, e, h in Augusto et al., 2017).

Augusto et al. (2017) further investigated the relative importance of actual N limitation versus P limitation and found soil parent materials appeared to be "*slightly*" more important than climate (Fig. 4c) based on the plant growth response to fertilization (index 1). However, when looking at plant N:P ratios, the relative limitation index of the plant leaf influenced by climate (+0.73) was more strongly than by soil parent material (-0.2) as shown by Fig. 4d in Augusto et al. (2017).

As shown above, there are different indexes for nutrient stresses, which differ with respect to the perspective (soil, individual plant, vegetation, ecosystem, etc). In the nutrient cycle, the vegetation and soil are tightly coupled: plants take nutrients from the soil for growing and return the nutrients to soil when they die. So all indexes have their use and a combination of indexes is the best to cover the big picture, like Augusto et al. (2017) did. In this study, we aimed to provide a dataset to evaluate the results of LSMs in their simulation of interactions between C, N and P cycling and LSMs mainly work at ecosystem scale. We focused on openness, nutrient use efficiencies and residence times in ecosystems. The openness is defined as the percentage of the total ***plant*** uptake of nutrients from new nutrient inputs (N fixation and N deposition for N; P deposition and release of P from rock weathering for P), and the nutrient use efficiencies are defined as the quotient between GPP and ***plant*** uptake of N and P from inorganic N and labile soil P. These indicators all work at ecosystem scale, so that we think it is more appropriate to made analysis at biome-scale rather than at soil scale in this study.

At last, other studies discussing about similar indicators also made analysis at biome scale. For example, Cleveland et al. (2013) discussed the patterns of new versus recycled nutrients, which is a similar concept as the openness defined in our study, for different biomes. The analysis of nutrient efficiencies made by Gill and Finzi (2016) were also made at the biome scale. We think, as already highlighted above, whether the analysis should be made at biome-scale or soil-type-scale should largely depend on what variables we are looking at.

To address the point raised by the referee and highlight the fact different studies define nutrient cycles at different scales, we revise the manuscript on page 5 line 2: "Different indices have been used to describe nutrient cycling from different perspectives (soil, individual plant, vegetation, ecosystem, etc) (Augusto et al., 2017; Cleveland et al., 2013; Gill and Finzi, 2016). In this study, we focused on the openness, nutrient use efficiencies and the residence time (Sect. 3.2) which are defined at ecosystem scale and thus correspond to the scale at which DGVMs are typically defined. For the presentation of results, we distinguish seven biomes: tropical rainforests (TRF), temperate deciduous forests (TEDF), …"

15. Page 5, lines 12-13: I am concerned at the ECMWF soil moisture product. Is it any good? Doesn't it have fixed layer depths? I'm not sure if that is appropriate here.

Response:

ERA-Interim/Land has four fixed layer depths: 0-0.07 m, 0.07-0.28 m, 0.28-1 m and

1-2.89 m. We admit that we do not have precise data set for the total soil content globally up till now, so that we only rely on some model results which were also constrained and evaluated against in situ measurements (Balsamo et al., 2015; Martens et al., 2017).

In our computation, the soil moisture impacts the estimate of inorganic N and labile soil P (Eqs. B7, E17 and E28). To address the question by the referee, we choose another widely used data set of root-zone soil moisture, GLEAM v3.2 (Martens et al., 2017). In GLEAM v3.2, the depth of the root zone is a function of the land-cover type and comprises three model layers for the fraction of tall vegetation (0–10, 10–100, and 100–250 cm), two for the fraction of low vegetation (0–10, 10–100 cm), and only one for the fraction of bare soil (0–10 cm). We multiplied the root-zone soil moisture by the depth of root zone derived from the biome map we showed in our study to estimate the total water content. To convert from the biome map to the classes defined in GLEAM v3.2, we assume forests biomes correspond to tall vegetation in GLEAM v3.2, grass biomes correspond to low vegetation and other land surfaces correspond to bare soil. The comparison between the resulting pool sizes of inorganic N and labile soil P using these two different data sets of soil moisture are shown in Fig. R1. It is not surprising that these two products have large uncertainties at grid scale, but the large-scale patterns of inorganic N and labile soil P using these two products are very similar.

To address the referee's concern, we revise the sentence on page 5, lines 12-13: "The spatially explicit estimate of total soil moisture was derived from the European Centre for Medium-Range Weather Forecasts (ECMWF) Interim Reanalysis (ERA-Interim/Land; Albergel et al., 2013; Balsamo et al., 2015). Gridded soil water content was provided in ERA-Interim/Land in four discretized layers until 2.89 m below ground, which is the soil depth we considered for the total soil moisture. Although some uncertainties exist at grid scale, the large-scale patterns in soil moisture from ERA-Interim/Land are consistent with other products (Rötzer et al., 2015), enabling us to use it to represent the large-scale spatial gradients in soil water moisture. The global gridded estimate of runoff data was obtained from the Global Runoff Data Centre (GRDC, http://www.grdc.sr.unh.edu/), …"

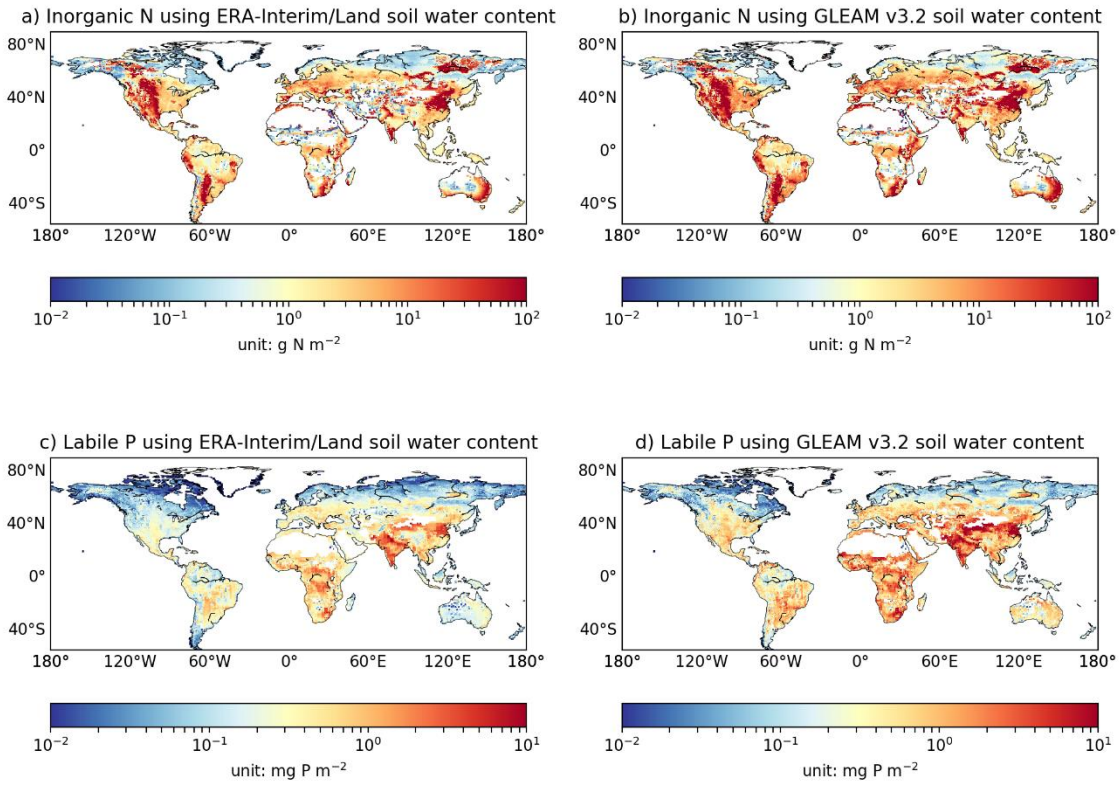

Figure R1 Comparison between inorganic N (a, c) and labile soil P (b, d) using different products of soil water content.

16. Page 8, lines 3-4: There is not much take-away here. I guess it is not too surprising that the number falls within the large range. But what is the range of your computed number? Is the ranage reduced or increased compared to CARDAMOM?

Response:

This section used input of C (NPP) to ecosystems and the residence time of C pools to compute a steady-state C cycle. The aim of this computation is not to improve CARDAMOM results, but to justify that the steady-state C cycle transformed from CARDAMOM is within the range of our best knowledge about the C cycle corresponding to non-steady state present-day conditions (provided by CARDAMOM). This section justifies the use of steady state transformation to derive the N and P cycle in GOLUM-CNP. For instance, the pool sizes of N and P in vegetation are computed as the product of C pool sizes (computed based on steady-state assumption) and the stoichiometry ratios of N:C and P:C based on a mass-balance approach.

We revised this section and highlighted the justification of using this steady-state C cycle rather than the original CARDAMOM in our GOLUM-CNP.

17. Page 8, lines 16-19: All of this seems like speculation, more appropriate for a "discussion" section than for "Results".

Response:

Thanks for the suggestion. We revise the manuscript:

- Sect. 4.1: "Table 2 shows the global C-pool sizes and main fluxes of the steady-state

C cycle transformed from CARDAMOM under the climate condition of 2001-2010, which are compared with the means and percentile ranges from the original non-steady-state CARDAMOM results. Although the steady-state C stocks do not exactly represent the C stocks at present day, the~~The~~ differences between the steady-state transformed pool sizes and the original non-steady-state CARDAMOM results were within 10% for most C pools and fluxes. The largest differences were for ~~the estimates of the~~ biomass (foliar, fine-root and wood) pools. The larger foliar and fine-root pools in the steady-state GOLUM-CNP model were due to adjustments done for grass dominated grid cells for which CARDAMOM provided some wood growth inconsistent with the biome distribution used in GOLUM-CNP. In these cases, we allocated wood growth from CARDAMOM into growth of fine root and foliage. ~~placing woody NPP into these two pools in the grassland grid cells~~. These pools in GOLUM-CNP, however, remained within the [5, 95th] percentile range of the original CARDAMOM values~~version~~. The pool size for global woody biomass was 37% smaller in the steady-state model (469 Pg) than the original CARDAMOM results but remained within its inter-quartile range (364-984 Pg). The differences between the gridded maps from original CARDAMOM and GOLUM-CNP are shown in Fig S1. The steady-state transformed C stocks in biomass, litter and SOM were within the 25th and 75th percentiles of the original CARDAMOM results at more than 90% of forest grid cells, indicating that our steady-state transformed C stocks are close to the actual C stocks at present day, given the large uncertainties in the state-of-the-art estimates. Due to the adjustment made for the grass dominated grid cells (see above), the C pools for grassland differ more strongly than forest-dominated area from the original CARDAMOM."

- Sect. 5.3 page 12 lines 35-37: "… Our results are a first step for evaluating global biogeochemical cycles. Although our steady-state C pool sizes (given the NPP and residence time at the condition of current climate) were within the [25, 75th] percentile range of the original non-steady-state CARDAMOM results (Fig. S1) at most grid cells, the biomass C stocks at 5%-10% of forest grid cells exceed the uncertainty range of CARDAMOM. In addition, independent remote-sensing estimates for 30 ℃N to 80 ℃N were 4.76 ±1.78 kg C m-2 for mean forest C density and 79.8 ±29.9 Pg C for total forest C (Thurner et al., 2014), which were lower than the GOLUM-CNP estimates (6.51 kg C m-2 for mean forest C density across pixels defined as forest in Fig. 2, and 181 Pg C for total forest C) for this region. This inconsistency was largely due to the fact that northern temperate and boreal forests may deviate substantially from their equilibrium for the current NPP (Pan et al., 2011), because of climate change and elevated CO2. Residual overestimation could be also due to the fact that biomass removal by harvesting and from disturbance other than fires was not explicitly constrained in CARDAMOM and thus not represented in GOLUM-CNP. A transient simulation of N and P cycling will be needed in future studies…"

18. Page 11, lines 4-18: There are also a fair amount of "results" in the "Discussion" section. Furthermore, these are some very ad hoc ways of making corrections when unexpected results

are obtained.

Response:

We think that these corrections are empirical because they are not directly a "data-driven" product like CARDAMOM (although CARDAMOM lacks strong constraints for the C allocation fractions, especially at high latitudes). This part of discussion aims to provide an example how to identify the major contributor of the uncertainties in the model and how to qualitatively estimate the impact of some biased input data on the results. In this context, we think that this part is more appropriate for the "Discussion" results rather than the "Results" section.

In order to clarify the logic of this section, we made the following revisions in the manuscript:

- Page 3 line 10-12: "… We first present the model structure (Sect. 2) and the data sets used to derive its outputs consisting of pools, fluxes and turnovers of C, N and P (Sect. 3). The model results and their sensitivities to the input observation-based data sets are then further analyzed in Sect. 4. In Sect. 5, we show examples of the application of this sensitivity analysis to identify the major differences in the results from our model framework and a synthesis of in situ measurements, and a qualitative example of how to compare the model and the independent data. These differences identify critical observations to reduce uncertainty in global C and nutrient cycling and highlight the future demand for model development, calibration and evaluation."
- Page 10 line 16: "… The data-driven estimates of steady-state global C, N and P cycles are the first that are fully consistent with a large set of global observation-based data sets, under the condition of current climate, deposition and CO2 concentration. The indicators for the coupling between nutrient and C cycling, which are emerging properties of GOLUM-CNP, are used to evaluate the capabilities of GOLUM-CNP to capture observed patterns among biomes. We found that there are some differences between our data-driven estimates and previous studies about the nutrient efficiencies at biome scales (Gill and Finzi, 2016) and the openness (Cleveland et al., 2013). In this section, we discussed the major uncertainties in our model and show how these uncertainties affect the computation of nutrient efficiencies and the openness (Sect. 5.1). Of note is that most of our discussions are for the C cycle (based on the sensitivity analysis, see below), and since CARDAMOM is the only data-driven C cycle to our knowledge, the modifications of the CARDAMOM dataset we made in this section are more qualitative and diagnostic rather than deterministic. Such an example highlights some important variables that should be investigated or considered in future data-driven products."

19. Page 11, lines 40-41: I do not see where this was shown.

Response:

We revise the sentence: "Our estimates of P openness were also larger than those ~~by~~of Cleveland et al. (2013), which ~~was~~ we attributed to the large differences in the estimates of P deposition between the two studies: Cleveland et al. (2013) used ~~values of~~ P deposition (0.26

Tg yr^{-1}) ~~reported by~~from Mahowald et al. (2008), which were ~~almost~~ an order of magnitude lower than ~~the~~ recent estimates from Wang et al. (2017) ~~that we~~ used in this study (5.8 Tg yr^{-1}), ~~arguably~~ because ~~of an underestimated~~ Wang et al. (2017) revised the contribution of anthropogenic P emissions and ~~not accounting for~~ P in particles with diameters >10 μm (Wang et al., 2015, 2017). …"

References:

Augusto, L., Achat, D. L., Jonard, M., Vidal, D. and Ringeval, B.: Soil parent material—A major driver of plant nutrient limitations in terrestrial ecosystems, Global Change Biology, 23(9), 3808–3824, doi:10.1111/gcb.13691, 2017.

Balsamo, G., Albergel, C., Beljaars, A., Boussetta, S., Brun, E., Cloke, H., Dee, D., Dutra, E., Muñoz-Sabater, J., Pappenberger, F. and others: ERA-Interim/Land: a global land surface reanalysis data set, Hydrol. Earth Syst. Sci., 19(1), 389–407, 2015.

Cleveland, C. C., Houlton, B. Z., Smith, W. K., Marklein, A. R., Reed, S. C., Parton, W., Grosso, S. J. D. and Running, S. W.: Patterns of new versus recycled primary production in the terrestrial biosphere, Proc. Natl. Acad. Sci., 110(31), 12733–12737, doi:10.1073/pnas.1302768110, 2013.

Cole, C. V., Innis, G. S. and Stewart, J. W. B.: Simulation of Phosphorus Cycling in Semiarid Grasslands, Ecology, 58(1), 1–15, doi:10.2307/1935104, 1977.

Gill, A. L. and Finzi, A. C.: Belowground carbon flux links biogeochemical cycles and resource-use efficiency at the global scale, Ecol Lett, 19(12), 1419–1428, doi:10.1111/ele.12690, 2016.

Goll, D. S., Brovkin, V., Parida, B. R., Reick, C. H., Kattge, J., Reich, P. B., van Bodegom, P. M. and Niinemets, Ü.: Nutrient limitation reduces land carbon uptake in simulations with a model of combined carbon, nitrogen and phosphorus cycling, Biogeosciences, 9, 3547–3569, doi:10.5194/bg-9-3547-2012, 2012.

Houlton, B. Z., Morford, S. L. and Dahlgren, R. A.: Convergent evidence for widespread rock nitrogen sources in Earth's surface environment, Science, 360(6384), 58–62, doi:10.1126/science.aan4399, 2018.

Jonard, M., Fürst, A., Verstraeten, A., Thimonier, A., Timmermann, V., Potočić, N., Waldner, P., Benham, S., Hansen, K., Merilä, P., Ponette, Q., Cruz, A. C. de la, Roskams, P., Nicolas, M., Croisé, L., Ingerslev, M., Matteucci, G., Decinti, B., Bascietto, M. and Rautio, P.: Tree mineral nutrition is deteriorating in Europe, Global Change Biology, 21(1), 418–430, doi:10.1111/gcb.12657, 2015.

Lawrence, D. M., Oleson, K. W., Flanner, M. G., Thornton, P. E., Swenson, S. C., Lawrence, P. J., Zeng, X., Yang, Z.-L., Levis, S., Sakaguchi, K., Bonan, G. B. and Slater, A. G.: Parameterization improvements and functional and structural advances in Version 4 of the Community Land Model, Journal of Advances in Modeling Earth Systems, 3(1), doi:10.1029/2011MS00045, 2011.

Luo, Y. and Weng, E.: Dynamic disequilibrium of the terrestrial carbon cycle under global change, Trends in Ecology & Evolution, 26(2), 96–104, 2011.

Martens, B., Miralles, D. G., Lievens, H., van der Schalie, R., de Jeu, R. A. M., Fernández-Prieto, D., Beck, H. E., Dorigo, W. A. and Verhoest, N. E. C.: GLEAM v3: satellite-based land evaporation and root-zone soil moisture, Geosci. Model Dev., 10(5), 1903–1925, doi:10.5194/gmd-10-1903-2017, 2017.

Mayor, J. R., Wright, S. J. and Turner, B. L.: Species-specific responses of foliar nutrients to long-term nitrogen and phosphorus additions in a lowland tropical forest, Journal of Ecology, 102(1), 36–44, doi:10.1111/1365-2745.12190, 2014.

Reed, S. C., Cleveland, C. C. and Townsend, A. R.: Functional Ecology of Free-Living Nitrogen Fixation: A Contemporary Perspective, Annu. Rev. Ecol. Evol. Syst., 42(1), 489–512, doi:10.1146/annurev-ecolsys-102710-145034, 2011.

Sardans, J. and Peñuelas, J.: The role of plants in the effects of global change on nutrient availability and stoichiometry in the plant-soil system, Plant Physiology, pp.112.208785, doi:10.1104/pp.112.208785, 2012.

Sardans, J., Rivas-Ubach, A. and Peñuelas, J.: The C:N:P stoichiometry of organisms and ecosystems in a changing world: A review and perspectives, Perspectives in Plant Ecology, Evolution and Systematics, 14(1), 33–47, doi:10.1016/j.ppees.2011.08.002, 2012.

Sardans, J., Alonso, R., Janssens, I. A., Carnicer, J., Vereseglou, S., Rillig, M. C., Fernández‐Martí

nez, M., Sanders, T. G. M. and Peñuelas, J.: Foliar and soil concentrations and stoichiometry of nitrogen and phosphorous across European Pinus sylvestris forests: relationships with climate, N deposition and tree growth, Functional Ecology, 30(5), 676–689, doi:10.1111/1365-2435.12541, 2016.

Sardans, J., Grau, O., Chen, H. Y. H., Janssens, I. A., Ciais, P., Piao, S. and Peñuelas, J.: Changes in nutrient concentrations of leaves and roots in response to global change factors, Global Change Biology, 23(9), 3849–3856, doi:10.1111/gcb.13721, 2017.

Sistla, S. A. and Schimel, J. P.: Stoichiometric flexibility as a regulator of carbon and nutrient cycling in terrestrial ecosystems under change, New Phytologist, 196(1), 68–78, doi:10.1111/j.1469-8137.2012.04234.x, 2012.

Thornton, P. E., Lamarque, J.-F., Rosenbloom, N. A. and Mahowald, N. M.: Influence of carbon-nitrogen cycle coupling on land model response to CO2 fertilization and climate variability, Glob. Biogeochem. Cycles, 21(4), GB4018, doi:10.1029/2006GB002868, 2007.

Wang, R., Goll, D., Balkanski, Y., Hauglustaine, D., Boucher, O., Ciais, P., Janssens, I., Penuelas, J., Guenet, B., Sardans, J. and others: Global forest carbon uptake due to nitrogen and phosphorus deposition from 1850 to 2100, Glob. Change Biol., 2017.

Wang, Y.-P., Houlton, B. Z. and Field, C. B.: A model of biogeochemical cycles of carbon, nitrogen, and phosphorus including symbiotic nitrogen fixation and phosphatase production, Global Biogeochem. Cycles, 21(1), GB1018, doi:10.1029/2006GB002797, 2007.

Wang, Y. P., Law, R. M. and Pak, B.: A global model of carbon, nitrogen and phosphorus cycles for the terrestrial biosphere, Biogeosciences, 7(7), 2010.

Xu-Ri and Prentice, I. C.: Terrestrial nitrogen cycle simulation with a dynamic global vegetation model, Glob. Change Biol., 14(8), 1745–1764, doi:10.1111/j.1365-2486.2008.01625.x, 2008.

Yang, X., Wittig, V., Jain, A. K. and Post, W.: Integration of nitrogen cycle dynamics into the Integrated Science Assessment Model for the study of terrestrial ecosystem responses to global change, Glob. Biogeochem. Cycles, 23(4), 2009.

Yang, X. and Post, W. M.: Phosphorus transformations as a function of pedogenesis: A synthesis of soil phosphorus data using Hedley fractionation method, Biogeosciences, 8(10), 2011.

Yang, Y., Fang, J., Ji, C., Datta, A., Li, P., Ma, W., Mohammat, A., Shen, H., Hu, H., Knapp, B. O. and Smith, P.: Stoichiometric shifts in surface soils over broad geographical scales: evidence from China's grasslands, Global Ecology and Biogeography, 23(8), 947–955, doi:10.1111/geb.12175, 2014b.

Yuan, Z. Y. and Chen, H. Y. H.: Decoupling of nitrogen and phosphorus in terrestrial plants associated with global changes, Nature Climate Change, 5(5), 465–469, doi:10.1038/nclimate2549, 2015.

Zaehle, S., Friend, A. D., Friedlingstein, P., Dentener, F., Peylin, P. and Schulz, M.: Carbon and nitrogen cycle dynamics in the O-CN land surface model: 2. Role of the nitrogen cycle in the historical terrestrial carbon balance, Global Biogeochemical Cycles, 24(1), doi:10.1029/2009GB003522, 2010.

Zaehle, S.: Terrestrial nitrogen–carbon cycle interactions at the global scale, Philos. Trans. R. Soc. Lond. B Biol. Sci., 368(1621), 20130125, doi:10.1098/rstb.2013.0125, 2013.

GOLUM-CNP v1.0: a data-driven modeling of carbon, nitrogen and phosphorus cycles in major terrestrial biomes

Yilong Wang[1,*], Philippe Ciais[1], Daniel Goll[1], Yuanyuan Huang[1], Yiqi Luo[2,3,4], Ying-Ping Wang[5], A. Anthony Bloom[6], Grégoire Broquet[1], Jens Hartmann[7], Shushi Peng[8], Josep Penuelas[9,10], Shilong Piao[8,11], Jordi Sardans[9,10], Benjamin D. Stocker[~~12,13~~10], Rong ~~Wang[14]~~Wang[12], Sönke ~~Zaehle[15]~~Zaehle[13], Sophie Zechmeister-~~Boltenstern[16]~~Boltenstern[14]

[1] Laboratoire des Sciences du Climat et de l'Environnement, CEA-CNRS-UVSQ- Université Paris Saclay, Gif-sur-Yvette, France

[2] Center for Ecosystem Science and Society, Northern Arizona University, Flagstaff, AZ, USA

[3] Department of Earth System Science, Tsinghua University, Beijing, China

[4] Department of Microbiology and Plant Biology, University of Oklahoma, Norman, OK, USA

[5] CSIRO Oceans and Atmosphere, PMB #1, Aspendale, Victoria, Australia

[6] Jet Propulsion Laboratory, California Institute of Technology, Pasadena, CA, USA

[7] Institute for Geology, KlimaCampus, Universität Hamburg, Bundesstrasse 55, D-20146 Hamburg, Germany

[8] Sino-French Institute for Earth System Science, College of Urban and Environmental Sciences, Peking University, Beijing, China

[9] CSIC, Global Ecology Unit CREAF-CSIC-UAB, Bellaterra, Catalonia, Spain

[10] CREAF, Cerdanyola del Vallès, Catalonia, Spain

[11] Institute of Tibetan Plateau Research, Chinese Academy of Sciences, Beijing, China

~~[12] AXA Chair of Biosphere and Climate Impacts, Grand Challenges in Ecosystems and the Environment and Grantham Institute – Climate Change and the Environment, Department of Life Sciences, Imperial College London, Silwood Park Campus, Ascot, UK~~

~~[13] Institute for Atmospheric and Climate Science, ETH Zürich, Universitätstrasse 16, Zürich, Switzerland~~

~~[14]~~[12] Department of Global Ecology, Carnegie Institution for Science, Stanford, CA, USA

~~[15]~~[13] Max Planck Institute for Biogeochemistry, Jena, Germany

~~[16]~~[14] University of Natural Resources and Life Sciences Vienna, Institute of Soil Research, Department of Forest and Soil Sciences, Vienna, Austria

**Corresponding to:* Yilong Wang[1] (yilong.wang@lsce.ipsl.fr)

Abstract. Global terrestrial nitrogen (N) and phosphorus (P) cycles are coupled to the global carbon (C) cycle for net primary production (NPP), plant C allocation and decomposition of soil organic matter, but N and P have distinct pathways of inputs and losses. Current C-nutrient models exhibit large uncertainties in their estimates of pool sizes, fluxes and turnover rates of nutrients, due to a lack of consistent global data for evaluating the models. In this study, we present a new model-data fusion framework called Global Observation-based Land-ecosystems Utilization Model of Carbon, Nitrogen and Phosphorus (GOLUM-CNP) that combines the CARbon DAta MOdel fraMework (CARDAMOM) data-constrained C-cycle analysis with spatially explicit data-driven estimates of N and P inputs and losses and with observed stoichiometric ratios. We calculated the steady-state N- and P-pool sizes and fluxes globally for large biomes. Our study showed that new N inputs from biological fixation and deposition supplied >20% of total plant uptake in most forest ecosystems but accounted for smaller fractions in boreal forests and grasslands. New P inputs from atmospheric deposition and rock weathering supplied a much smaller fraction of total plant uptake than new N inputs, indicating the importance of internal P recycling within ecosystems to support plant growth~~that the terrestrial C sink may ultimately be constrained by low P~~. Nutrient-use efficiency, defined as the ratio of gross primary production (GPP) to plant nutrient uptake, ~~can be~~were diagnosed from our model results and compared between biomes. Tropical forests had the lowest N-use efficiency and the highest P-use efficiency of the

forest biomes. An analysis of sensitivity and uncertainty indicated that the NPP-allocation fractions to leaves, roots and wood contributed the most to the uncertainties in the estimates of nutrient-use efficiencies. Correcting for biases in NPP-allocation fractions produced more plausible gradients of N- and P-use efficiencies from tropical to boreal ecosystems and highlighted the critical role of accurate measurements of C allocation for understanding the N and P cycles.

1 Introduction

Nitrogen (N) and phosphorus (P) cycling are tightly coupled with the global carbon (C) cycle (Cleveland et al., 2013; Elser et al., 2007; Gruber and Galloway, 2008; Ver et al., 1999; Turner et al., 2018) in terrestrial ecosystems. N and P availability affects vegetation productivity, growth and other processes ~~N and P uptake by plants control productivity and growth~~ (Norby et al., 2010; Sutton et al., 2008; Vitousek and Howarth, 1991). N and P also affect soil C by nutrient controls on the mineralization of litter and soil organic matter (Gärdenäs et al., 2011; Melillo et al., 2011). Global vegetation models suggest that the ~~The~~ coupling between the C, N and P cycles ~~affects~~ is among the major factors determining ~~the~~ projected changes in the terrestrial C ~~cycle~~ balance under scenarios of climate change and rising atmospheric CO_2, because additional productivity will only be realized if plants can increase their uptake or recycling of nutrients (Hungate et al., 2003; Sun et al., 2017; Wang and Houlton, 2009; Zaehle et al., 2015). ~~The e~~Estimates of the magnitudes of these responses of ecosystems in the future, however, are highly uncertain (Peñuelas et al., 2013; Wieder et al., 2015).

Nutrients are important for understanding the current perturbation and future projections of the global C cycle, so several ~~land surface models~~ Dynamic Global Vegetation Models (DGVMs) ~~(LSMs)~~ have incorporated terrestrial N cycling (Goll et al., 2012; Medvigy et al., 2009; Parton et al., 2010; Thornton et al., 2007; Wang et al., 2001, 2010; Weng and Luo, 2008; Xu-Ri and Prentice, 2008; Yang et al., 2009; Zaehle et al., 2014; Zaehle and Friend, 2010). Fewer models have incorporated the cycling of P and its interactions with C dynamics (Goll et al., 2012, 2017a; Wang et al., 2010). Many of the underlying processes are not fully understood, and comprehensive data for evaluation are lacking to constrain the representation of some key processes (Zaehle et al., 2014), so model structure, the processes included and the prescribed parameters differ widely among ~~LSMs~~ DGVMs (Zaehle and Dalmonech, 2011). For example, some models assume constant stoichiometry (N:C and P:C ratios) in plant tissues (Thornton et al., 2007; Weng and Luo, 2008), ~~but~~ while others have a flexible stoichiometry (Wang et al., 2010; Xu-Ri and Prentice, 2008; Yang et al., 2009; Zaehle and Friend, 2010). For the N cycle, for instance, some ~~Some~~ models do not include losses of gaseous N ~~due to~~from denitrification (Medvigy et al., 2009), some use the "hole-in-the-pipe" approach to simulate the denitrification flux (Thornton et al., 2007; Wang et al., 2010), assuming it is proportional to net N mineralization, ~~and~~ while others calculate this flux as a function of soil N-pool size and soil conditions (temperature, moisture, pH, etc.) (Parton et al., 2010; Xu-Ri and Prentice, 2008; Zaehle and Friend, 2010). For the P cycle, for instance, Jahnke (2000) estimated that the global total amount of soil P was 200 Pg and that the P contained in plants was 3 Pg, based on empirical P content of soils (0.1%) and soil thickness (60 cm). These estimates were questioned by recent studies from Wang et al. (2010) and Goll et al. (2012), who estimated that P in plants ranged between 0.23 and 0.39 Pg and that P in soil was only 26.5 Pg based on P:C ratios derived from more comprehensive stoichiometric data sets. Furthermore, ~~these models~~terrestrial ecosystem models are usually only evaluated for specific ecosystems or at a limited number of sites (Goll et al., 2017a; Yang et al., 2014a). The application of these models for simulations with global coverage is thus highly uncertain (Goll et al., 2012; Wang et al., 2010; Zhang et al., 2011). ~~Jahnke (2000) estimated that the global total amount of soil P was 200 Pg and that the P contained in plants was 3 Pg. These estimates, though, were questioned by Wang et al. (2010) and Goll et al. (2012), who estimated that P in plants ranged between 0.23 and 0.39 Pg and that P in soil was only 26.5 Pg.~~

A growing number of data sets in recent decades have addressed many aspects of the nutrient cycles and their interactions with C dynamics. For example, Zechmeister-Boltenstern et al. (2015) synthesized the stoichiometry in different ecosystem compartments and highlighted the latitudinal gradients of plant, litter and soil stoichiometry. Liu et al. (2017)

evaluated soil net N mineralization among different ecosystems at the global scale and found that net N mineralization decreased with increasing latitude. They also found that the N mineralization at higher latitudes ~~are~~ is more sensitive to temperature changes than at lower latitudes, indicating potential alleviation of N limitation for plants' productivity at boreal regions under global warming. Yang et al. (2013) provided spatially explicit estimates of different forms of soil P globally and thus made it possible to assess the P content that is available for plant uptake. These data help to improve the understanding of the global terrestrial biogeochemical cycles across large climatic and ecological gradients and can in principle be combined to provide an integrated analysis of terrestrial C, N and P ~~dynamics~~cycles. Estimates of C, N and P cycles consistent with all these data sets, however, have not yet been successfully provided due to the difficulties in combining these data sets with different uncertainties and inconsistent spatial/temporal representations.

We present a new global data-driven diagnostic of C, N and P pools and fluxes, called GOLUM-CNP (~~modeling framework called~~ Global Observation-based Land-ecosystems Utilization Model of Carbon, Nitrogen and Phosphorus) which is based on the assumption that these cycles are equilibrated with present day conditions (see below for limitations of this approach). The goals of this study are to: 1) establish a global data-driven diagnostics of C, N and P fluxes and pools in order to compare nutrient use efficiencies, nutrient turnover rates and other relevant indicators across biomes; and 2) provide a new dataset that can be used to evaluate the results of global terrestrial biosphere models with consistent state of C, N and P cycles. ~~(GOLUM-CNP) for providing observation-based estimates of C, N and P pools and fluxes~~. In GOLUM-CNP, ~~We calculated~~ the C, N and P cycles were estimated for different biomes ~~for an~~ assum~~inged~~ steady state ~~corresponding to~~with present-day input of carbon (NPP), nitrogen (N deposition and N fixation) and phosphorus (P deposition and release from rock weathering)~~conditions~~ (see Sect. 3.2). The reason for this steady-state computation lies in the fact that only few global long-term observations associated with N and P cycles are available and are insufficient to constrain a transient simulation under the model framework. For example, field-scale manipulation experiments have shown that warming, elevated atmospheric CO_2, and N and P fertilization can drive changes in stoichiometry and nutrient resorptions (Sistla and Schimel, 2012; Sardans et al., 2012; Sardans and Peñuelas, 2012; Mayor et al., 2014; Yang et al., 2014b; Yuan and Chen, 2015; Sardans et al., 2016; Sardans et al., 2017) in terrestrial ecosystems, but these data are insufficient to infer these changes in terrestrial ecosystems during the past decades. As more data becomes available, the model framework can be adjusted to simulate a transient present day state. Although, the steady-state assumption hampers the comparison of stocks with present day observations, a direct comparison with simulated steady states of DGVM is possible as these model can simulate the steady-state for present day conditions.

Starting from a CARbon DAta MOdel fraMework (CARDAMOM) data-constrained analysis of the terrestrial C cycle (Bloom et al., 2016), which is based on the Data Assimilation Linked Ecosystem Carbon Model version two (DALEC2, Bloom and Williams, 2015; Williams et al., 2005) and on observations of biomass, soil C, leaf area index (LAI) and fire emissions, we incorporated observed stoichiometric ratios (C:N:P) in each pool, N and P external input fluxes, transformations and losses in ecosystems and ~~losses and observation-based information for~~ the fraction of gaseous losses of N to total (gaseous and leaching) losses of N from a global dataset of ^{15}N measurements in soils. Although the diagnostics is presented for steady state, the methods used to compute fluxes and pools are generic and could be extended to non-steady state (see Sect. 2 and equations in Appendix A-C) when more data will become available in the future (see Sect. 5.3).

We first present the model structure (Sect. 2) and the data sets used to derive its outputs consisting of pools, fluxes and turnovers of C, N and P (Sect. 3). The model results and their sensitivities to the input observation-based data sets are then further analyzed in Sect. 4. In Sect. 5, we show examples of the application of this sensitivity analysis to identify the major differences in the results from our model framework and a synthesis of *in situ* measurements, and a qualitative example of how to compare the model and the independent data. These differences identify critical observations to reduce uncertainty in global C and nutrient cycling and highlight the future demand for model development, calibration and evaluation. ~~Finally, we discuss the potential applications of the framework for model development, calibration and evaluation.~~

2 Model structure

~~The~~ GOLUM-CNP ~~framework~~ describes the C, N and P cycles in natural (i.e. non-agricultural) terrestrial ecosystems (Fig. 1). ~~We follow the model structure of DALEC2 and CARDAMOM for the C cycle.~~ We used the same C pools and fluxes as in the CARDAMOM diagnostic (see Sect. 2.1 for details) to describe the C cycle and we computed associated N and P pools and fluxes. Biomass is divided into three pools: foliage, fine roots and wood. The wood pool includes woody stems, branches and coarse roots. The litter pool in Fig. 1 corresponds to fine litter from leaves and fine roots. Soil organic matter (SOM) receives C from fine litter and woody biomass. Two additional pools not present in CARDAMOM are added, representing soil inorganic N and labile soil P. These ~~two~~ inorganic N and labile soil P pools are assumed to represent nutrients accessible by plants (see Sect. 2.1 and 2.2). Of note is that these inorganic N and labile soil P pools represent an integration of various forms of N and P. For example, P has various forms in the soil and can be transformed between those forms (Wang et al., 2007; Yang and Post, 2011). Some forms of organic P (e.g. bicarbonate Po in Hedley method, Yang and Post, 2011) can easily be mineralized and thus were implicitly included in our labile soil P pool. Other forms of P that are not easily accessible to plants are referred to as "occluded P" and labile soil P can become occluded P (Wang et al., 2010; Goll et al., 2017a). Fluxes connecting the pools are described by the differential equations given in Appendices A-C. An overview of the C, N and P cycles and their interactions are presented in the following sections. A full list of the symbols and their definitions is given in Table 1.

2.1 C cycle

The C cycle in the GOLUM-CNP model ~~structure~~ is based on the DALEC2 model (Bloom et al., 2016; Bloom and Williams, 2015). We used a similar structure to define the C pools of GOLUM-CNP but grouped the DALEC2 foliar and labile vegetation C pools into a single foliar pool (Fig. 1). Net primary production (NPP) is allocated to the three biomass pools. The outgoing fluxes from biomass pools include losses from fire, the transfer of foliage and root detritus to litter and the transfer of wood debris directly to the SOM pool. The outgoing fluxes from litter include losses from fire and decomposition. A fraction of decomposed litter is respired and returned to the atmosphere as CO_2, the remaining fraction being converted to SOM. The SOM pool loses C by fire and decomposition. Differential equations governing the dynamics of C pools are given in Appendix A.

2.2 N cycle

The N cycle in GOLUM-CNP is coupled to the C cycle: the pool sizes of N are ~~decided~~ determined by the C-pool sizes and their respective N:C ratios; the N fluxes from different pools are determined by the N-pool sizes and corresponding turnover rates. The N cycle includes a specific soil inorganic-N pool in addition to the five pools of the C cycle. The inputs of N to ecosystems include atmospheric N deposition and N fixation (N_d+N_{fix} in Fig. 1), both of which are assumed to enter the inorganic-N pool. The total N-fixation flux in this study includes both symbiotic and asymbiotic fixation (see Sect. 3.1), separately estimated from a previous study (see Sect. 3.1). We~~, but we~~ do not separate the two fixation processes and assume that they together contribute to the inorganic-N pool, although these two pathways of N fixation are differed in terms of the relationships between N_2-fixing microorganisms and plants~~even though N fixation is controlled by plants~~. We did not consider the flux of N mobilized from near-surface rocks, although a recent paper by Houlton et al. (2018) pointed out this flux may be an important N sources in montane and high-latitude ecosystems. N uptake (F_N) by plants is assumed to be solely from the inorganic-N pool. Organic N is an important N supply for plants (Näsholm et al., 2009)~~, especially~~ in boreal-forest and tundra ecosystems (Schimel and Bennett, 2004; Schimel and Chapin, 1996; Zhu and Zhuang, 2013), but the quantitative importance of this process is still unknown for other ecosystems globally. We thus ignored the uptake of organic soil N. N uptake by plants from the inorganic-N pool is modeled from the N:C ratio of NPP allocated to biomass pools minus the resorbed N. In the real world, N is only resorbed at the end of the growing season or leaf lifespan and then stored

in plant organs and remobilized during the next growing season. Here, because our model does not have a sub-annual time step, rates of resorption described by a resorption coefficient (Appendix B) are assumed to be constant over time. We also assumed that N is not resorbed from fine roots or wood, because evidence for this process is inconclusive (Gordon and Jackson, 2000; Zechmeister-Boltenstern et al., 2015). N mineralization is modeled along with litter and SOM decomposition. N immobilization due to the uptake of inorganic soil N by soil organisms is modeled to match the higher N:C ratio of the SOM pool than its donor (wood and litter) pools. ~~The output~~Loss of N from ecosystems occurs ~~from~~ through fire, denitrification and leaching. The N lost due to fire is assumed to be emitted only in gaseous form, because the proportion of N retained in the residual ash is very small ~~during a fire~~ (Niemeyer et al., 2005; Qian et al., 2009). We consider the gaseous loss of inorganic N from denitrification but ignore the volatilization of N in the form of NH_4^+ ~~N~~. This flux usually occurs at a soil pH >8 (Freney et al., 1983) or after application of N fertilizers (Yang et al., 2009), and NH_3 emissions from soils under non-agricultural~~natural~~ vegetation are relatively small globally (5 Tg N y^{-1}, Bouwman et al., 1997; Houlton et al., 2015), representing <5% of total gaseous loss, so the omission of NH_4^+ N volatilization will not introduce large biases in our model for most regions. The dynamics of N in the pools are summarized by the differential equations in Appendix B.

2.3 P cycle

The P cycle, like the N cycle, is also coupled to the C cycle; the dynamics of P in the pools are ~~depicted~~ described by the differential equations in Appendix C. The external inputs of P to ecosystems include atmospheric P deposition and P released from P-bearing minerals by chemical weathering (P_d+P_w in Fig. 1). P from deposition and rock weathering enters the soil inorganic-P pool. The structure of the P cycle is the same as for the N cycle described above for foliar-P resorption, P released from the decomposition of litter and SOM and the immobilization of inorganic soil P by soil organisms. Inorganic P, unlike inorganic N, can be sorbed onto/into soil particles and subsequently become occluded. This form is assumed to be unavailable to plants. We modeled ~~strong sorption~~the flux from the labile soil P to occluded P with a constant rate. ~~Output~~ Loss pathways of P ~~from the ecosystem~~ include fire, leaching and conversion to ~~strongly sorbed and~~ occluded P. Notably, not all P mobilized by fire is emitted in gaseous form, ~~and some of the P~~but is partly retained in the residual ash (Niemeyer et al., 2005; Qian et al., 2009). We used a constant fraction of 75% (Niemeyer et al., 2005; Qian et al., 2009) to model the P retained in the residual ash during a fire, and this fraction of P enters the ~~inorganic~~ labile soil P pool.

3 Methods

3.1 Input data sets

All parameters used as inputs for the calibration of GOLUM-CNP are listed in Table 1. A steady state was assumed to infer remaining ~~The~~ variables ~~(inferred assuming a steady state are~~ also listed in Table 1). The estimates of fluxes and C-pool sizes were based on mass balances, and the estimates of N- and P-pool sizes were derived from the C-pool size and stoichiometric data (see below and Appendix E). We used the C fluxes and turnover times of C pools derived from CARDAMOM for the C cycle (Bloom et al., 2016), which offered a data-consistent analysis of terrestrial C cycling on a global 1 °×1 ° grid for 2001-2010 by optimizing the DALEC2 model parameters to match the state and process variables with the global observations of MODIS LAI (Myneni et al., 2015), soil C (Hiederer and K öchy, 2011), burned area (Giglio et al., 2013) and tropical biomass (Saatchi et al., 2011). Although the CARDAMOM data-driven analysis only reported the C pools and fluxes, the impacts of N and P on the C cycle have been implicitly reflected in CARDAMOM through the constraints by some of the observations. For example, the availability of N and/or P limits the growth of vegetation and thus the LAI observed (Klodd et al., 2016; Reich et al., 2010); the N and P contents in soil control the decomposition of soil C and thus the soil C pool observed (Manzoni et al., 2010). In this sense, it is appropriate to use C cycle from CARDAMOM as inputs to estimate the pool and fluxes of N and P.~~CARDAMOM as a basis for the GOLUM-CNP data-driven modeling of C, N and~~

~~P cycles.~~

Different indices have been used to describe nutrient cycling from different perspectives (soil, individual plant, vegetation, ecosystem, etc) (Augusto et al., 2017; Cleveland et al., 2013; Gill and Finzi, 2016). In this study, we focused on the openness, nutrient use efficiencies and the residence time (Sect. 3.2) which are defined at ecosystem scale and thus correspond to the scale at which DGVMs are typically defined. For the presentation of results, we distinguish seven biomes~~The current synthesis of site data for pool stoichiometry was mainly aggregated at the scale of the biomes, so we divided the global vegetation into seven biomes, following Zechmeister-Boltenstern et al. (2015)~~: tropical rainforests (TRF), temperate deciduous forests (TEDF), temperate coniferous forests (TECF), boreal coniferous forests (BOCF), tundra (TUN), tropical/C4 grasslands (TRG) and temperate/C3 grasslands (TEG). Note that similar empirical land-cover maps have been also used in previous studies to simulate C, N and P cycles (Cleveland et al., 2013; Wang et al., 2010). We applied observed biome-specific ~~used observed biome-averaged values of the~~ N:C ratios ~~of~~ for each pool ~~for the seven biomes~~ from the synthesis by Zechmeister-Boltenstern et al. (2015).

We used the spatially explicit estimates of N deposition (Wang et al., 2017) for 2001-2010 (Fig. S2a), which were evaluated with globally distributed *in-situ* measurements. The spatially explicit estimate for N fixation (Fig. S2b) was taken from the CABLE model simulation for 2001-2010 (Peng et al., submitted) with a N fixation model developed by Wang et al. (2007). The simulation result matches the relative abundance of N_2-fixing legumes in different ecosystems. Globally, the N fixation is 116 Tg N yr^{-1} and is within the range of empirical estimates (100-290 Tg N yr^{-1}; Cleveland et al., 1999; Galloway et al., 2004), but larger than the estimate of 44 Tg N yr^{-1} by Vitousek et al. (2013) for pre-industrial conditions. The large range (44-290 TgN yr^{-1}) in the estimates of nitrogen fixation reflects both a paucity of measurements of N fixation, as well as incomplete understanding of the biophysical and biochemical controls on N fixation. And to our knowledge, CABLE simulation is the only product that has spatially explicit and processed-based estimates of N fixation, and is therefore used in this study.~~We used the spatially explicit estimates of N deposition (Wang et al., 2017) and N fixation (both symbiotic and asymbiotic) (Peng et al., submitted) for 2001-2010 for the N inputs, which were constrained by the observation-based estimates of C:N ratios of the various plant pools, soil microbial biomass and organic matter under present conditions.~~ The resorption coefficients of leaves for the seven biomes were derived from the N:C ratios of leaves and leaf litter reported by Zechmeister-Boltenstern et al. (2015). The rate of loss of inorganic N by leaching was determined from data for total soil moisture and runoff (Eq. B7). The spatially explicit estimate of total soil moisture was derived from the European Centre for Medium-Range Weather Forecasts (ECMWF) Interim Reanalysis (ERA-Interim/Land; Albergel et al., 2013; Balsamo et al., 2015). Gridded soil water content was provided in ERA-Interim/Land in four discretized layers until 2.89 m below ground, which is the soil depth we considered for the total soil moisture. Although some uncertainties exist at grid scale, the large-scale patterns in soil moisture from ERA-Interim/Land are consistent with other products (Rötzer et al., 2015), enabling us to use it to represent the large-scale spatial gradients in soil water moisture. The global gridded estimate of runoff data was obtained from the Global Runoff Data Centre (GRDC, http://www.grdc.sr.unh.edu/), which is constrained by observed river discharges from 663 stations globally. We used observation-based estimates of the fraction of N lost by denitrification to the total inorganic-N loss (denitrification + leaching) pathways (Goll et al., 2017b) to calibrate the denitrification-loss flux. This fraction of denitrification loss (f_{denit}) was derived using a process-based statistical model fitted to global soil $\delta^{15}N$ data sets, based on the distinct ^{15}N fractionation effect of denitrification versus loss from leaching (Bai et al., 2012; Houlton and Bai, 2009).

We constrained the P cycle using ~~the~~ spatially explicit estimates by Wang et al. (2017) for P deposition for 2001-2010 (Fig. S3a). Spatially explicit estimates of P input from rock weathering (Fig. S3b) were derived from data for river discharge and the chemical composition of minerals by Hartmann et al. (2014). The P:C ratios and resorption coefficients for the seven biomes were obtained from Zechmeister-Boltenstern et al. (2015). Only a fraction of total inorganic P can be lost by leaching, and this fraction of dissolved inorganic P in total labile P was derived based on the observations of Hedley soil P fractions as

the resin-extractible P divided by total labile P reported by Yang and Post (2011) for the twelve USDA soil orders. The constant rate at which inorganic P becomes strongly sorbed (f_{sorb}, Eq. C6) was fixed at 0.04 y^{-1} (Goll et al., 2017a).

Zechmeister-Boltenstern et al. (2015) only reported the stoichiometric ratios and the N and P resorption coefficients for seven large non-agricultural~~natural~~ biomes, but other input variables were grid-based products. A land-cover map was used to aggregate the grid-based C-cycle variables from Bloom et al. (2016) into the biomes used by Zechmeister-Boltenstern et al. (2015). The land-cover map was derived from the dominant land-cover type for each grid cell for the globe, excluding croplands, from the land-cover map of the Climate Change Initiative (LC_CCI) established by the European Space Agency (ESA) (Bontemps et al., 2013) at 0.25 °×0.25 ° resolution. Specifically, we used the 2010 map to classify all grid cells into one of the seven non-agricultural~~natural~~ biomes of Zechmeister-Boltenstern et al. (2015) (Fig. 2), following the methodology presented by Poulter et al. (2015).

3.2 Model integration and output diagnostics

We applied the model framework described in Sect. 2 to derive a data-driven estimate of steady-state C, N and P cycling. A steady state indicates that annual mean input fluxes for all pools are assumed to be balanced by annual mean outgoing fluxes, with the annual mean outgoing fluxes from organic pools calculated as the quotient of the pool sizes to the corresponding turnover times. Assuming that all pool sizes were in a steady state, the left side of the equations in Appendices A-C (Eqs. A1-A5, B1-B6 and C1-C6) ~~were~~ are all equal to zero. Adding the constraints in Appendix D (Eqs. D1-D11), we derived a system with 28 equations and 28 unknown variables (Table 1), thereby defining all~~so the estimates of the~~ unknowns in GOLUM-CNP ~~were all well constrained~~. The unknown variables were solved by applying the 33 global spatially explicit observation-based estimates listed in Table 1 in these equations (Appendix E). The set of equations of the GOLUM-CNP model was solved for each 0.25 °×0.25 ° grid cell using biome-mean N:C and P:C stoichiometric ratios, grid-cell specific values of C variables from Bloom et al. (2016) and the gridded external N- and P-input and -output fields described above. In this computation, some processes were~~are~~ only solved by mass balance and the steady-state assumption~~s~~ instead of explicitly being calibrated. For example, we did not explicitly simulate various pathways of N and P mineralization and immobilization. The N and P mineralization fluxes are computed as the product of the decomposition of C in litter and SOM and their respective stoichiometries, and N and P immobilization fluxes are computed by mass balance to match the higher N:C and P:C ratios in the SOM pool ~~than~~ compared to the ratios in inputs to SOM from wood and litter decomposition. ~~Similar computations have been widely used in previous studies.~~ For instance, N and P mineralization were computed as the difference between nutrient demand of vegetation and the sum of external inputs and resorption in Cleveland et al. (2013, Eqs. S5 and S6), assuming that the nutrients available to plants in soil do not change significantly at current stage. Some variables were computed by mass balance and do not rely on steady state assumption, e.g. the uptake of N (F_N) and P (F_P) by plants (Table 1). Such computations based on mass balance and steady-state assumptions allow us to have a diagnostic modelling framework, but at the same time capture observations of carbon fluxes, pools and pool stoichiometries.

The inputs of the C cycle from the original CARDAMOM dataset were provided as probability distributions, while other datasets were provided only as mean values. In this study, we compute the GOLUM-CNP using the mean values of all the input datasets to represent the mean behaviour of the C, N and P cycling.

We present the C, N and P pools and the fluxes between them for each biome. We also aggregated the results at the global scale and compared them with previous studies. We calculated some ecologically relevant quantities from the GOLUM-CNP output. Following Cleveland et al. (2013), we defined the *openness* of N and P cycles as NO and PO that were calculated as the ratio of nutrients inputs (I_x, $X \in \{N,P\}$, taken as the sum of deposition (N_d) and biological fixation (N_{fix}) for N and as the sum of deposition (P_d) and release from rock weathering (P_w) for P, over the amount of nutrients in

production, taken as the sum of uptake from inorganic N or labile soil P pools (F_x, $X \in \{N,P\}$) and resorbed nutrients (RSB_x, $X \in \{N,P\}$), ~~percentage of the total plant uptake of nutrients (I_x, $X \in \{N,P\}$) from new nutrient inputs. Here, new nutrient inputs included deposition (N_d) and biological fixation (N_{fix}) for N and deposition (P_d) and rock weathering (P_w) for P, and the total uptake of nutrients by vegetation included the uptake from inorganic N or P pools (F_x, $X \in \{N,P\}$) and the resorbed nutrients (RSB_x, $X \in \{N,P\}$),~~ leading to:

$$XO = \frac{I_x}{F_x + RSB_x} \quad (1)$$

The mean residence time of N and P for the entire ecosystem ($\tau_{X,eco}$, $X \in \{N,P\}$) was defined as the ratio of total modeled pool mass (including plant, litter, SOM and inorganic pools) to all outgoing fluxes. The sum of all steady-state outgoing fluxes ~~equaled~~ was set equal to the sum of external input fluxes, so we calculated the mean residence time of N and P by:

$$\tau_{N,eco} = \frac{\sum_{i=1}^{5} N_i + N_{inorg}}{N_d + N_{fix}}$$
$$\tau_{P,eco} = \frac{\sum_{i=1}^{5} P_i + P_{inorg}}{P_d + P_w} \quad (2)$$

The *nutrient-use efficiencies* (NUE and PUE) were defined by:

$$XUE = \frac{GPP}{Fx} = \frac{NPP / f_{NPP}}{Fx} \quad (3)$$

where F_x ($X \in \{N,P\}$) is the annual uptake of inorganic soil N or P by plants, and f_{NPP} is the ratio of NPP to gross primary production (GPP) from CARDAMOM. Our model used NPP as the input C flux for ecosystems, but we used GPP instead of NPP in Eq. (3) to calculate XUE for comparing with the estimates based on *in situ* measurements by Gill and Finzi (2016), which were also based on GPP. We thus used f_{NPP} only as an external variable in our modeling framework, and f_{NPP} was not targeted when evaluating the sensitivities and uncertainties of the results (see below).

We tested the steady-state sensitivity (SS) of the model results to the observational data sets (inputs of the model listed in Table 1) by linearizing the GOLUM-CNP model and its solver for calculating the first-order partial derivative of all outputs relative to each input parameter:

$$SS = \partial \mathbf{O} / \partial \mathbf{I} \quad (4)$$

where **I** is the vector of the input variables, and **O** is the vector of the output variables. This approach directly provided a sensitivity matrix, which allowed us to test the effect of the accuracy of the measurement of each input variable on the model results for the N and P cycles. This method was similar to the "one-at-a-time" (OAT) approach used for sensitivity analysis in previous C-N coupled modeling studies (Orwin et al., 2011; Shi et al., 2016; Zaehle and Friend, 2010) but did not require running simulations by changing the inputs one at a time. This approach did not fully explore the possible range of values for a given parameter, but provided comparable SS values for different parameters, which is useful when the full uncertainty ranges of some parameters are unknown, e.g. uncertainty due to the inconsistent definitions between the measured pools in the real world and the conceptual pools in the model, or the large uncertainty due to sparse observations for some biomes. The input parameters had distinct magnitudes (and units), so we used the relative sensitivities, e.g. $SS = \partial \mathbf{O} / \mathbf{O} / (\partial \mathbf{I} / \mathbf{I})$, to compare the sensitivities to different model inputs. For the sensitivity analysis, an SS of 1 indicates that a 1% increase (or decrease) in a model input produces a 1% increase (or decrease) in the model output, and an SS of -0.5 indicates that a 1%

increase (or decrease) in the model input produces a -0.5% decrease (or increase) in the model output. The results of this sensitivity analysis could be further used to investigate the sources of uncertainty in the outputs and to evaluate variances of the model outputs using error propagation:

$$\boldsymbol{\varepsilon}_{\mathbf{O},i} = \frac{\partial \mathbf{O}}{\partial \mathbf{I}_i}\varepsilon_{\mathbf{I},i}$$

$$\boldsymbol{\varepsilon}_{\mathbf{O}} = \sum_{i=1}^{n} \frac{\partial \mathbf{O}}{\partial \mathbf{I}_i}\varepsilon_{\mathbf{I},i} \quad (5)$$

$$\Sigma_{\mathbf{O}} = \mathrm{E}(\boldsymbol{\varepsilon}_{\mathbf{O}}{}^{\mathrm{T}}\boldsymbol{\varepsilon}_{\mathbf{O}})$$

where $\varepsilon_{I,i}$ is the error in the *i*th input data, $\varepsilon_{O,i}$ is the error propagated from the error in input *i*, $\boldsymbol{\varepsilon}_O$ is the error that accounts for errors in all input data, E represents the expectation of a variable and ~~$\boldsymbol{\Sigma}$~~$\boldsymbol{\varepsilon}_O$ is the covariance matrix whose diagonal entries are the variances of the outputs.

3.3 Adjustments of CARDAMOM C cycle

In CARDAMOM, there was no explicit separation between forests and grasslands and CARDAMOM provided low woody biomass in grassland dominated regions (Saatchi et al., 2011; Williams et al., 2013), while grasslands are considered as biomes and have no woody biomass in GOLUM-CNP. In order to represent the grassland biomes in GOLUM-CNP and to conserve the global NPP from CARDAMOM, ~~Biomass distributions in grassland-dominated biomes, including savannas, are skewed to low biomass, but has a high tail, particularly in the dry tropics (Saatchi et al., 2011; Williams et al., 2013).~~ we~~We~~ approximated the C-cycle state of the non-forest biomes (TRG, TEG and TUN) by partitioning half of CARDAMOM woody NPP to foliar NPP and half to fine roots, in order to better represent grassland C, N and P cycling across these biomes.

The CARDAMOM terrestrial C analysis did not assume steady states. Our goal, however, was to describe the steady states of C, N and P cycling, because few global long-term observations associated with N and P were available to constrain the model. We recalculated the C cycle based on a subset of the CARDAMOM results. Specifically, we used NPP and turnover times of the C pools for 2001-2010 (Table 1) and recalculated the steady-state sizes of these pools and the transfers of C between the pools represented in Fig. 1, solving Eqs. A1-A5 with their left sides as zeros. This steady-state transformation of the CARDAMOM C cycle is assessed in Sect. 4.1.

4 Results

4.1 Steady state C cycle

Table 2 shows the global C-pool sizes and main fluxes of the steady-state C cycle transformed from CARDAMOM under the climate conditions of 2001-2010.~~, which are compared with the means and percentile ranges from the original non-steady-state CARDAMOM results~~. Although the steady-state C stocks do not exactly represent the C stocks at present day, ~~The~~the differences between the steady-state transformed pool sizes and the original non-steady-state CARDAMOM results were within 10% for most C pools and fluxes. The largest differences were for ~~the estimates of the~~ biomass (foliar, fine-root and wood) pools. The larger foliar and fine-root pools in the steady-state GOLUM-CNP model were due to adjustments done for grass dominated grid cells for which CARDAMOM provided some wood growth inconsistent with the biome distribution used in GOLUM-CNP. In these cases, we allocated wood growth from CARDAMOM into growth of fine root and foliage. ~~placing woody NPP into these two pools in the grassland grid cells.~~ These pools in GOLUM-CNP, however, remained within the [5, 95th] percentile range of the original CARDAMOM values~~version~~. The pool size for global woody biomass was 37% smaller in the steady-state model (469 Pg) than the original CARDAMOM results but remained within its inter-quartile range (364-984 Pg). The differences between the gridded maps from original CARDAMOM and GOLUM-CNP are shown in Fig S1. The steady-state transformed C stocks in biomass, litter and SOM were within the 25th and 75th percentiles

of the original CARDAMOM results at more than 90% of forest grid cells, indicating that our steady-state transformed C stocks are close to the actual C stocks at present day, given the large uncertainties in the state-of-the-art estimates. Due to the adjustment made for the grass dominated grid cells (see above), the C pools for grassland differ more strongly than forest-dominated area from the original CARDAMOM. ~~The largest difference in woody biomass in the steady state model was for the northern temperate and boreal region (>35 °N) (Fig. S1). Independent remote sensing estimates for 30 °N to 80 °N were 4.76 ± 1.78 kg C m^{-2} for mean forest C density and 79.8 ± 29.9 Pg C for total forest C (Thurner et al., 2014), which were much lower than the original CARDAMOM values (9.55 kg C m^{-2} for mean forest C density across pixels defined as forest in Fig. 2, and 361 Pg C for total forest C) for this region. The forest woody biomass in the steady state model for the C cycle for this region (6.51 kg C m^{-2} for mean forest C density and 181 Pg C for total forest C) was lower than that in the original CARDAMOM data set but still higher than that reported by Thurner et al. (2014). This inconsistency was largely due to the limited extent of the Thurner et al. (2014) map, which only covered ecosystems categorized as forests. Residual overestimation could also be due to the assumption of a steady state, and northern temperate and boreal forests may deviate substantially from their equilibrium for the current NPP (Pan et al., 2011), due to climate change and elevated CO_2. Furthermore, biomass removal by harvesting and from disturbance other than fires was not explicitly constrained in CARDAMOM, which also contributed to a high bias of the steady state transformation of CARDAMOM. In the following sections, we used the steady state CARDAMOM results in the GOLUM CNP model, which was more appropriate for the interpretation of biome-scale C, N and P cycling, using the methodological steps outlined in Sect. 3.2 and 3.3.~~

4.2 Steady-state ~~pool sizes~~nutrient stocks and fluxes

Figure 3 and Fig. S4 summarizes the ~~pool sizes~~stocks and fluxes of N and P for the seven biomes and for the globe ~~(Fig. 3 a-g)~~. The uptake fluxes of N and P were largest for tropical forests, mainly driven by the large NPP of this biome. Rates of N and P uptake were lower for temperate and boreal forests than tropical forests and for non-forest biomes than forests. The pool sizes of N and P in plants tended to decrease from tropical to boreal regions, ~~mostly consistent with~~following the C-pool sizes and their observed stoichiometries. Conversely, N and P contents in litter were larger for boreal forests, temperate grasslands and tundra ecosystems than the other biomes, mainly due to a longer turnover of the litter pool in these biomes. The N-pool size of SOM was also larger in boreal forests, temperate grasslands and tundra than the other biomes. The P-pool size in SOM, however, was smaller for boreal forests and tundra than the other biomes, consistent with the differences between the N:C and P:C ratios of boreal biomes compared to other biomes (Table S1). Inorganic- N and labile soil P pools and leaching rates of N and P were higher in tropical forests, where runoff was higher than in the other biomes. Semi-arid tropical grassland (TRG) had high losses of N and P by fire and a low loss from leaching. The internal N and P fluxes within ecosystems were usually much larger than the external input fluxes and the output fluxes for all biomes, highlighting the dominant role of internal cycling of N and P, which differed from C cycles where NPP and losses by respiration were larger than any internal C flux.

Here we compared the estimates of N and P stocks for global terrestrial biosphere with other studies. Our estimate of N in plants (3.9 Pg N) was close to the estimate modeled by Zaehle et al. (2013) (3.5 Pg N), and was within the range of other studies, from 1.8 Pg N by Yang et al. (2009) and 6.57 Pg N by Wang et al. (2010) (6.57 Pg N). Our estimate of N in litter and SOM was lower than the estimate of 65 Pg N by Xu-ri et al. (2008) and Yang et al. (2009), but smaller than the estimate of 126 Pg N by Wang et al. (2010). Our estimate of the P mass in plants (0.17 Pg P) was smaller than the estimates modeled by Wang et al. (2010) (0.39 Pg P) and Goll et al. (2012) (0.23 Pg P). Our estimate of the litter P mass (0.03 Pg P) was similar to the estimate of 0.04 Pg P by the CABLE model (Wang et al. 2010) but was two-fold lower than the estimate (0.08 Pg P) modeled by Goll et al. (2012).

The rate of total N input (deposition and fixation) aggregated to ~~a~~ global scale was 0.19 Pg N y^{-1} and equa~~l~~ted (by construction) to the steady-state rate of total N loss. Total N uptake by plants was 0.68 Pg N y^{-1}. Our estimate of N

denitrification was 0.10 Pg N y^{-1}, consistent with the independent estimate of global soil denitrification of 0.12 Pg N y^{-1} by Seitzinger et al. (2006) and within the range reported by other studies, from 0.04 Pg N y^{-1} (Houlton and Bai, 2009) to 0.29 Pg N y^{-1} (Galloway et al., 2013). The global loss of N was 0.05 Pg from fire and 0.04 Pg N y^{-1} from leaching ~~was 0.04 Pg N y^{-1}~~, the latter being~~also~~ similar to the independent estimates by Galloway et al. (2004, 2013) of 0.013-0.18 Pg N y^{-1} and by Houlton and Bai (2009) of 0.09 Pg N y^{-1}. Globally, the loss of N by fire accounted for 26% of the total N loss. The total input of P to the terrestrial ecosystem was 0.007 Pg P y^{-1}, 86% from deposition (range from 71% for BOCF to 92% for TRG); only a small fraction was from rock weathering (ranging from 8 to 29% across biomes). ~~The loss of N by fire globally was 48 Tg N y^{-1} and accounted for 26% of the total N loss.~~ The loss of P is mainly from leaching and the loss by fire accounted for only 18% of the total P loss, much smaller than the fraction for N. ~~Our estimate of the litter P mass (0.03 Pg P) was similar to the estimate of 0.04 Pg P by the CABLE model (Wang et al. 2010) but was two fold lower than the estimate (0.08 Pg P) modeled by Goll et al. (2012). Our estimate of the P mass in plants (0.17 Pg P) was smaller than the estimates modeled by Wang et al. (2010) (0.39 Pg P) and Goll et al. (2012) (0.23 Pg P).~~

4.3 Implications for ecological research

Figure 4 shows the latitudinal distribution of foliar N:P ratios in our model. This~~, a~~ result ~~directly from~~reflects the distribution of the seven biomes and respective C:N and C:P ratios – both of which are prescribed here. Foliar N:P ratios decreased on average from low to high latitudes. Estimates from previous studies also followed this trend (Kerkhoff et al., 2005; McGroddy et al., 2004; Reich and Oleksyn, 2004) based on foliar measurements. The mean N:P ratios in our study were in the middle of the range of observations for all latitudes. The results of GOLUM-CNP better indicated the high N:P ratios between 20 ° to 40 °, where grassland is the dominant biome, than the monotonic regressions (colored lines in Fig. 4) derived by Reich and Oleksyn (2004) and Kerkhoff et al. (2005) for foliar data, implying that the use of stoichiometries at the scale of large biomes can identify the general features of the spatial gradients of N and P cycling.

Figure 5a and 5b show the distribution of the openness (defined as the ratio of new nutrient inputs to the total plant uptake of nutrients, Sect. 3.2) for N and P in different ecosystems~~.~~ and Fig. S5a and S5b show the gridded maps of these indices. New N in forest ecosystems (~~due to~~sum of deposition and biological fixation) accounted for 10% (BOCF) to 51% (TECF) of the total plant uptake of N, and new P (due to deposition and rock weathering) accounted for only 3.5% (BOCF) to 15% (TRF) of the total plant uptake of P. The openness of both N and P in grassland ecosystems decreased from the tropics to high latitudes. The residence times of N and P in ecosystems were much longer ~~for N and P~~ than those of C (Table S2) and decreased from the tropics to boreal areas (Fig. 5c, ~~and~~ 5d, S6a and S6b).

The openness and residence times of N and P together allow to assess the relative importance of ~~demonstrated the support of plant growth by~~ external inputs and internal cycling to support plant growth. For example, TECF are characterized by a more open N cycle and a longer N residence times compared to TRF. The difference in the openness of N cycle indicates that the TECF intends to invest more resources to obtain N from external inputs than TRF. The differences in residence times indicate that N is more efficiently conserved within the ecosystem in TECF compared to TRF, and such a conservation within ecosystems is primarily driven by differences in the turnover of dead organic matter (Fig. 3). The P cycle is less open than N cycle in all ecosystems, highlighting the importance of ecosystem P recycling within ecosystems to support plant growth.~~For example, the residence time of N was longer in TECF than TRF, indicating lower rates of N fixation and deposition in TECF than TRF. The openness of N, however, was higher in TECF than TRF, because the turnover times of litter and SOM in TECF were almost twice those in TRF (Fig. 3), so a large amount of N was "locked" in litter and SOM in TECF, and the net mineralization (gross mineralization minus gross immobilization) was much lower in TECF than TRF. The importance of external N inputs was thus much larger in TECF than TRF. More N and P will be needed to support the additional productivity in the future due to, for example, climate change or elevated CO_2 (Sun et al., 2017), so that areas with more external inputs will more likely meet the additional nutrient demands. Meanwhile,~~

~~consistently lower P than N openness in all ecosystems suggested that plant growth may be ultimately constrained in the future by low P availability.~~

Figure 6 shows the diagnosed nutrient-use efficiencies from GOLUM-CNP outputs for the seven biomes and Fig. S7a and S7b show the gridded maps of nutrient-use efficiencies. Among forest biomes, ~~Tropical~~ tropical forest had the lowest NUE and the highest~~, and its~~ PUE ~~was much higher than those of the~~compared to other forest biomes (Fig. 6a), consistent with the ~~general view that~~higher P ~~limits productivity more than~~and lower N stresses in tropical ecosystems (Gill and Finzi, 2016; Reich and Oleksyn, 2004). The values of NUE and PUE were similar to each other for TEDF, TECF and BOCF. Nutrient-use efficiencies were about 3-fold lower for non-forest biomes (Fig. 6b) than forest biomes, and both NUE and PUE decreased from tropical/C4 grassland to tundra.

4.4 Sensitivity analysis

Figure 7 shows the mean sensitivity of the nutrient-uptake fluxes (F_N and F_P), nutrient-use efficiencies (NUE and PUE), pool sizes of inorganic N and P (N_{inorg} and P_{inorg}), N and P openness, residence times of N and P in the ecosystem ($\tau_{N,eco}$ and $\tau_{P,eco}$) and residence times of N and P in plants ($\tau_{N,plant}$ and $\tau_{P,plant}$) to the input variables for the tropical-rainforest biome (TRF). The sensitivities were similar for the other biomes (Figs. ~~S2 and S3~~S8-S13). The uptake of nutrients in GOLUM-CNP was determined by NPP, NPP-allocation fractions, observation-based nutrient:C ratios and resorption coefficients (Eqs E7 and E18), so N uptake for tropical forest (Fig. ~~6a~~7a) was highly sensitive to NPP (1.0), NPP-allocation fractions (0.3) and the N:C ratio (0.4) of the woody pool, and P uptake was sensitive to NPP (1.0) and foliar variables (0.5 for $\gamma_{C,1}$ and 0.5 for $\rho_{P,1}$; see Table 1 for the definition of these variables). The nutrient-use efficiencies, defined in Eq. (1) as the ratio between GPP and the nutrient-uptake fluxes (Eq. 3), were negatively sensitive to the input variables mentioned above. Estimates of the openness of N and P were sensitive to input fluxes, NPP, NPP-allocation fractions and stoichiometric inputs. The residence times of nutrients in the ecosystem were influenced by variables affecting vegetation growth (e.g. NPP and allocation fractions of NPP) and those affecting inputs (e.g. deposition, N fixation and P release from rock weathering) to about equal extent. They were also very sensitive to variables related to soil, e.g. the N:C and P:C ratios in soil and residence times of soil. This reflect the large stocks of C and nutrients in soils than in the vegetation. The ~~turnover~~ residence times of nutrients in whole plants ($\tau_{N,plant}$ and $\tau_{P,plant}$) were ~~sensitive to the input data in turnover times of the plant tissues ($\tau_{1,2,3}$), the allocation fractions of NPP to different biomass pools ($\gamma_{1,2,3}$), the stoichiometry ($\rho_{X,1,2,3}$, X$\in${N,P}) and the resorption coefficients ($\epsilon_{X,1}$, X$\in${N,P}).~~more sensitive to the variables affecting woody biomass than those affecting foliage and fine roots. The sensitivity of residence times in the ecosystem and whole plants suggested that the nutrient cycling in the terrestrial biosphere were primarily determined by the largest pools.

5 Discussion

We developed a new observation-based modeling framework of global terrestrial N and P cycling built on a data-driven C-cycle model and observed N:C and P:C stoichiometric ratios in different pools spatially averaged at the scale of large biomes and observation-based estimates of the external input and output fluxes of N and P. This model was then used to estimate the pool sizes and fluxes in N and P cycles and indicators of the coupling between nutrient and C cycling, including nutrient openness, residence times in ecosystems and nutrient-use efficiencies. The data-driven estimates of steady-state global C, N and P cycles are the first that are fully consistent with a large set of global observation-based data sets, under the condition of current climate, deposition and CO_2 concentration. The indicators for the coupling between nutrient and C cycling, which are emerging properties of GOLUM-CNP, are used to evaluate the capabilities of GOLUM-CNP to capture observed patterns among biomes. We found that there are some differences between our data-driven estimates and previous studies about the nutrient efficiencies at biome scales (Gill and Finzi, 2016) and the openness (Cleveland et al., 2013). In this

section, we discussed the major uncertainties in our model and show how these uncertainties affect the computation of nutrient efficiencies and the openness (Sect. 5.1). Of note is that most of our discussions are for the C cycle (based on the sensitivity analysis, see below), and since CARDAMOM is the only data-driven C cycle to our knowledge, the modifications of the CARDAMOM dataset we made in this section are more qualitative and diagnostic rather than deterministic. Such an example highlights some important variables that should be investigated or considered in future data-driven products.

5.1 Sensitivity to C variables

Our estimates of nutrient-use efficiencies differed significantly from those estimated from *in situ* measurements (red squares and diamonds in Fig. 4) by Gill and Finzi (2016), particularly the values of PUE for all biomes and NUE for temperate and boreal forests. NUE and PUE ~~are~~ were ~~functions of the~~determined by NPP-allocation fractions, stoichiometric ratios, resorption coefficients and fractions of fire in the total outgoing C flux (Eqs. 3 and E7, where NPP is canceled by the division). The CARDAMOM observation-based analysis of the C cycle is the basis of the GOLUM-CNP modeling framework, so that errors and uncertainties in CARDAMOM for the C cycle translate into errors and uncertainties of GOLUM-CNP. Quantitatively, the sensitivity analysis (Figs. 7, ~~S2 and S3~~S8-S13) indicated that F_N and F_P, and thus NUE and PUE, were most sensitive to the NPP-allocation fractions (especially to woody biomass) and foliar stoichiometry. We applied the sensitivity matrix (Eq. 5) to further calculate the contribution of variances from each of these input variables, in which the uncertainties in the NPP-allocation and fire fractions were obtained from CARDAMOM and the uncertainties (1-sigma) in the N:C and P:C stoichiometric ratios and resorption coefficients were assumed to be 40%. This 40% uncertainty was larger than the uncertainty (20%) of the N:C ratios used by Wang et al. (2010), so our estimate of the contribution of uncertainties from the stoichiometric ratios was relatively large. The contribution of these different sources of uncertainty to the variances of NUE and PUE is shown in Fig. 8 for temperate coniferous forests whose NUE and PUE deviated the most from the estimate by Gill and Finzi (2016). Fig. 8 shows that the NPP-allocation fractions were the largest contributors to the total variances in NUE and PUE, which totaled >80%.

The NPP-allocation coefficients in CARDAMOM were only constrained indirectly by the satellite observations of LAI and tropical aboveground biomass. The uncertainty of the CARDAMOM allocation fractions was thus substantial, especially for non-tropical biomes where no biomass data were used (allocation-fraction 25^{th} – 75^{th} percentile ranges are typically >50% of the mean). For example, the mean fraction of NPP allocated to woody biomass in CARDAMOM was >60% in most grids (Fig. S~~4~~14a), which is rare for field measurements (Chen et al., 2013; Doughty et al., 2015). The mean allocation of NPP to fine roots may have been underestimated, characterized by too long a turnover time in CARDAMOM (range from <1 to 10 y) compared to field measurements (<3 y for all ecosystems, Gill and Jackson, 2000; Green et al., 2005). The CARDAMOM results indicated a turnover time of leaves in temperate and boreal biomes of <1 y, while Reich et al. (2014) indicated that the typical life span of conifer needles in evergreen coniferous forests depended on temperature and ranged from 2.5 to >10 y, this inconsistency being attributed by Bloom et al. (2016) to the potential roles of seasonal MODIS LAI biases and to the presence of understory vegetation across high-latitude ecosystems (Heiskanen et al., 2012).

Considering these inconsistencies between mean CARDAMOM values and *in situ* measurements, we conducted an additional experiment in which the CARDAMOM fields were further adapted: 1) the mean NPP-allocation fractions to woody biomass and the turnover time of woody biomass was divided by 1.5 to make sure that the NPP-allocation fractions to woody biomass fall in the range of field measurements, 2) the foliage turnover time of TECF and BOCF forests and associated NPP-allocation fractions were adjusted (keeping foliar biomass not changed) to match *in situ* observations (Reich et al., 2014) based on the fitted relationship between the needle longevity and mean annual temperature from Reich et al. (2014), assuming that understory vegetation plays a minimal role in C, N and P cycling and 3) Since in CARDAMOM, the NPP was constrained by GPP (GPP being constrained by the observation of LAI and the relationship between LAI and GPP) and the observation of biomass, additional adjustments were made to conserve the total NPP and pool sizes estimated from

CARDAMOM by allocating the residual NPP after the modifications from step 1 and 2 to fine roots, and adjusting the turnover time of fine roots to conserve exactly the pool size of CARDAMOM (see Figs. ~~S4-S7~~S14-S17 for the adjusted variables and original CARDAMOM values). ~~With these adjustments, the new C cycle is more consistent with the reality, especially for variables that were not well constrained in original CARDAMOM analysis~~. Fig. 9 shows the NUE and PUE from this new experiment based on this modified version of the C cycle from CARDAMOM. The NUE and PUE were lower than those in Fig. 6 for the forest biomes, especially for TECF and BOCF, which tended to decrease PUE from tropical to boreal forest. This distribution of PUE among the biomes in Fig. 9 better matched the differences between biomes presented by Gill and Finzi (2016). ~~The differences between Fig. 9 and Fig. 6 illustrate how the results of the NUE and PUE are sensitive to the C variables and how the uncertainties in the C cycle would be propagated to the estimates of N and P cycles. However,~~ Remaining inconsistencies could be attributed to~~exist because~~ the different methods used in this study and by Gill and Finzi (2016) are different. For example, Gill and Finzi (2016) notably used the net mineralization rates of N and P to approximate plant uptake, because their differences were an order of magnitude smaller than net nutrient mineralization. These authors used *in situ* measurements of net N mineralization but used a statistical model to estimate P mineralization based on a soil-order-specific soil-P pool due to the lack of data (Yang and Post, 2011) and a regression between soil-P turnover times and mean annual temperature. Their estimate of plant uptake was thus independent of vegetation stoichiometry, which differed from our study. Gill and Finzi (2016) also used bootstrapping to sample the NPP and net N (or P) mineralization from independent studies. Their estimates of NUE and PUE were thus not based on paired data, so their estimates may contain some sampling errors.

5.2 Uncertainty of nutrient-cycle openness

The distribution of nutrient-cycle openness in the seven biomes was presented in Sect. 4.3 and Fig. 5. Our estimate of a small openness of N and P in BOCF, and that the openness was smaller for the P than the N cycle, were consistent with the estimates by Cleveland et al. (2013). Our estimates of the N openness, however, were about twice as large as the estimates of Cleveland et al. (2013). This difference was due to the larger deposition fluxes in our study (globally 72 Tg N y^{-1}) than those used by Cleveland et al. (2013) (33 Tg N y^{-1}; from Dentener, 2006), because Wang et al. (2017) used an atmospheric model with higher horizontal resolution and an updated inventory of reactive-N (e.g. NO_x and NH_3) emission (Wang et al., 2017) and also because Cleveland et al. (2013) ~~also~~ assumed that only 15% of deposited N was available to plants. Cleveland et al. (2013) demonstrated that changing the fraction of biologically available deposited N to 100% did not significantly change the openness, because N-deposition fluxes were generally smaller than N fixation and accounted for a small fraction of external N inputs in their study. Our estimates of P openness were also larger than those ~~by~~ of Cleveland et al. (2013), which ~~was~~ we attributed to the large differences in the estimates of P deposition between the two studies. Cleveland et al. (2013) used ~~values of~~ P deposition (0.26 Tg yr^{-1}) ~~reported by~~ from Mahowald et al. (2008), which were ~~almost~~ an order of magnitude lower than ~~the~~ recent estimates from Wang et al. (2017) ~~that we~~ used in this study (5.8 Tg yr^{-1}), ~~arguably~~ because ~~of an underestimated~~ Wang et al. (2017) revised the contribution of anthropogenic P emissions and ~~not accounting for~~ P in particles with diameters >10 μm (Wang et al., 2015, 2017). We also found that the P-cycle openness decreased from the tropics to the boreal region, in contrast to the results by Cleveland et al. (2013). This also derives from the differences in the spatial gradients of P deposition in the two studies. Mahowald et al. (2008) found that P deposition was largest in northern Africa and that P deposition was within the same order of magnitude for tropical and temperate forests. Wang et al. (2017), however, found that P deposition was much larger over tropical forests than other regions. The contrasting spatial gradients in P deposition was likely due to the different models of atmospheric transport used by Wang et al. (2017) and Mahowald et al. (2008). More importantly, most stations measuring total P deposition are in temperate regions, and measurements of P deposition over tropical forests are very limited (Mahowald et al., 2008; Wang et al., 2017), so the estimates of P deposition in the tropics were not well constrained by *in situ* observations and thus had large uncertainties. Differences in the spatial

gradients in nutrient-cycle openness between our study and the study by Cleveland et al. (2013) demonstrated the impact of uncertain input data sets on the estimate of ecologically relevant quantities. The quantitative assessment of the uncertainties in our estimates of openness, however, was difficult, because the potential uncertainties in these data sets were not systematically evaluated within and between different estimates, and should therefore be addressed in future studies.

5.3 Future research and data needs

Our estimates of global N and P cycles were at the scale of large biomes. Recent studies of N and P cycles have relied on biome-specific stoichiometry (Cleveland et al., 2013; Wang et al., 2010). Stoichiometry, however, is also highly variable within biomes (Reich and Oleksyn, 2004). For example, Kattge et al. (2011) found that 40% of the variability in foliar N content was within species (finer scale than that of large biomes) and suggested that these stoichiometric ratios may be better represented by future trait-based estimates rather than fixed species-specific values. Some improvements have been made on the variation of stoichiometric ratios across climatic and ecological gradients within and across biomes, and on the contribution of plant traits and environmental conditions to these variations (Dong et al., 2017; Han et al., 2005; Meyerholt and Zaehle, 2015). However, it is still not sufficient to derive a globally gridded overview of the N and P cycles on current knowledge. A better understanding of the stoichiometric variability and its drivers is still needed in terms of not only representing the large-scale gradients but also reducing the uncertainties at local scale. New and spatially interpolated stoichiometric data sets should partly overcome this problem, although uncertainties in the interpolation will need to be carefully propagated on GOLUM-CNP outputs.

We assumed that all terrestrial ecosystems were at a steady state for 2001-2010 due to a lack of global constraints on the dynamics of N and P cycling over a long period. Terrestrial ecosystems, however, are not currently at steady states (Luo, 2017; Luo and Weng, 2011), due to climate change, increasing atmospheric CO_2, ~~and~~ anthropogenic disturbance etc, (Friedlingstein et al., 2006; Sitch et al., 2015). Zaehle (2013) reported that the terrestrial biosphere has accumulated 1.2 Pg N and 134.0 Pg C since the pre-industrial period. Wang et al. (2017) also found that N and P deposition have changed dramatically over time. The simulations by different models varies considerably, e.g. the responses of the biosphere to the increasing atmospheric CO_2 (Zaehle et al., 2014) and thus in future projections, because the current data sets have had little success in constraining all key processes in most DGVMs~~LSMs~~. Our results contribute to ~~are a first step for~~ evaluating models simulating global biogeochemical cycles. Although our steady-state C pool sizes (given the NPP and residence time at the condition of current climate) were within the [25, 75th] percentile range of the original non-steady-state CARDAMOM results (Fig. S1) at most grid cells, the biomass C stocks at 5%-10% of forest grid cells exceed the uncertainty range of CARDAMOM. In addition, independent remote-sensing estimates for 30 °N to 80 °N were 4.76 ± 1.78 kg C m^{-2} for mean forest C density and 79.8 ± 29.9 Pg C for total forest C (Thurner et al., 2014), which were lower than the GOLUM-CNP estimates (6.51 kg C m^{-2} for mean forest C density across pixels defined as forest in Fig. 2, and 181 Pg C for total forest C) for this region. This inconsistency was largely due to the fact that northern temperate and boreal forests may deviate substantially from their equilibrium for the current NPP (Pan et al., 2011), because of climate change and elevated CO_2. Residual overestimation could be also due to the fact that biomass removal by harvesting and from disturbance other than fires was not explicitly constrained in CARDAMOM and thus not represented in GOLUM-CNP. A transient simulation of N and P cycling will be needed in future studies as more constraints on N and P cycles emerge to study the effects of climate change, increasing CO_2 levels and disturbance on N and P cycles and their feedbacks. In such a transient simulation, a key process would be to simulate both the short-term and long-term responses of plants to the changing environment, e.g. how the plants would react when the inorganic N or labile soil P was not sufficient. Different models assumed different hypotheses under these conditions. For instance, N:C and P:C ratios are fixed and the photosynthesis rate is reduced to meet the low uptake of nutrients in Thornton et al., (2007). In Wang et al. (2010), the N:C and P:C ratios in biomass can vary within certain ranges, insufficient nutrient uptake would first result in a low concentration of N and/or P in plant tissues and

the low concentration of nutrient would then limit the photosynthesis according to an empirical relationship between nutrient concentration and NPP. Similarly, when the N:C and P:C ratios in litter change, the decomposition rate of litter would change as a result of altered activity of microbes (Manzoni et al., 2017). In the future, more data are required to test these hypotheses and the transient simulation of next version of GOLUM-CNP should incorporate these interactions between the plants and environments.

In addition, some processes, such as the N inputs from rock weathering (Houlton et al., 2018) were not considered in this study, because 1) as stated in Houlton et al. (2018), it is still unknown how much of rock-released N can be used by plants when rock weathering happens deep beneath the soils; 2) in GOLUM-CNP, adding rock N inputs has the same effect than N fixation and N deposition (Eqs. B6 and E17); and 3) the estimate of total input of N to ecosystems (188 Tg N yr^{-1}) in this study are already at the higher end of the estimate (mean 147 Tg yr^{-1}, and range between 99.1 and 185.1 Tg yr^{-1}) of Houlton et al. (2018), even if rock N inputs are not accounted for, due to our larger estimates of N fixation and N deposition than Houlton et al. (2018). In the future, the rock N inputs and the fraction of these N inputs are accessible to plants should be further quantified and the quantity of total N inputs to the ecosystems should be reconciled between different studies. With these improvements, the future development of data-driven GOLUM-CNP should take into all these processes and fluxes.

The model structure of GOLUM-CNP is mainly described by the inputs (NPP for C cycle, N deposition and fixation for N cycle, P deposition and release from rock weathering for P cycle) and residence times. Most DGVMs (e.g. Goll et al., 2012, 2017a; Medvigy et al., 2009; Parton et al., 2010; Thornton et al., 2007; Wang et al., 2010; Weng and Luo, 2008; Xu-Ri and Prentice, 2008; Yang et al., 2009; Zaehle et al., 2014; Zaehle and Friend, 2010) can be summarized by these two components, although these models have more processes and use complex equations to describe the dynamics controlling carbon and nutrient distribution among pools and the turnover of each pool. In this context, the output of the GOLUM-CNP provides a traceable tool that can be used in the future to compare the results between GOLUM-CNP and different DGVMs. As DGVMs are capable of computing the steady state of the biogeochemical cycles for present conditions, a direct comparison between GOLUM-CNP estimate and DGVMs' estimates is possible.

At last, ~~Th~~the sensitivity matrix presented in Sect. 4.4 provides a useful tool for assessing the uncertainties in model outputs by propagating the uncertainties in the model inputs. We applied this method to quantitatively assess the sources of uncertainties in the estimated nutrient-use efficiencies (Sect. 5.1 and Fig. 8), but we also found that the uncertainties for some other quantities were currently difficult to obtain, because the estimates of uncertainties were not available for all spatially explicit input data. This sensitivity analysis can be used in future studies to quantify the contribution of each input data set to the uncertainty in other model outputs, to characterize the dominant sources of uncertainties in the estimated C, N and P processes, to identify the major differences between different models (e.g. GOLUM-CNP versus DGVMs) and thus to identify priorities for future data syntheses to fill the largest gaps in uncertainty. Future studies that provide global data sets will need to include systematic evaluations and spatially explicit estimates of uncertainties in their data sets.

6 Concluding remarks

This study is a first attempt to combine observation-based estimates of C, N, P fluxes and pools in terrestrial ecosystems into a consistent (steady-state) diagnostic model. Although there are considerable uncertainties in our results due to uncertain and incomplete carbon cycle and nutrient observations, the main findings are: 1) external inputs of P from outside the ecosystem contributes to a smaller plant P uptake than that of N, indicating a more important role of internal P recycling than that of internal N recycling in supporting plant growth ~~a likely ultimate constraints of P on plant growth in the future~~, 2) tropical forests have the lowest N use efficiency and the largest P use efficiency, suggesting the adaptive response of this biome to the low P availability in the tropics. The structure of GOLUM-CNP is analogous to most other process-based ~~LSMs~~ DGVMs describing carbon and nutrient interactions ~~(e.g. Goll et al., 2012, 2017a; Medvigy et al., 2009; Parton et al., 2010;~~

~~Thornton et al., 2007; Wang et al., 2010; Weng and Luo, 2008; Xu-Ri and Prentice, 2008; Yang et al., 2009; Zaehle et al., 2014; Zaehle and Friend, 2010), although these models have more processes and use complex equations to describe the dynamics controlling carbon and nutrient distribution among pools and the turnover of each pool~~. The output of the GOLUM-CNP provides a traceable tool and~~, in which a consistency between different datasets of global C, N and P cycles has been achieved. Such a framework~~ can ~~thus~~ be used in the future to test the performance of ~~these~~ complex ~~LSMs~~ DGVMs in the simulation of interactions between C, N and P cycling.

Code and data availability

The source code and the map of the classification of seven large biomes are included in the Supplement. For the other datasets that are listed in Table 1, it is encouraged to contact the first authors of the original references.

Appendix A Equations for carbon cycle

The carbon cycle framework is based on DALEC2 model (Bloom and Williams, 2015), except that we combined the labile and foliage pools together since the labile pool in DALEC2 only transfer to foliage. There are five pools in the C cycle (1: foliage; 2: fine roots; 3: wood; 4: litter; 5: SOM). The equations governing the change of C pools are given by:

$$\frac{dC_1}{dt} = -{\tau_1}^{-1}C_1 + \gamma_1 Fc \quad \text{(A1)}$$

$$\frac{dC_2}{dt} = -{\tau_2}^{-1}C_2 + \gamma_2 Fc \quad \text{(A2)}$$

$$\frac{dC_3}{dt} = -{\tau_3}^{-1}C_3 + \gamma_3 Fc \quad \text{(A3)}$$

$$\frac{dC_4}{dt} = {\tau_1}^{-1}C_1\left(1 - f_{fireC,1}\right) + {\tau_2}^{-1}C_2\left(1 - f_{fireC,2}\right) - {\tau_4}^{-1}C_4 \quad \text{(A4)}$$

$$\frac{dC_5}{dt} = {\tau_3}^{-1}C_3(1 - f_{fireC,3}) + \eta{\tau_4}^{-1}C_4 - {\tau_5}^{-1}C_5 \quad \text{(A5)}$$

The definitions of the symbols are listed in Table 1.

Appendix B Equations for nitrogen cycle

There are five organic N pools and one inorganic soil N pool. The N cycle are described by the following equations:

$$\frac{dN_1}{dt} = -{\tau_1}^{-1}N_1(1 - \varepsilon_1) + \beta_1 Fn \quad \text{(B1)}$$

$$\frac{dN_2}{dt} = -{\tau_2}^{-1}N_2 + \beta_2 Fn \quad \text{(B2)}$$

$$\frac{dN_3}{dt} = -{\tau_3}^{-1}N_3 + \beta_3 Fn \quad \text{(B3)}$$

$$\frac{dN_4}{dt} = {\tau_1}^{-1}N_1(1 - \varepsilon_1)(1 - f_{fireC,1}) + {\tau_2}^{-1}N_2(1 - f_{fireC,2}) - {\tau_4}^{-1}N_4 \quad \text{(B4)}$$

$$\frac{dN_5}{dt} = {\tau_3}^{-1}N_3(1 - f_{fireC,3}) + \eta{\tau_4}^{-1}N_4 + N_{imob} - {\tau_5}^{-1}N_5 \quad \text{(B5)}$$

$$\frac{dN_{inorg}}{dt} = {\tau_5}^{-1}N_5\left(1 - f_{fireC,5}\right) + {\tau_4}^{-1}N_4\left(1 - \eta - f_{fireC,4}\right) + N_d + N_{fix} - N_{imob} - f_{leach}N_{inorg} - f_{denit}N_{inorg} - Fn \quad \text{(B6)}$$

The definitions of the symbols are listed in Table 1.

In Eq. B6, the fraction of inorganic N (f_{leach}) that is lost due to leaching is computed by soil water (Θ) and the sum of drainage and surface runoff (q). We use the spatially explicit estimate of daily soil moisture derived from the European Centre for Medium-Range Weather Forecasts (ECMWF) Interim Reanalysis (ERA-Interim/Land; Albergel et al., 2013; Balsamo et al., 2015) (see Table 1), and the global gridded estimate of monthly mean runoff data from the Global Runoff Data Centre (GRDC, http://www.grdc.sr.unh.edu/). Since the runoff data only have a monthly time step, we use the same

value of runoff for each day within one month. The leaching fraction at annual scale is thus computed by:

$$f_{leach} = \sum_{d=1}^{365} \frac{q_i}{\Theta_i + q_i} \quad \text{(B7)}$$

Of note is that in this computation, f_{leach} can exceed one, meaning that the turnover time of inorganic N pool is smaller than one year (Wang et al., 2010).

Appendix C Equations for phosphorus cycle

There are five organic P pools and one inorganic soil P pool. The P cycle are described by the following equations:

$$\frac{dP_1}{dt} = -{\tau_1}^{-1} P_1 (1 - \theta_1) + \varphi_1 Fp \quad \text{(C1)}$$

$$\frac{dP_2}{dt} = -{\tau_2}^{-1} P_2 + \varphi_2 Fp \quad \text{(C2)}$$

$$\frac{dP_3}{dt} = -{\tau_3}^{-1} P_3 + \varphi_3 Fp \quad \text{(C3)}$$

$$\frac{dP_4}{dt} = {\tau_1}^{-1} P_1 (1 - \theta_1)(1 - f_{fireC,1}) + {\tau_2}^{-1} P_2 (1 - f_{fireC,2}) - {\tau_4}^{-1} P_4 \quad \text{(C4)}$$

$$\frac{dP_5}{dt} = {\tau_3}^{-1} P_3 (1 - f_{fireC,3}) + \eta {\tau_4}^{-1} P_4 + P_{imob} - {\tau_5}^{-1} P_5 \quad \text{(C5)}$$

$$\frac{dP_{inorg}}{dt} = {\tau_5}^{-1} P_5 \left(1 - f_{fireC,5}\right) + + {\tau_4}^{-1} P_4 \left(1 - \eta - f_{fireC,4}\right) + P_d + P_w + 0.75 Fire_P - P_{imob} - f_{leach} f_{dissolve} P_{inorg} - f_{sorb} P_{inorg} + Fp \quad \text{(C6)}$$

Where $Fire_P$ represent the P in the ecosystem that suffers from fire events:

$$Fire_P = {\tau_1}^{-1} P_1 (1 - \theta_1) f_{fireC,1} + {\tau_2}^{-1} P_2 f_{fireC,2} + {\tau_3}^{-1} P_3 f_{fireC,3} + {\tau_4}^{-1} P_4 f_{fireC,4} + {\tau_5}^{-1} P_5 f_{fireC,5} \quad \text{(C7)}$$

Appendix D Additional constraints

1) Under steady-state, the N:C and P:C ratios for the plants and soil are assumed to be constant, so that N_i and P_i can be calculated by the production of the C pool size from CARDAMOM and the stoichiometry ratios for each pool from Zechmeister-Boltenstern et al. (2015), except litter which has different definitions in CARDAMOM and Zechmeister-Boltenstern et al. (2015):

$$N_i = \rho_{N,i} C_i \ (i = 1,2,3,5) \quad \text{(D1-D4)}$$

$$P_i = \rho_{P,i} C_i \ (i = 1,2,3,5) \quad \text{(D5-D8)}$$

2) The fraction of NPP, F_N and F_P allocations sum up to 1:

$$\beta_1 + \beta_2 + \beta_3 = 1 \quad \text{(D9)}$$

$$\varphi_1 + \varphi_2 + \varphi_3 = 1 \quad \text{(D10)}$$

3) The fraction of gaseous loss of N due to denitrification to the total inorganic N loss should satisfy the estimates by using global $\delta^{15}N$ observations (f_{gasN}, Goll et al., 2017b):

$$\frac{f_{denit} N_{inorg}}{f_{leach} N_{inorg} + f_{denit} N_{inorg}} = f_{gasN} \quad \text{(D11)}$$

7 Appendix E Solutions under steady-state assumption

$$C_i = F_c \gamma_{C,i} \tau_i \ (i = 1,2,3) \quad \text{(E1-E4)}$$

$$C_4 = \left[\frac{C_1}{\tau_1}\left(1 - f_{fireC,1}\right) + \frac{C_2}{\tau_2}(1 - f_{fireC,2})\right] \tau_4 \quad \text{(E5)}$$

$$C_5 = \left[\frac{C_3}{\tau_3}\left(1 - f_{fireC,3}\right) + \frac{C_4}{\tau_4}(1 - f_{fireC,4})\right] \tau_5 \quad \text{(E6)}$$

$$F_N = F_c \left[\rho_{N,1} \gamma_{C,1} \left(1 - f_{fireC,1}\right)\left(1 - \varepsilon_{N,1}\right) + \rho_{N,1} \gamma_{C,1} f_{fireC,1} + \rho_{N,2} \gamma_{C,2} + \rho_{N,2} \gamma_{C,3}\right] \quad \text{(E7)}$$

$$\gamma_{N,2} = \frac{\rho_{N,2}C_2}{\tau_2 F_N} \quad \text{(E8)}$$

$$\gamma_{N,3} = \frac{\rho_{N,3}C_3}{\tau_3 F_N} \quad \text{(E9)}$$

$$\gamma_{N,1} = 1 - \gamma_{N,2} - \gamma_{N,3} \quad \text{(E10)}$$

$$N_i = \rho_{N,i}C_i \ \ (i = 1,2,3,5) \quad \text{(E11-E14)}$$

$$N_4 = \frac{\frac{\rho_{N,1}C_1}{\tau_1}(1-f_{fireC,1})+\frac{\rho_{N,2}C_2}{\tau_2}(1-f_{fireC,2})}{\frac{C_1}{\tau_1}(1-f_{fireC,1})+\frac{C_2}{\tau_2}(1-f_{fireC,2})}C_4 \quad \text{(E15)}$$

$$N_{imorb} = \eta\left(\rho_{N,5} - \frac{N_4}{C_4}\right)\frac{C_4}{\tau_4} + \left(\rho_{N,5} - \frac{N_3}{C_3}\right)\frac{C_3}{\tau_3}(1 - f_{fireC,3}) \quad \text{(E16)}$$

$$N_{inorg} = \frac{N_d + N_{fix} - \sum_{i=1}^{5}(\frac{N_i}{\tau_i}f_{fireC,i})}{f_{leach}} \quad \text{(E17)}$$

$$F_P = F_c\left[\rho_{P,1}\gamma_{C,1}(1 - f_{fireC,1})(1 - \varepsilon_{P,1}) + \rho_{P,1}\gamma_{C,1}f_{fireC,1} + \rho_{P,2}\gamma_{C,2} + \rho_{P,2}\gamma_{C,3}\right] \quad \text{(E18)}$$

$$\gamma_{P,2} = \frac{\rho_{P,2}C_2}{\tau_2 F_P} \quad \text{(E19)}$$

$$\gamma_{P,3} = \frac{\rho_{P,3}C_3}{\tau_3 F_P} \quad \text{(E20)}$$

$$\gamma_{P,1} = 1 - \gamma_{P,2} - \gamma_{P,3} \quad \text{(E21)}$$

$$P_i = \rho_{P,i}C_i \ \ (i = 1,2,3,5) \quad \text{(E22-E25)}$$

$$P_4 = \frac{\frac{\rho_{P,1}C_1}{\tau_1}(1-f_{fireC,1})+\frac{\rho_{P,2}C_2}{\tau_2}(1-f_{fireC,2})}{\frac{C_1}{\tau_1}(1-f_{fireC,1})+\frac{C_2}{\tau_2}(1-f_{fireC,2})}C_4 \quad \text{(E26)}$$

$$P_{imorb} = \eta\left(\rho_{P,5} - \frac{P_4}{C_4}\right)\frac{C_4}{\tau_4} + \left(\rho_{P,5} - \frac{P_3}{C_3}\right)\frac{C_3}{\tau_3}(1 - f_{fireC,3}) \quad \text{(E27)}$$

$$P_{inorg} = \frac{P_d + P_w - \sum_{i=1}^{5}(\frac{P_i}{\tau_i}f_{fireC,i})}{f_{leach}f_{dissolve} + f_{sorb}} \quad \text{(E28)}$$

Acknowledgement

The idea of GOLUM was initially discussed at a workshop held at the Northwest Agricultural and Forestry, China. We are grateful for the financial support of the workshop by the State Key Laboratory of Soil Erosion and Dryland Farming on the Loess Plateau of Northwest A & F University and the National Basic Research Programme of China grant 2013CB956602. Funding was provided by the Laboratory for Sciences of Climate and Environment (LSCE), CEA, CNRS and UVSQ. PC, DG, SP, JP and JS acknowledge support from the European Research Council Synergy grant ERC-2013-SyG-610028 IMBALANCE-P. Contribution by AAB was carried out at the Jet Propulsion Laboratory, California Institute of Technology, under a contract with the National Aeronautics and Space Administration. BDS was funded by ERC H2020-MSCA-IF-2015, grant number 701329.

References

Albergel, C., Dorigo, W., Reichle, R. H., Balsamo, G., De Rosnay, P., Muñoz-Sabater, J., Isaksen, L., De Jeu, R. and Wagner, W.: Skill and global trend analysis of soil moisture from reanalyses and microwave remote sensing, J. Hydrometeorol., 14(4), 1259–1277, 2013.

Augusto, L., Achat, D. L., Jonard, M., Vidal, D. and Ringeval, B.: Soil parent material—A major driver of plant nutrient limitations in terrestrial ecosystems, Global Change Biology, 23(9), 3808–3824, doi:10.1111/gcb.13691, 2017.

Bai, E., Houlton, B. Z. and Wang, Y. P.: Isotopic identification of nitrogen hotspots across natural terrestrial ecosystems, Biogeosciences, 9(8), 3287–3304, doi:10.5194/bg-9-3287-2012, 2012.

Balsamo, G., Albergel, C., Beljaars, A., Boussetta, S., Brun, E., Cloke, H., Dee, D., Dutra, E., Muñoz-Sabater, J., Pappenberger, F. and others: ERA-Interim/Land: a global land surface reanalysis data set, Hydrol. Earth Syst. Sci., 19(1), 389–407, 2015.

Bloom, A. A. and Williams, M.: Constraining ecosystem carbon dynamics in a data-limited world: integrating ecological

"common sense" in a model–data fusion framework, Biogeosciences, 12(5), 1299–1315, 2015.
Bloom, A. A., Exbrayat, J.-F., Velde, I. R. van der, Feng, L. and Williams, M.: The decadal state of the terrestrial carbon cycle: Global retrievals of terrestrial carbon allocation, pools, and residence times, Proc. Natl. Acad. Sci., 113(5), 1285–1290, doi:10.1073/pnas.1515160113, 2016.
Bontemps, S., Defourny, P., Radoux, J., Van Bogaert, E., Lamarche, C., Achard, F., Mayaux, P., Boettcher, M., Brockmann, C., Kirches, G. and others: Consistent global land cover maps for climate modelling communities: current achievements of the ESA's land cover CCI, in Proceedings of the ESA Living Planet Symposium, Edimburgh, pp. 9–13. [online] Available from: https://ftp.space.dtu.dk/pub/Ioana/papers/s274_2bont.pdf (Accessed 20 April 2017), 2013.
Bouwman, A. F., Lee, D. S., Asman, W. a. H., Dentener, F. J., Van Der Hoek, K. W. and Olivier, J. G. J.: A global high-resolution emission inventory for ammonia, Glob. Biogeochem. Cycles, 11(4), 561–587, doi:10.1029/97GB02266, 1997.
Chen, G., Yang, Y. and Robinson, D.: Allocation of gross primary production in forest ecosystems: allometric constraints and environmental responses, New Phytol., 200(4), 1176–1186, doi:10.1111/nph.12426, 2013.
Cleveland, C. C., Townsend, A. R., Schimel, D. S., Fisher, H., Howarth, R. W., Hedin, L. O., Perakis, S. S., Latty, E. F., Von Fischer, J. C., Elseroad, A. and Wasson, M. F.: Global patterns of terrestrial biological nitrogen (N2) fixation in natural ecosystems, Global Biogeochem. Cycles, 13(2), 623–645, doi:10.1029/1999GB900014, 1999.
Cleveland, C. C., Houlton, B. Z., Smith, W. K., Marklein, A. R., Reed, S. C., Parton, W., Grosso, S. J. D. and Running, S. W.: Patterns of new versus recycled primary production in the terrestrial biosphere, Proc. Natl. Acad. Sci., 110(31), 12733–12737, doi:10.1073/pnas.1302768110, 2013.
Dentener, F. J.: Global Maps of Atmospheric Nitrogen Deposition, 1860, 1993, and 2050, , doi:10.3334/ornldaac/830, 2006.
Dong, N., Prentice, I. C., Evans, B. J., Caddy-Retalic, S., Lowe, A. J. and Wright, I. J.: Leaf nitrogen from first principles: field evidence for adaptive variation with climate, Biogeosciences, 14(2), 481–495, doi:10.5194/bg-14-481-2017, 2017.
Doughty, C. E., Metcalfe, D. B., Girardin, C. A. J., Amézquita, F. F., Cabrera, D. G., Huasco, W. H., Silva-Espejo, J. E., Araujo-Murakami, A., Da Costa, M. C., Rocha, W. and others: Drought impact on forest carbon dynamics and fluxes in Amazonia, Nature, 519(7541), 78–82, 2015.
Elser, J. J., Bracken, M. E. S., Cleland, E. E., Gruner, D. S., Harpole, W. S., Hillebrand, H., Ngai, J. T., Seabloom, E. W., Shurin, J. B. and Smith, J. E.: Global analysis of nitrogen and phosphorus limitation of primary producers in freshwater, marine and terrestrial ecosystems, Ecol. Lett., 10(12), 1135–1142, doi:10.1111/j.1461-0248.2007.01113.x, 2007.
Fekete, B. M., Vörösmarty, C. J. and Grabs, W.: High-resolution fields of global runoff combining observed river discharge and simulated water balances, Glob. Biogeochem. Cycles, 16(3) [online] Available from: http://onlinelibrary.wiley.com/doi/10.1029/1999GB001254/full (Accessed 8 May 2017), 2002.
Freney, J. R., Simpson, J. R. and Denmead, O. T.: Volatilization of ammonia, in Gaseous loss of nitrogen from plant-soil systems, pp. 1–32, Springer. [online] Available from: http://link.springer.com/chapter/10.1007/978-94-017-1662-8_1 (Accessed 19 April 2017), 1983.
Friedlingstein, P., Cox, P., Betts, R., Bopp, L., Von Bloh, W., Brovkin, V., Cadule, P., Doney, S., Eby, M., Fung, I. and others: Climate–carbon cycle feedback analysis: results from the C4MIP model intercomparison, J. Clim., 19(14), 3337–3353, 2006.
Galloway, J. N., Dentener, F. J., Capone, D. G., Boyer, E. W., Howarth, R. W., Seitzinger, S. P., Asner, G. P., Cleveland, C. C., Green, P. A., Holland, E. A., Karl, D. M., Michaels, A. F., Porter, J. H., Townsend, A. R. and Vöosmarty, C. J.: Nitrogen Cycles: Past, Present, and Future, Biogeochemistry, 70(2), 153–226, doi:10.1007/s10533-004-0370-0, 2004.
Galloway, J. N., Dentener, F. J., Capone, D. G., Boyer, E. W., Howarth, R. W., Seitzinger, S. P., Asner, G. P., Cleveland, C. C., Green, P. A., Holland, E. A., Karl, D. M., Michaels, A. F., Porter, J. H., Townsend, A. R. and Vöosmarty, C. J.: Nitrogen Cycles: Past, Present, and Future, Biogeochemistry, 70(2), 153–226, doi:10.1007/s10533-004-0370-0, 2004.
Galloway, J. N., Leach, A. M., Bleeker, A. and Erisman, J. W.: A chronology of human understanding of the nitrogen cycle, Philos. Trans. R. Soc. B Biol. Sci., 368(1621), 20130120, doi:10.1098/rstb.2013.0120, 2013.
Gärdenäs, A. I., Ågren, G. I., Bird, J. A., Clarholm, M., Hallin, S., Ineson, P., Kätterer, T., Knicker, H., Nilsson, S. I., Näsholm, T., Ogle, S., Paustian, K., Persson, T. and Stendahl, J.: Knowledge gaps in soil carbon and nitrogen interactions – From molecular to global scale, Soil Biol. Biochem., 43(4), 702–717, doi:10.1016/j.soilbio.2010.04.006, 2011.
Giglio, L., Randerson, J. T. and Werf, G. R.: Analysis of daily, monthly, and annual burned area using the fourth-generation global fire emissions database (GFED4), J. Geophys. Res. Biogeosciences, 118(1), 317–328, 2013.
Gill, A. L. and Finzi, A. C.: Belowground carbon flux links biogeochemical cycles and resource-use efficiency at the global scale, Ecol. Lett., 19(12), 1419–1428, doi:10.1111/ele.12690, 2016.
Gill, R. A. and Jackson, R. B.: Global patterns of root turnover for terrestrial ecosystems, New Phytol., 147(1), 13–31, doi:10.1046/j.1469-8137.2000.00681.x, 2000.
Goll, D. S., Brovkin, V., Parida, B. R., Reick, C. H., Kattge, J., Reich, P. B., van Bodegom, P. M. and Niinemets, Ü.: Nutrient limitation reduces land carbon uptake in simulations with a model of combined carbon, nitrogen and phosphorus cycling, Biogeosciences, 9, 3547–3569, doi:10.5194/bg-9-3547-2012, 2012.
Goll, D. S., Vuichard, N., Maignan, F., Jornet-Puig, A., Sardans, J., Violette, A., Peng, S., Sun, Y., Kvakic, M., Guimberteau, M., Guenet, B., Zaehle, S., Peñuelas, J., Janssens, I. and Ciais, P.: A representation of the phosphorus cycle for ORCHIDEE (revision 3985), Geosci Model Dev Discuss, 2017, 1–39, doi:10.5194/gmd-2017-62, 2017a.
Goll, D. S., Winkler, A. J., Raddatz, T., Dong, N., Prentice, I. C., Ciais, P. and Brovkin, V.: Carbon-nitrogen interactions in idealized simulations with JSBACH (version 3.10), Geosci Model Dev Discuss, 2017, 1–28, doi:10.5194/gmd-2016-304, 2017b.

Gordon, W. S. and Jackson, R. B.: Nutrient concentrations in fine roots, Ecology, 81(1), 275–280, 2000.
Green, J. J., Dawson, L. A., Proctor, J., Duff, E. I. and Elston, D. A.: Fine Root Dynamics in a Tropical Rain Forest is Influenced by Rainfall, Plant Soil, 276(1–2), 23–32, doi:10.1007/s11104-004-0331-3, 2005.
Gruber, N. and Galloway, J. N.: An Earth-system perspective of the global nitrogen cycle, Nature, 451(7176), 293–296, doi:10.1038/nature06592, 2008.
Han, W., Fang, J., Guo, D. and Zhang, Y.: Leaf nitrogen and phosphorus stoichiometry across 753 terrestrial plant species in China, New Phytol., 168(2), 377–385, doi:10.1111/j.1469-8137.2005.01530.x, 2005.
Hartmann, J., Moosdorf, N., Lauerwald, R., Hinderer, M. and West, A. J.: Global chemical weathering and associated P-release — The role of lithology, temperature and soil properties, Chem. Geol., 363, 145–163, doi:10.1016/j.chemgeo.2013.10.025, 2014.
Heiskanen, J., Rautiainen, M., Stenberg, P., Mõttus, M., Vesanto, V.-H., Korhonen, L. and Majasalmi, T.: Seasonal variation in MODIS LAI for a boreal forest area in Finland, Remote Sens. Environ., 126, 104–115, 2012.
Hiederer, R. and Köchy, M.: Global soil organic carbon estimates and the harmonized world soil database, EUR, 79, 25225, 2011.
Houlton, B. Z. and Bai, E.: Imprint of denitrifying bacteria on the global terrestrial biosphere, Proc. Natl. Acad. Sci., 106(51), 21713–21716, doi:10.1073/pnas.0912111106, 2009.
Houlton, B. Z., Marklein, A. R. and Bai, E.: Representation of nitrogen in climate change forecasts, Nat. Clim. Change, 5(5), 398–401, doi:10.1038/nclimate2538, 2015.
Houlton, B. Z., Morford, S. L. and Dahlgren, R. A.: Convergent evidence for widespread rock nitrogen sources in Earth's surface environment, Science, 360(6384), 58–62, doi:10.1126/science.aan4399, 2018.
Hungate, B. A., Dukes, J. S., Shaw, M. R., Luo, Y. and Field, C. B.: Nitrogen and Climate Change, Science, 302(5650), 1512–1513, doi:10.1126/science.1091390, 2003.
Jahnke, R. A.: The phosphorus cycle, in Earth system science: From biogeochemical cycles to global change, pp. 360–376, Elservier Academic Press, San Diego. ~~[online] Available from: https://books.google.fr/books?hl=en&lr=&id=85YkdAm5tdoC&oi=fnd&pg=PA360&dq=The+Phosphorus+Cycle&ots=ImiRpJyZLU&sig=ho0YXiy7pOAleQOCstOZc0iGtYs~~, 2000.
Kattge, J., Díaz, S., Lavorel, S., Prentice, I. C., Leadley, P., Bönisch, G., Garnier, E., Westoby, M., Reich, P. B., Wright, I. J., Cornelissen, J. H. C., Violle, C., Harrison, S. P., Van BODEGOM, P. M., Reichstein, M., Enquist, B. J., Soudzilovskaia, N. A., Ackerly, D. D., Anand, M., Atkin, O., Bahn, M., Baker, T. R., Baldocchi, D., Bekker, R., Blanco, C. C., Blonder, B., Bond, W. J., Bradstock, R., Bunker, D. E., Casanoves, F., Cavender-Bares, J., Chambers, J. Q., Chapin Iii, F. S., Chave, J., Coomes, D., Cornwell, W. K., Craine, J. M., Dobrin, B. H., Duarte, L., Durka, W., Elser, J., Esser, G., Estiarte, M., Fagan, W. F., Fang, J., Fernández-Méndez, F., Fidelis, A., Finegan, B., Flores, O., Ford, H., Frank, D., Freschet, G. T., Fyllas, N. M., Gallagher, R. V., Green, W. A., Gutierrez, A. G., Hickler, T., Higgins, S. I., Hodgson, J. G., Jalili, A., Jansen, S., Joly, C. A., Kerkhoff, A. J., Kirkup, D., Kitajima, K., Kleyer, M., Klotz, S., Knops, J. M. H., Kramer, K., Kühn, I., Kurokawa, H., Laughlin, D., Lee, T. D., Leishman, M., Lens, F., Lenz, T., Lewis, S. L., Lloyd, J., Llusià, J., Louault, F., Ma, S., Mahecha, M. D., Manning, P., Massad, T., Medlyn, B. E., Messier, J., Moles, A. T., Müller, S. C., Nadrowski, K., Naeem, S., Niinemets, Ü., Nöllert, S., Nüske, A., Ogaya, R., Oleksyn, J., Onipchenko, V. G., Onoda, Y., Ordoñez, J., Overbeck, G., et al.: TRY – a global database of plant traits, Glob. Change Biol., 17(9), 2905–2935, doi:10.1111/j.1365-2486.2011.02451.x, 2011.
Kerkhoff, A. J., Enquist, B. J., Elser, J. J. and Fagan, W. F.: Plant allometry, stoichiometry and the temperature-dependence of primary productivity, Glob. Ecol. Biogeogr., 14(6), 585–598, doi:10.1111/j.1466-822X.2005.00187.x, 2005.
Klodd, A. E., Nippert, J. B., Ratajczak, Z., Waring, H. and Phoenix, G. K.: Tight coupling of leaf area index to canopy nitrogen and phosphorus across heterogeneous tallgrass prairie communities, Oecologia, 182(3), 889–898, doi:10.1007/s00442-016-3713-3, 2016.
Liu, Y., Wang, C., He, N., Wen, X., Gao, Y., Li, S., Niu, S., Butterbach-Bahl, K., Luo, Y. and Yu, G.: A global synthesis of the rate and temperature sensitivity of soil nitrogen mineralization: latitudinal patterns and mechanisms, Glob. Change Biol., 23(1), 455–464, doi:10.1111/gcb.13372, 2017.
Luo, Y.: The Third Dimension of Terrestrial Carbon Cycle Dynamics, 2017.
Luo, Y. and Weng, E.: Dynamic disequilibrium of the terrestrial carbon cycle under global change, Trends Ecol. Evol., 26(2), 96–104, 2011.
Mahowald, N., Jickells, T. D., Baker, A. R., Artaxo, P., Benitez-Nelson, C. R., Bergametti, G., Bond, T. C., Chen, Y., Cohen, D. D., Herut, B., Kubilay, N., Losno, R., Luo, C., Maenhaut, W., McGee, K. A., Okin, G. S., Siefert, R. L. and Tsukuda, S.: Global distribution of atmospheric phosphorus sources, concentrations and deposition rates, and anthropogenic impacts, Glob. Biogeochem. Cycles, 22(4), GB4026, doi:10.1029/2008GB003240, 2008.
Manzoni, S., Trofymow, J. A., Jackson, R. B. and Porporato, A.: Stoichiometric controls on carbon, nitrogen, and phosphorus dynamics in decomposing litter, Ecol. Monogr., 80(1), 89–106, 2010.
Manzoni, S., Čapek, P., Mooshammer, M., Lindahl, B. D., Richter, A. and Šantrůčková, H.: Optimal metabolic regulation along resource stoichiometry gradients, Ecology Letters, 20(9), 1182–1191, doi:10.1111/ele.12815, 2017.
Mayor, J. R., Wright, S. J. and Turner, B. L.: Species-specific responses of foliar nutrients to long-term nitrogen and phosphorus additions in a lowland tropical forest, Journal of Ecology, 102(1), 36–44, doi:10.1111/1365-2745.12190, 2014.
McGroddy, M. E., Daufresne, T. and Hedin, L. O.: Scaling of C:n:p Stoichiometry in Forests Worldwide: Implications of Terrestrial Redfield-Type Ratios, Ecology, 85(9), 2390–2401, doi:10.1890/03-0351, 2004.
Medvigy, D., Wofsy, S. C., Munger, J. W., Hollinger, D. Y. and Moorcroft, P. R.: Mechanistic scaling of ecosystem function

and dynamics in space and time: Ecosystem Demography model version 2, J. Geophys. Res. Biogeosciences, 114(G1), G01002, doi:10.1029/2008JG000812, 2009.
Melillo, J. M., Butler, S., Johnson, J., Mohan, J., Steudler, P., Lux, H., Burrows, E., Bowles, F., Smith, R., Scott, L. and others: Soil warming, carbon–nitrogen interactions, and forest carbon budgets, Proc. Natl. Acad. Sci., 108(23), 9508–9512, 2011.
Meyerholt, J. and Zaehle, S.: The role of stoichiometric flexibility in modelling forest ecosystem responses to nitrogen fertilization, New Phytol., 208(4), 1042–1055, doi:10.1111/nph.13547, 2015.
Myneni, R., Knyazikhin, Y. and Park, T.: MOD15A2H MODIS/Terra Leaf Area Index/FPAR 8-Day L4 Global 500m SIN Grid V006, 2015.
Näsholm, T., Kielland, K. and Ganeteg, U.: Uptake of organic nitrogen by plants, New Phytol., 182(1), 31–48, doi:10.1111/j.1469-8137.2008.02751.x, 2009.
Niemeyer, T., Niemeyer, M., Mohamed, A., Fottner, S. and Härdtle, W.: Impact of prescribed burning on the nutrient balance of heathlands with particular reference to nitrogen and phosphorus, Appl. Veg. Sci., 8(2), 183–192, 2005.
Norby, R. J., Warren, J. M., Iversen, C. M., Medlyn, B. E. and McMurtrie, R. E.: CO2 enhancement of forest productivity constrained by limited nitrogen availability, Proc. Natl. Acad. Sci., 107(45), 19368–19373, doi:10.1073/pnas.1006463107, 2010.
Orwin, K. H., Kirschbaum, M. U. F., St John, M. G. and Dickie, I. A.: Organic nutrient uptake by mycorrhizal fungi enhances ecosystem carbon storage: a model-based assessment, Ecol. Lett., 14(5), 493–502, doi:10.1111/j.1461-0248.2011.01611.x, 2011.
Pan, Y., Birdsey, R. A., Fang, J., Houghton, R., Kauppi, P. E., Kurz, W. A., Phillips, O. L., Shvidenko, A., Lewis, S. L., Canadell, J. G., Ciais, P., Jackson, R. B., Pacala, S. W., McGuire, A. D., Piao, S., Rautiainen, A., Sitch, S. and Hayes, D.: A large and persistent carbon sink in the world's forests, Science, 333(6045), 988–93, doi:10.1126/science.1201609, 2011.
Parton, W. J., Hanson, P. J., Swanston, C., Torn, M., Trumbore, S. E., Riley, W. and Kelly, R.: ForCent model development and testing using the Enriched Background Isotope Study experiment, J. Geophys. Res. Biogeosciences, 115(G4), G04001, doi:10.1029/2009JG001193, 2010.
Peng, J, Wang Y-P and Houlton B.Z. Estimates of biological nitrogen fixation and implication of land carbon uptake from 1901 to 2100. under review in Global Biogeochemical Cycles.
Peñuelas, J., Poulter, B., Sardans, J., Ciais, P., Velde, M. van der, Bopp, L., Boucher, O., Godderis, Y., Hinsinger, P., Llusia, J., Nardin, E., Vicca, S., Obersteiner, M. and Janssens, I. A.: Human-induced nitrogen–phosphorus imbalances alter natural and managed ecosystems across the globe, Nat. Commun., 4, ncomms3934, doi:10.1038/ncomms3934, 2013.
Poulter, B., MacBean, N., Hartley, A., Khlystova, I., Arino, O., Betts, R., Bontemps, S., Boettcher, M., Brockmann, C., Defourny, P., Hagemann, S., Herold, M., Kirches, G., Lamarche, C., Lederer, D., Ottlé, C., Peters, M. and Peylin, P.: Plant functional type classification for earth system models: results from the European Space Agency's Land Cover Climate Change Initiative, Geosci Model Dev, 8(7), 2315–2328, doi:10.5194/gmd-8-2315-2015, 2015.
Qian, Y., Miao, S. L., Gu, B. and Li, Y. C.: Estimation of postfire nutrient loss in the Florida Everglades, J. Environ. Qual., 38(5), 1812–1820, 2009.
Reich, P. B. and Oleksyn, J.: Global patterns of plant leaf N and P in relation to temperature and latitude, Proc. Natl. Acad. Sci. U. S. A., 101(30), 11001–11006, 2004.
Reich, P. B., Oleksyn, J., Wright, I. J., Niklas, K. J., Hedin, L. and Elser, J. J.: Evidence of a general 2/3-power law of scaling leaf nitrogen to phosphorus among major plant groups and biomes, Proc. R. Soc. Lond. B Biol. Sci., 277(1683), 877–883, doi:10.1098/rspb.2009.1818, 2010.
Reich, P. B., Rich, R. L., Lu, X., Wang, Y.-P. and Oleksyn, J.: Biogeographic variation in evergreen conifer needle longevity and impacts on boreal forest carbon cycle projections, Proc. Natl. Acad. Sci., 111(38), 13703–13708, 2014.
Rötzer, K., Montzka, C. and Vereecken, H.: Spatio-temporal variability of global soil moisture products, Journal of Hydrology, 522, 187–202, doi:10.1016/j.jhydrol.2014.12.038, 2015.
Saatchi, S. S., Harris, N. L., Brown, S., Lefsky, M., Mitchard, E. T., Salas, W., Zutta, B. R., Buermann, W., Lewis, S. L., Hagen, S. and others: Benchmark map of forest carbon stocks in tropical regions across three continents, Proc. Natl. Acad. Sci., 108(24), 9899–9904, 2011.
Sardans, J. and Peñuelas, J.: The role of plants in the effects of global change on nutrient availability and stoichiometry in the plant-soil system, Plant Physiology, pp.112.208785, doi:10.1104/pp.112.208785, 2012.
Sardans, J., Rivas-Ubach, A. and Peñuelas, J.: The C:N:P stoichiometry of organisms and ecosystems in a changing world: A review and perspectives, Perspectives in Plant Ecology, Evolution and Systematics, 14(1), 33–47, doi:10.1016/j.ppees.2011.08.002, 2012.
Sardans, J., Alonso, R., Janssens, I. A., Carnicer, J., Vereseglou, S., Rillig, M. C., Fernández‐Martínez, M., Sanders, T. G. M. and Peñuelas, J.: Foliar and soil concentrations and stoichiometry of nitrogen and phosphorous across European Pinus sylvestris forests: relationships with climate, N deposition and tree growth, Functional Ecology, 30(5), 676–689, doi:10.1111/1365-2435.12541, 2016.
Sardans, J., Grau, O., Chen, H. Y. H., Janssens, I. A., Ciais, P., Piao, S. and Peñuelas, J.: Changes in nutrient concentrations of leaves and roots in response to global change factors, Global Change Biology, 23(9), 3849–3856, doi:10.1111/gcb.13721, 2017.
Schimel, J. P. and Bennett, J.: Nitrogen mineralization: challenges of a changing paradigm, Ecology, 85(3), 591–602, 2004.
Schimel, J. P. and Chapin, F. S.: Tundra Plant Uptake of Amino Acid and NH4+ Nitrogen in Situ: Plants Complete Well for Amino Acid N, Ecology, 77(7), 2142–2147, doi:10.2307/2265708, 1996.

Seitzinger, S., Harrison, J. A., Böhlke, J. K., Bouwman, A. F., Lowrance, R., Peterson, B., Tobias, C. and Drecht, G. V.: Denitrification across landscapes and waterscapes: a synthesis, Ecol. Appl., 16(6), 2064–2090, 2006.
Shi, Z., Yang, Y., Zhou, X., Weng, E., Finzi, A. C. and Luo, Y.: Inverse analysis of coupled carbon–nitrogen cycles against multiple datasets at ambient and elevated CO2, J. Plant Ecol., 9(3), 285–295, 2016.
Sistla, S. A. and Schimel, J. P.: Stoichiometric flexibility as a regulator of carbon and nutrient cycling in terrestrial ecosystems under change, New Phytologist, 196(1), 68–78, doi:10.1111/j.1469-8137.2012.04234.x, 2012.
Sitch, S., Friedlingstein, P., Gruber, N., Jones, S. D., Murray-Tortarolo, G., Ahlström, A., Doney, S. C., Graven, H., Heinze, C., Huntingford, C. and others: Recent trends and drivers of regional sources and sinks of carbon dioxide, Biogeosciences, 12(3), 653–679, 2015.
Sun, Y., Peng, S., Goll, D. S., Ciais, P., Guenet, B., Guimberteau, M., Hinsinger, P., Janssens, I. A., Peñuelas, J., Piao, S., Poulter, B., Violette, A., Yang, X., Yin, Y. and Zeng, H.: Diagnosing phosphorus limitations in natural terrestrial ecosystems in carbon cycle models, Earths Future, 5(7), 730–749, doi:10.1002/2016EF000472, 2017.
Sutton, M. A., Simpson, D., Levy, P. E., Smith, R. I., Reis, S., Van Oijen, M. and De Vries, W. I. M.: Uncertainties in the relationship between atmospheric nitrogen deposition and forest carbon sequestration, Glob. Change Biol., 14(9), 2057–2063, 2008.
Thornton, P. E., Lamarque, J.-F., Rosenbloom, N. A. and Mahowald, N. M.: Influence of carbon-nitrogen cycle coupling on land model response to CO2 fertilization and climate variability, Glob. Biogeochem. Cycles, 21(4), GB4018, doi:10.1029/2006GB002868, 2007.
Thurner, M., Beer, C., Santoro, M., Carvalhais, N., Wutzler, T., Schepaschenko, D., Shvidenko, A., Kompter, E., Ahrens, B., Levick, S. R. and Schmullius, C.: Carbon stock and density of northern boreal and temperate forests, Glob. Ecol. Biogeogr., 23(3), 297–310, doi:10.1111/geb.12125, 2014.
Turner, B. L., Brenes-Arguedas, T. and Condit, R.: Pervasive phosphorus limitation of tree species but not communities in tropical forests, Nature, 555(7696), 367–370, doi:10.1038/nature25789, 2018.
Ver, L. M. B., Mackenzie, F. T. and Lerman, A.: Biogeochemical responses of the carbon cycle to natural and human perturbations; past, present, and future, Am. J. Sci., 299(7–9), 762–801, 1999.
Vitousek, P. M. and Howarth, R. W.: Nitrogen limitation on land and in the sea: how can it occur?, Biogeochemistry, 13(2), 87–115, 1991.
Vitousek, P. M., Menge, D. N. L., Reed, S. C. and Cleveland, C. C.: Biological nitrogen fixation: rates, patterns and ecological controls in terrestrial ecosystems, Philos Trans R Soc Lond B Biol Sci, 368(1621), doi:10.1098/rstb.2013.0119, 2013.
Wang, R., Balkanski, Y., Boucher, O., Ciais, P., Peñuelas, J. and Tao, S.: Significant contribution of combustion-related emissions to the atmospheric phosphorus budget, Nature Geosci, 8(1), 48–54, doi:10.1038/ngeo2324, 2015.
Wang, R., Goll, D., Balkanski, Y., Hauglustaine, D., Boucher, O., Ciais, P., Janssens, I., Penuelas, J., Guenet, B., Sardans, J. and others: Global forest carbon uptake due to nitrogen and phosphorus deposition from 1850 to 2100, Glob. Change Biol. [online] Available from: http://onlinelibrary.wiley.com/doi/10.1111/gcb.13766/full, 2017.
Wang, S., Grant, R. F., Verseghy, D. L. and Black, T. A.: Modelling plant carbon and nitrogen dynamics of a boreal aspen forest in CLASS — the Canadian Land Surface Scheme, Ecol. Model., 142(1–2), 135–154, doi:10.1016/S0304-3800(01)00284-8, 2001.
Wang, Y.-P., Houlton, B. Z. and Field, C. B.: A model of biogeochemical cycles of carbon, nitrogen, and phosphorus including symbiotic nitrogen fixation and phosphatase production, Global Biogeochem. Cycles, 21(1), GB1018, doi:10.1029/2006GB002797, 2007.
Wang, Y. P., Law, R. M. and Pak, B.: A global model of carbon, nitrogen and phosphorus cycles for the terrestrial biosphere, Biogeosciences, 7(7) [online] Available from: http://search.proquest.com/docview/757608124/abstract/B62E84E06C7F4CC7PQ/1 (Accessed 7 March 2017), 2010.
Wang, Y.-P. and Houlton, B. Z.: Nitrogen constraints on terrestrial carbon uptake: Implications for the global carbon-climate feedback, Geophys. Res. Lett., 36(24), L24403, doi:10.1029/2009GL041009, 2009.
Weng, E. and Luo, Y.: Soil hydrological properties regulate grassland ecosystem responses to multifactor global change: A modeling analysis, J. Geophys. Res. Biogeosciences, 113(G3) [online] Available from: http://onlinelibrary.wiley.com/doi/10.1029/2007JG000539/full, 2008.
Wieder, W. R., Cleveland, C. C., Smith, W. K. and Todd-Brown, K.: Future productivity and carbon storage limited by terrestrial nutrient availability, Nat. Geosci., 8(6), 441, 2015.
Williams, M., Schwarz, P. A., Law, B. E., Irvine, J. and Kurpius, M. R.: An improved analysis of forest carbon dynamics using data assimilation, Glob. Change Biol., 11(1), 89–105, 2005.
Williams, M., Hill, T. C. and Ryan, C. M.: Using biomass distributions to determine probability and intensity of tropical forest disturbance, Plant Ecol. Divers., 6(1), 87–99, doi:10.1080/17550874.2012.692404, 2013.
Xu-Ri and Prentice, I. C.: Terrestrial nitrogen cycle simulation with a dynamic global vegetation model, Glob. Change Biol., 14(8), 1745–1764, doi:10.1111/j.1365-2486.2008.01625.x, 2008.
Yang, X. and Post, W. M.: Phosphorus transformations as a function of pedogenesis: A synthesis of soil phosphorus data using Hedley fractionation method, Biogeosciences, 8(10) [online] Available from: http://search.proquest.com/docview/1012313736/abstract/28DB515C4ABC499BPQ/1 (Accessed 7 March 2017), 2011.
Yang, X., Wittig, V., Jain, A. K. and Post, W.: Integration of nitrogen cycle dynamics into the Integrated Science Assessment Model for the study of terrestrial ecosystem responses to global change, Glob. Biogeochem. Cycles, 23(4) [online] Available from: http://onlinelibrary.wiley.com/doi/10.1029/2009GB003474/full (Accessed 6 April 2017), 2009.
Yang, X., Post, W. M., Thornton, P. E. and Jain, A.: The distribution of soil phosphorus for global biogeochemical modeling,

Biogeosciences, 10(4), 2525, 2013.
Yang, X., Thornton, P. E., Ricciuto, D. M. and Post, W. M.: The role of phosphorus dynamics in tropical forests – a modeling study using CLM-CNP, Biogeosciences, 11(6), 1667–1681, doi:10.5194/bg-11-1667-2014, 2014a.
Yang, Y., Fang, J., Ji, C., Datta, A., Li, P., Ma, W., Mohammat, A., Shen, H., Hu, H., Knapp, B. O. and Smith, P.: Stoichiometric shifts in surface soils over broad geographical scales: evidence from China's grasslands, Global Ecology and Biogeography, 23(8), 947–955, doi:10.1111/geb.12175, 2014b.
Yuan, Z. Y. and Chen, H. Y. H.: Decoupling of nitrogen and phosphorus in terrestrial plants associated with global changes, Nature Climate Change, 5(5), 465–469, doi:10.1038/nclimate2549, 2015.
Zaehle, S.: Terrestrial nitrogen–carbon cycle interactions at the global scale, Philos. Trans. R. Soc. Lond. B Biol. Sci., 368(1621), 20130125, doi:10.1098/rstb.2013.0125, 2013.
Zaehle, S. and Dalmonech, D.: Carbon–nitrogen interactions on land at global scales: current understanding in modelling climate biosphere feedbacks, Curr. Opin. Environ. Sustain., 3(5), 311–320, doi:10.1016/j.cosust.2011.08.008, 2011.
Zaehle, S. and Friend, A. D.: Carbon and nitrogen cycle dynamics in the O-CN land surface model: 1. Model description, site-scale evaluation, and sensitivity to parameter estimates, Glob. Biogeochem. Cycles, 24(1), GB1005, doi:10.1029/2009GB003521, 2010.
Zaehle, S., Medlyn, B. E., De Kauwe, M. G., Walker, A. P., Dietze, M. C., Hickler, T., Luo, Y., Wang, Y.-P., El-Masri, B., Thornton, P., Jain, A., Wang, S., Warlind, D., Weng, E., Parton, W., Iversen, C. M., Gallet-Budynek, A., McCarthy, H., Finzi, A., Hanson, P. J., Prentice, I. C., Oren, R. and Norby, R. J.: Evaluation of 11 terrestrial carbon–nitrogen cycle models against observations from two temperate Free-Air CO2 Enrichment studies, New Phytol., 202(3), 803–822, doi:10.1111/nph.12697, 2014.
Zaehle, S., Jones, C. D., Houlton, B., Lamarque, J.-F. and Robertson, E.: Nitrogen availability reduces CMIP5 projections of twenty-first-century land carbon uptake, J. Clim., 28(6), 2494–2511, 2015.
Zechmeister-Boltenstern, S., Keiblinger, K. M., Mooshammer, M., Peñuelas, J., Richter, A., Sardans, J. and Wanek, W.: The application of ecological stoichiometry to plant–microbial–soil organic matter transformations, Ecol. Monogr., 85(2), 133–155, 2015.
Zhang, Q., Wang, Y. P., Pitman, A. J. and Dai, Y. J.: Limitations of nitrogen and phosphorous on the terrestrial carbon uptake in the 20th century, Geophys. Res. Lett., 38(22), L22701, doi:10.1029/2011GL049244, 2011.
Zhu, Q. and Zhuang, Q.: Modeling the effects of organic nitrogen uptake by plants on the carbon cycling of boreal forest and tundra ecosystems, Biogeosciences, 10(12), 7943–7955, 2013.

Table 1 Global spatially explicit observation-based estimates of model variables used as input data sets and the unknowns estimated in this study (including the symbols for each variable/parameter).

Variable	Definition	Description	Computation method	References
		Inputs: carbon cycle		
Fc	NPP	Spatially resolved model-data fusion estimates	Input	CARDAMOM; Bloom et al., 2016
$\tau_{i=1,2,3,4,5}$	Residence time of foliage, fine roots, wood, litter and SOM	Spatially resolved model-data fusion estimates	Input	CARDAMOM; Bloom et al., 2016
$\gamma_{C,i=1,2,3}$	Fraction of NPP allocated to foliage, fine roots and wood	Spatially resolved model-data fusion estimates	Input	CARDAMOM; Bloom et al., 2016
$f_{fire,C,\ i=1,2,3,4,5}$	Fraction of fire to total outgoing flux from foliage, fine roots, wood, litter and SOM	Spatially resolved model-data fusion estimates	Input	CARDAMOM; Bloom et al., 2016
η	Fraction of litter outflux that enters SOM	Spatially resolved model-data fusion estimates	Input	CARDAMOM; Bloom et al., 2016
		Inputs: nitrogen cycle		
$\rho_{N,i=1,2,3,5}$	N:C ratio in foliage, fine roots, wood and SOM	Biome-scale synthesis based on *in situ* measurements	Input	Zechmeister-Boltenstern et al., 2015
f_{leach}	Fraction of inorganic N (or P) lost due to leaching (Eq. B7)	Spatially resolved reanalysis by model; Model result, scaled to match measurements	Input	Balsamo et al., 2015 Fekete et al., 2002
$\varepsilon_{N,1}$	Resorption coefficient of N in foliage	Biome-scale synthesis based on *in situ* measurements	Input	Zechmeister-Boltenstern et al., 2015
N_d	N deposition	Spatially resolved model result, scaled to match *in situ* measurements	Input	Wang et al., 2017
N_{fix}	N fixation	Spatially resolved model result, scaled to match the estimates of NPP and N:C ratios	Input	Peng et al., submitted
f_{gas}	Fraction of denitrification to the total loss of inorganic N	Spatially resolved process-based statistical model result	Input	Goll et al., 2017b
		Inputs: phosphorus cycle		
$\rho_{P,i=1,2,3,5}$	P:C ratio in foliage, fine roots, wood and SOM	Biome-scale synthesis based on *in situ* measurements	Input	Zechmeister-Boltenstern et al., 2015
$f_{dissolved}$	Fraction of ~~inorganic~~ labile soil P that is dissolved in the soil water	*In situ* measurements, averaged based on soil order	Input	Yang and Post, 2011
f_{sorp}	Fraction of inorganic P that is transformed to strongly sorbed P	Assumed constant	Input	Goll et al., 2017a
$\varepsilon_{P,1}$	Resorption coefficient of P in foliage	Biome-scale synthesis based on *in situ* measurements	Input	Zechmeister-Boltenstern et al., 2015
P_d	P deposition	Spatially resolved model result, scaled to match *in situ* measurements	Input	Wang et al., 2017
P_d	P weathering	Spatially resolved model result, scaled to match observed data	Input	Hartmann et al., 2014
		Unknowns estimated from mass balance assuming steady state		

$C_{i=1,2,3,4,5}$	C pool of foliage, fine roots, wood, litter and SOM	Pools	Based on steady-state assumption
F_N	N uptake from inorganic-N pool by vegetation	Flux	Mass balance approach based on NPP (input) and stoichiometry ratios (input)
$\gamma_{N,i=1,2,3}$	Fraction of F_N allocated to foliage, fine roots and wood	Allocation fractions	Mass balance approach based on NPP (input) and stoichiometry ratios (input)
$N_{i=1,2,3,4,5}$	N in foliage, fine roots, wood, litter and SOM	Pools	Mass balance approach based on stoichiometry ratios (input) and steady-state C pools ($C_{i=1,2,3,4,5}$), assuming N:C ratios do not change over time
N_{immob}	N immobilization flux	Pools	Based on steady-state assumption that stoichiometry ratios (input), litter C and soil C do not change at annual scale
f_{denit}	Annual denitrification rate	Rate	Mass balance approach, assuming annual mean inorganic N pool size does not change at annual scale
N_{inorg}	Inorganic-N pool	Pool	Based on steady-state assumption that inorganic N do not change at annual scale
F_P	P uptake from inorganic-P pool by vegetation	Flux	Mass balance approach based on NPP (input) and stoichiometry ratios (input)
$\gamma_{P,i=1,2,3}$	Fraction of Fp allocated to foliage, fine roots and wood	Allocation fractions	Mass balance approach based on NPP (input) and stoichiometry ratios (input)
$P_{i=1,2,3,4,5}$	P in foliage, fine roots, wood, litter and SOM	Pools	Mass balance approach based on stoichiometry ratios (input) and steady-state C pools ($C_{i=1,2,3,4,5}$)
P_{immob}	P immobilization flux	Flux	Based on steady-state assumption that stoichiometry ratios (input), litter C and soil C do not change at annual scale
P_{inorg}	Inorganic-P pool	Pool	Based on steady-state assumption that labile P do not change at annual scale

Table 2 Global annual mean C-pool sizes, NPP and heterotrophic-respiration fluxes in the C-cycle model assuming steady states under the climate conditions of 2001-2010, compared to the means and percentile ranges from the original CARDAMOM results during 2001-2010.

	This study	Original CARDAMOM				
		5th percentile	25th percentile	Mean	75th percentile	95th percentile
Foliage-pool size (Pg C)	23	3.2	7	15	21	34
Fine-root-pool size (Pg C)	27	1.9	5	18	25	56
Wood-pool size (Pg C)	493	193	364	755	984	1850
Litter-pool size (Pg C)	20	1.3	4	22	26	88
SOM-pool size (Pg C)	1421	749	1100	1557	1882	2771
NPP (Pg C y^{-1})	52.5	Not given	39	52	63	Not given
Fire (Pg C y^{-1})	1.5	Not given	1.3	1.7	2.0	Not given
Heterotrophic respiration (Pg C y^{-1})	51	Not given	37	54	67	Not given

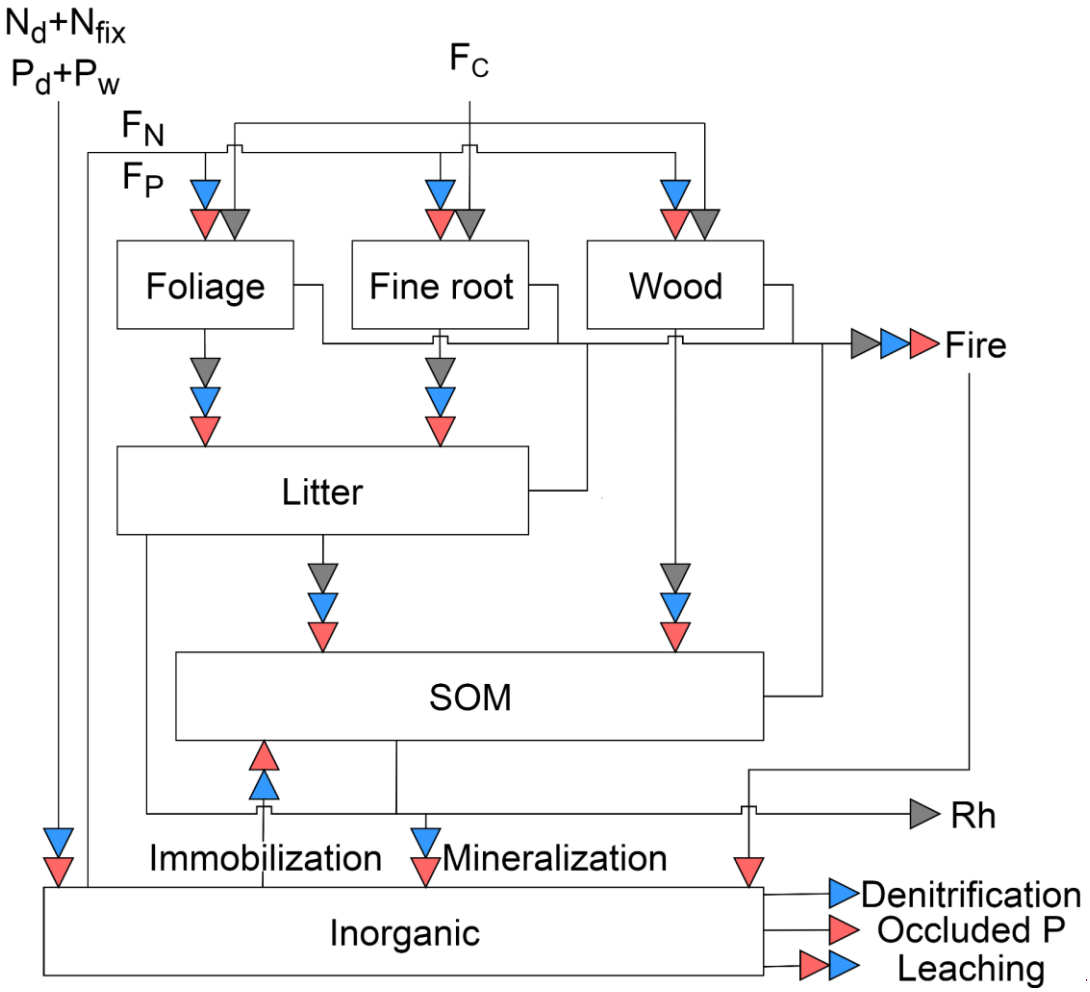
N_d+N_{fix}
P_d+P_w
F_C
F_N
F_P
Foliage
Fine root
Wood
Fire
Litter
SOM
Rh
Immobilization
Mineralization
Inorganic
Denitrification
Occluded P
Leaching

1

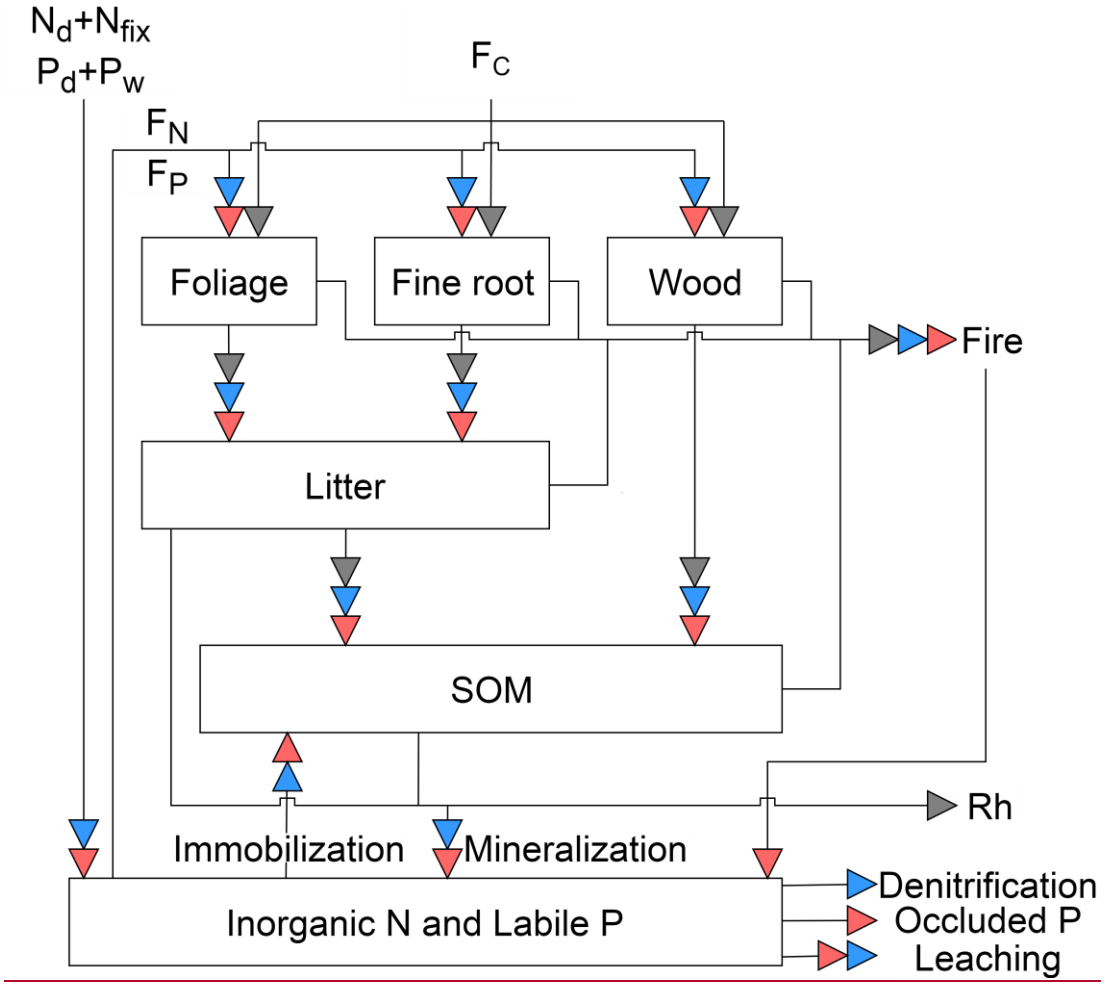
N_d+N_{fix}
P_d+P_w
F_C
F_N
F_P
Foliage
Fine root
Wood
Fire
Litter
SOM
Rh
Immobilization
Mineralization
Inorganic N and Labile P
Denitrification
Occluded P
Leaching

2

Figure 1 Schematic representation of the pools and fluxes in the C, N and P cycles within GOLUM-CNP. The gray, blue and red arrows represent C, N and P fluxes, respectively. Plants are divided into foliar, fine root and wood pools, where the wood pool includes woody stems and coarse roots. Litter and soil are two separate pools. The inorganic pool represents the nutrient sources in the soil that are available for plant uptake. Arrows between the pools represent the directions of C, N and P flow between pools. External inputs of N are atmospheric deposition (N_d) and biological N fixation (N_{fix}). External inputs of P are atmospheric deposition (P_d) and P released by rock weathering (P_w). F_C is net primary production (NPP). F_N and F_P are plant uptake of N and P from the inorganic N and labile P pools, respectively. R_h is release of C due to heterotrophic respiration. Mineralization of N and P is modeled along with litter and SOM decomposition, and N and P immobilization is modeled by a flux from the inorganic pool to SOM. External losses of N occur by fire, leaching and denitrification. External losses of P occur by fire, leaching and transfer to occluded P in the soil. ~~External inputs of N and P are atmospheric deposition (N_d and P_d), biological N fixation (N_{fix}) and P released by rock weathering (P_w). External losses of N occur by fire, leaching and denitrification. External losses of P occur by fire, leaching and transfer to occluded P in the soil. F_C is net primary production (NPP) and Rh is heterotrophic respiration. F_N and F_P are the plant uptake of N and P from the inorganic pool, respectively. Mineralization of N and P is modeled along with litter and SOM decomposition, and N and P immobilization is modeled by a flux from the inorganic pool to SOM.~~

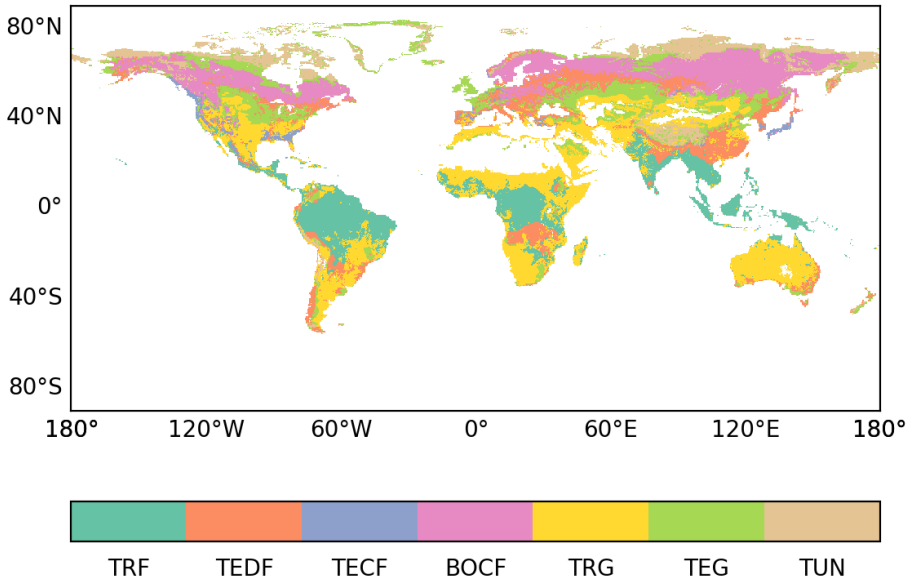

Figure 2 ESA CCI land-cover map classified into the seven large biomes for which average N:C and P:C ratios for each carbon pool are available, at 0.25 °×0.25 ° resolution: tropical rainforests (TRF), temperate deciduous forests (TEDF), temperate coniferous forests (TECF), boreal coniferous forests (BOCF), tropical/C4 grasslands (TRG), temperate/C3 grasslands (TEG) and tundra (TUN).

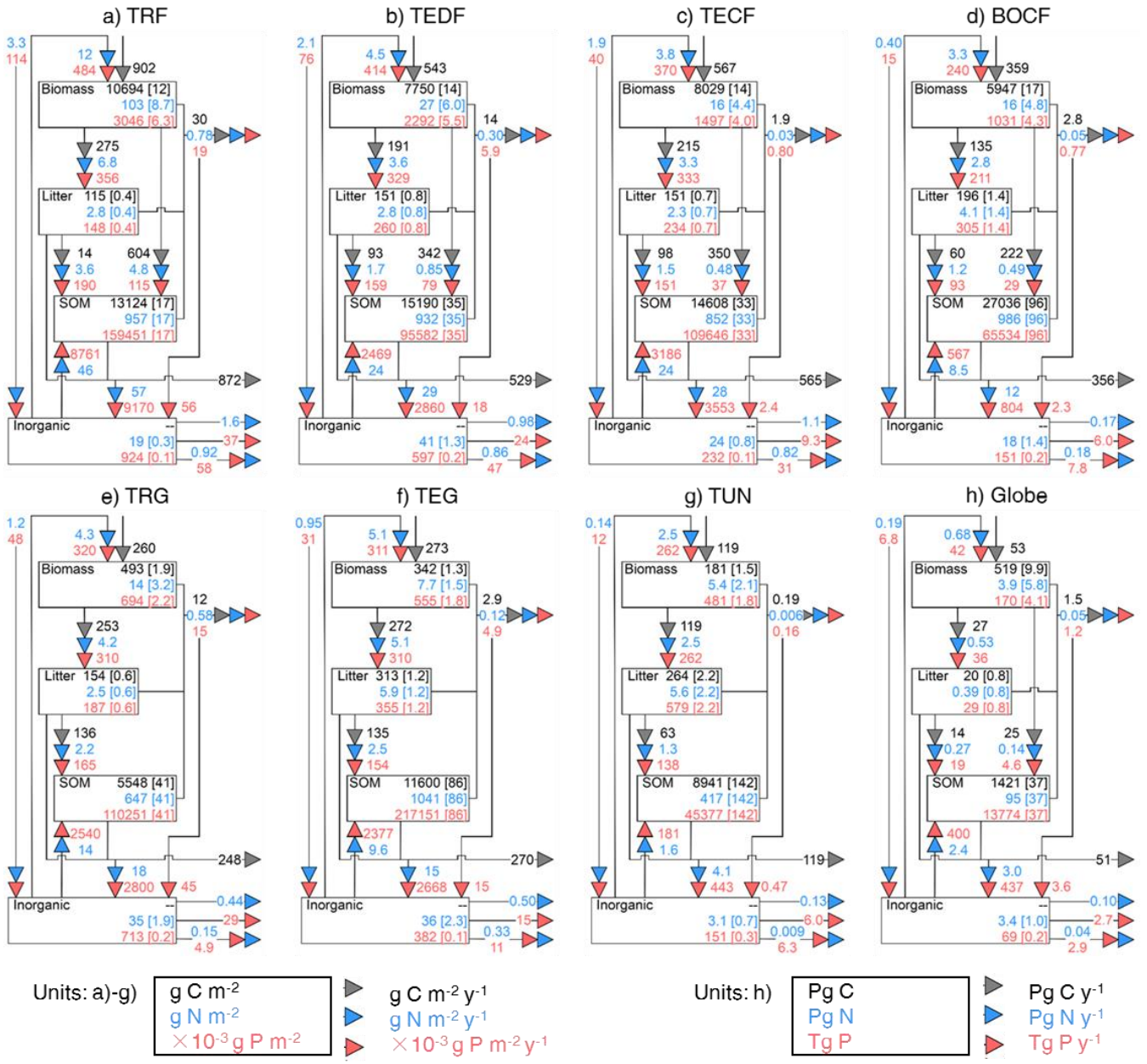
a) TRF
b) TEDF
c) TECF
d) BOCF
e) TRG
f) TEG
g) TUN
h) Globe
Biomass
Litter
SOM
Inorganic
Units: a)-g)
g C m-2
g N m-2
×10-3 g P m-2
g C m-2 y-1
g N m-2 y-1
×10-3 g P m-2 y-1
Units: h)
Pg C
Pg N
Tg P
Pg C y-1
Pg N y-1
Tg P y-1

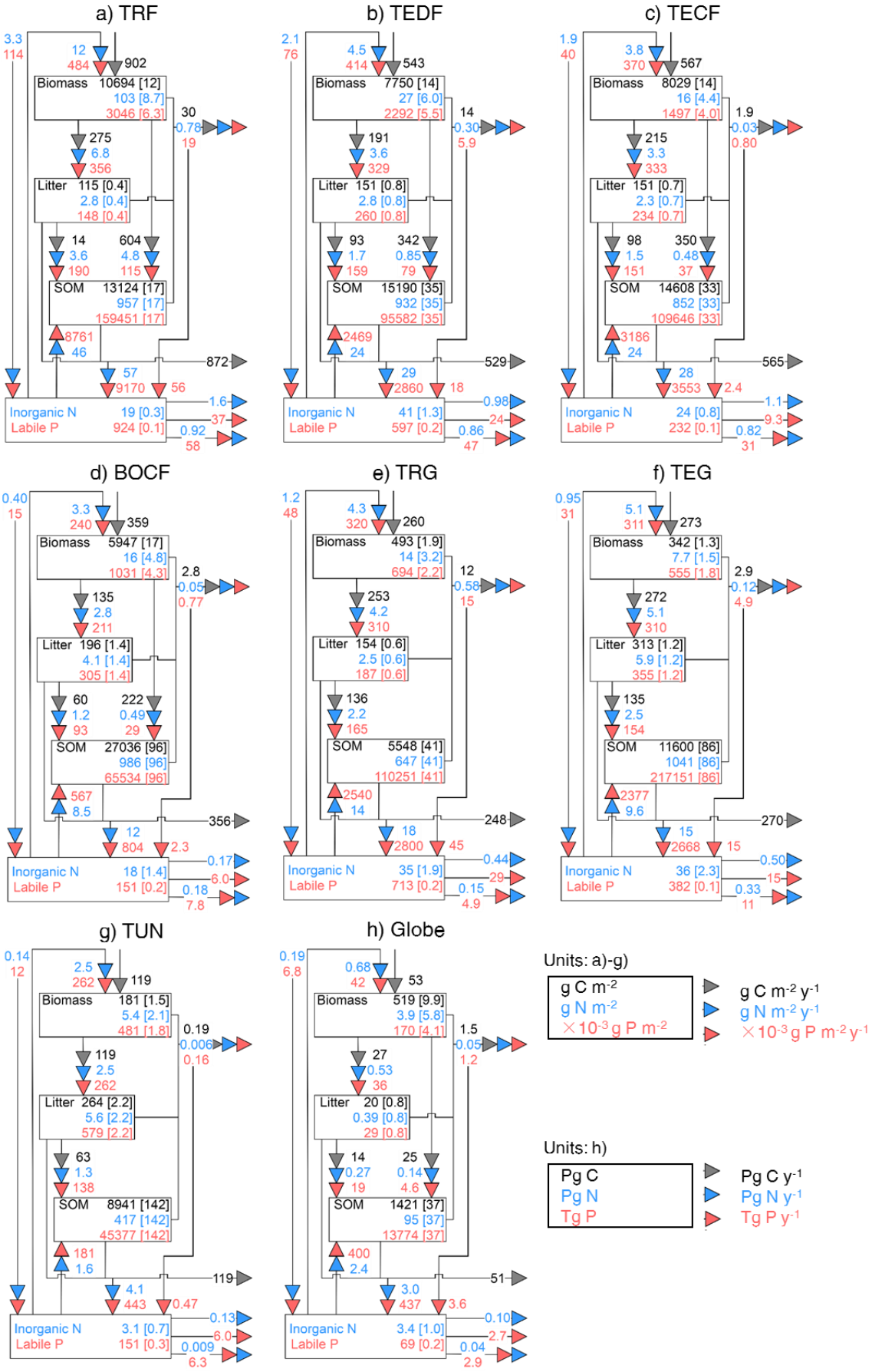

Figure 3 Fluxes (numbers along arrows), mean residence times (in parentheses) and pool sizes of the N (blue) and P (red) cycles in the terrestrial biosphere at steady state for the large biomes (a-g) and globe (h). The targeted biomes are tropical rainforests (TRF, a), temperate deciduous forests (TEDF, b), temperate coniferous forests (TECF, c), boreal coniferous forests (BOCF, d), tropical/C4 grasslands (TRG, e), temperate/C3 grasslands (TEG, f) and tundra (TUN, g).

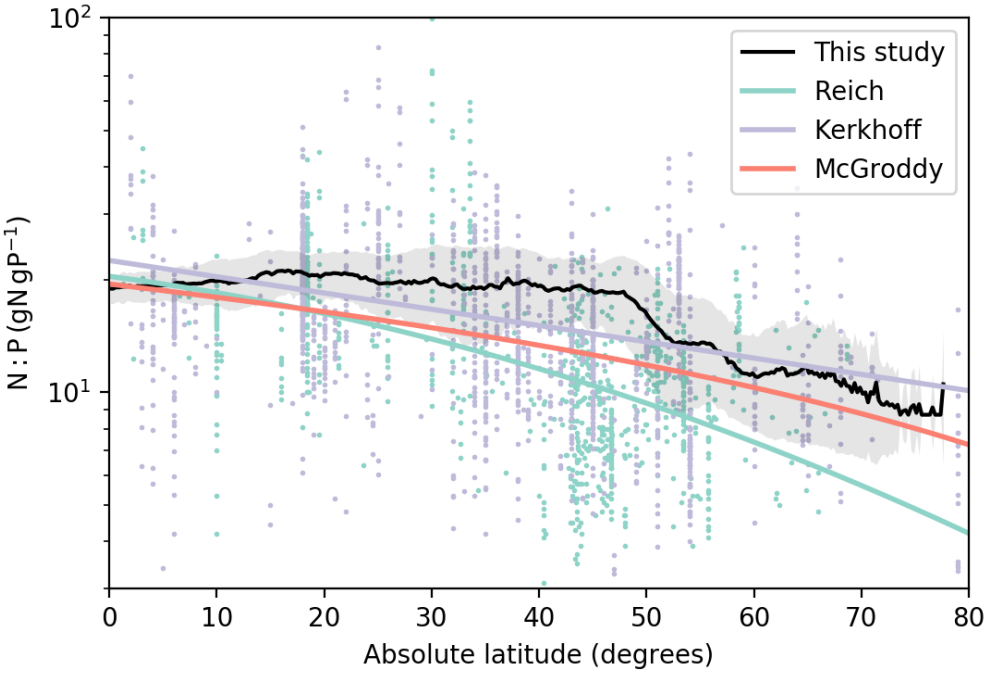

Figure 4 Relationship between foliar N:P ratios (gN gP^{-1}) and absolute latitude. The black line is the mean N:P ratios from this study, and the shaded area is the one-sigma standard deviation of the N:P ratios for specific latitude. Colored lines are the regression trends of foliar N:P ratios as a function of absolute latitude from Reich and Oleksyn (2004; green), Kerkhoff et al. (2005; blue) and McGroddy et al. (2004; red). Dots are the raw data that Reich and Oleksyn (2004; green) and Kerkhoff et al. (2005; blue) used to derive their regression trends.

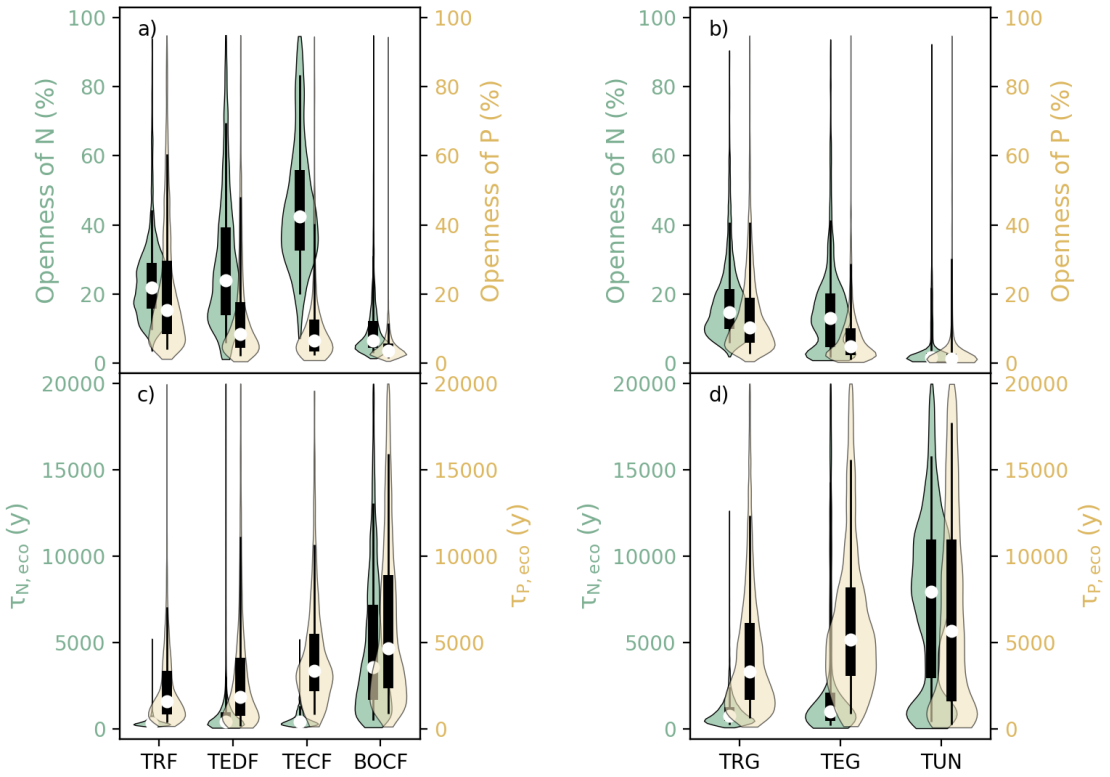

Figure 5 Violin plots of the openness of N and P cycling (the percentage of total plant uptake of N and P attributed to new nutrient inputs) for a) forest and b) grassland biomes. Residence times of N ($\tau_{N,eco}$) and P ($\tau_{P,eco}$) in c) forest ecosystems and d) grassland biomes. Open circles are medians of all grid cells within each biome, with balloons representing the probability density distribution of each value. Black whiskers indicate interquartile (thick) and 95% confidence intervals (thin). The biomes are tropical rainforests (TRF), temperate deciduous forests (TEDF), temperate coniferous forests (TECF), boreal coniferous forests (BOCF), tropical/C4 grasslands (TRG), temperate/C3 grasslands (TEG) and tundra (TUN).

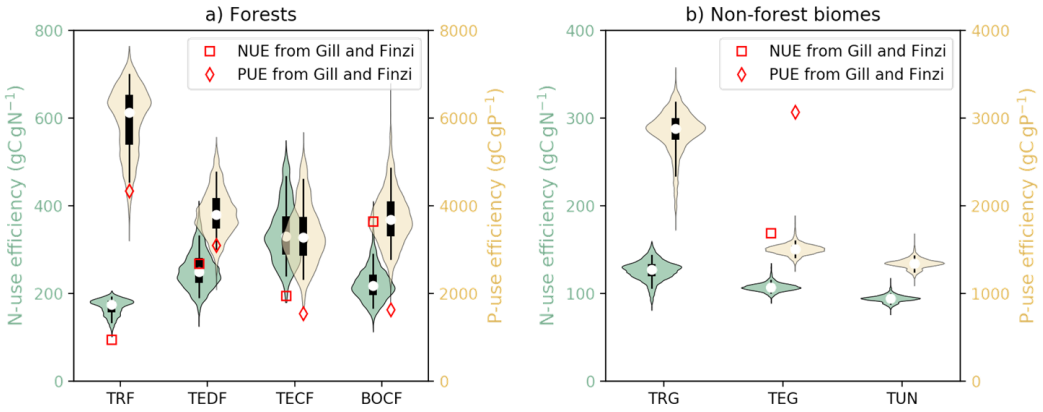

Figure 6 Violin plots of N- and P-use efficiencies (NUE and PUE, the nutrient uptake by plants divided by GPP) of seven biomes. Open circles are medians of all grid cells within each biome, with balloons representing the probability density distribution of each value. Black whiskers indicate interquartile (thick) and 95% confidence intervals (thin). a) Forest biomes, including tropical rainforests (TRF), temperate deciduous (TEDF), temperate coniferous (TECF) and boreal coniferous forests (BOCF). b) Grassland biomes, including tropical/C4 (TRG), temperate/C3 grasslands (TEG) and tundra (TUN). Red squares (NUE) and diamonds (PUE) are the independent estimates from site observations and other generic data sets compiled and harmonized by Gill and Finzi (2016) based on site measurements of GPP and net N/P mineralization.

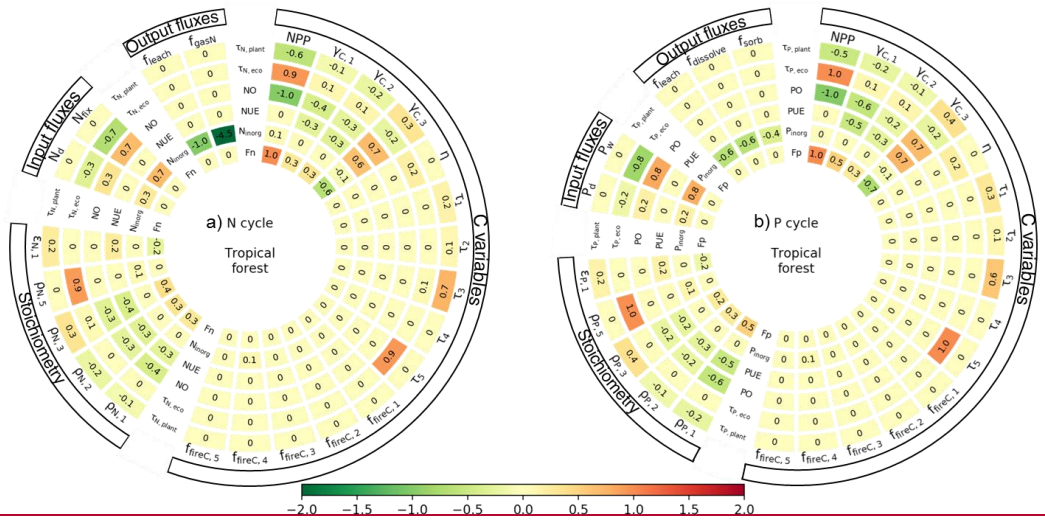
a) N cycle
Tropical forest
b) P cycle
Tropical forest
Output fluxes
Input fluxes
C variables
Stoichiometry
NPP
−2.0 −1.5 −1.0 −0.5 0.0 0.5 1.0 1.5 2.0

1

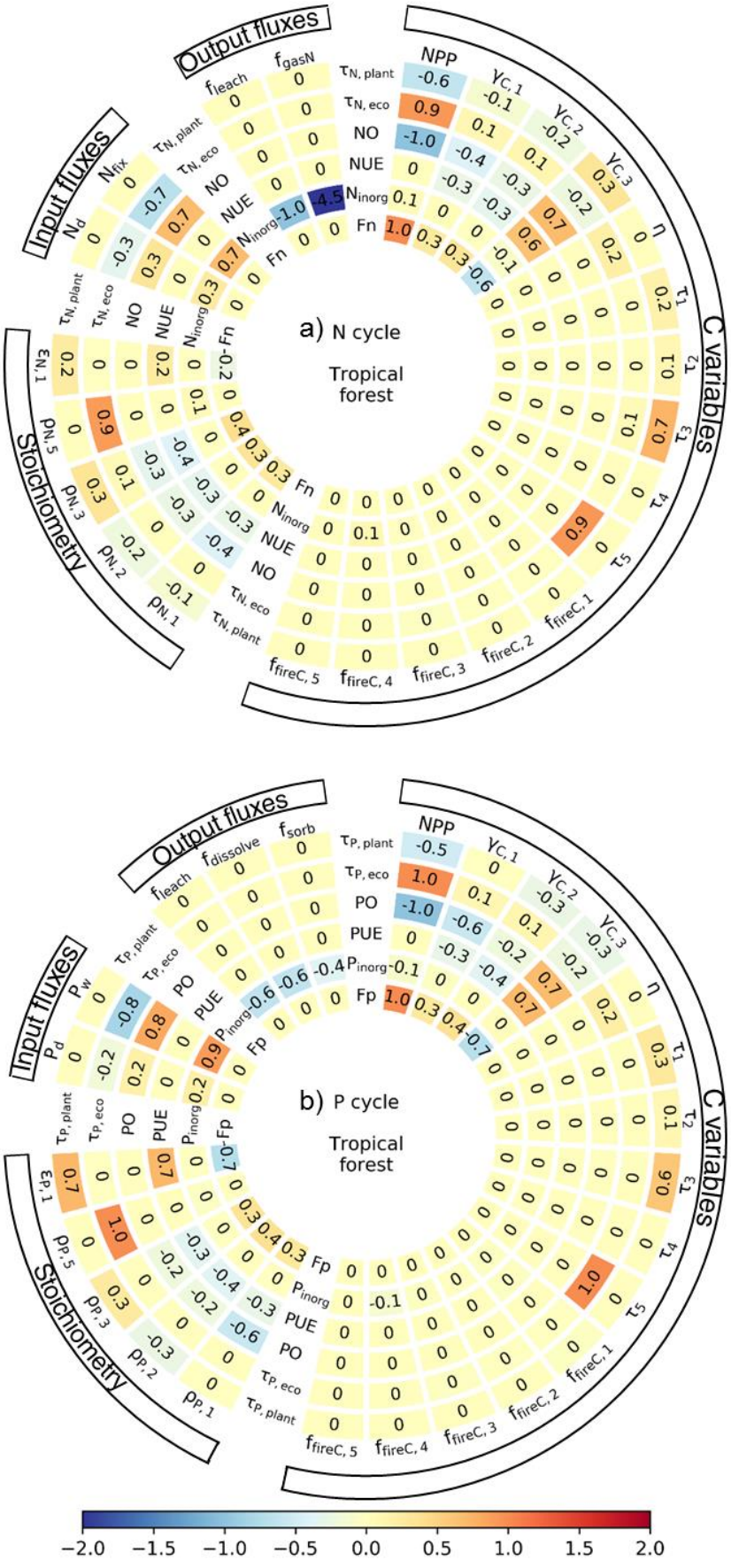

Figure 7 Mean **s**ensitivity of the estimates of rates of nutrient uptake, inorganic nutrients, nutrient-use efficiencies, openness, turnover time of nutrients in the ecosystem and turnover time of nutrients in plants to the input variables for tropical forest. Results for other biomes are shown in Figs. ~~S2 and S3~~S8-S13.

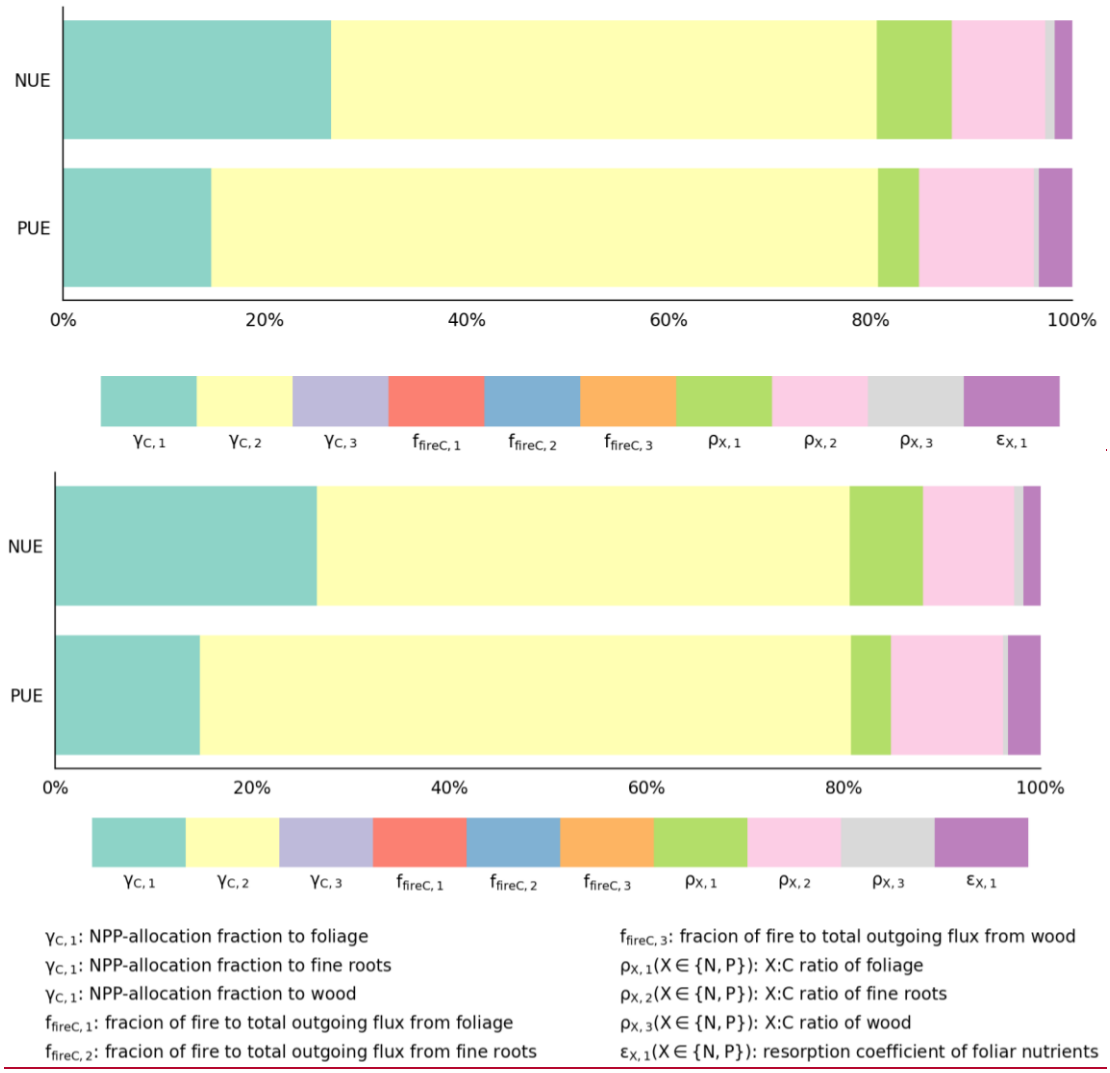

Figure 8 Contribution of input data to the variance of the estimates of nutrient-use efficiencies (X ∈ {N,P}) for temperate coniferous forests. $\gamma_{C,\,i=1,2,3}$ are NPP-allocation fractions to foliage, fine roots and wood, respectively. $f_{fireC,\,i=1,2,3}$ are fractions of fire to total outgoing flux from foliage, fine roots and wood, respectively. $\rho_{x,\,i=1,2,3}$ (X ∈ {N,P}) are X:C ratios of foliage, fine roots and wood, respectively. $\varepsilon_{X,\,1}$ (X ∈ {N,P}) is the resorption coefficient of foliar nutrients.

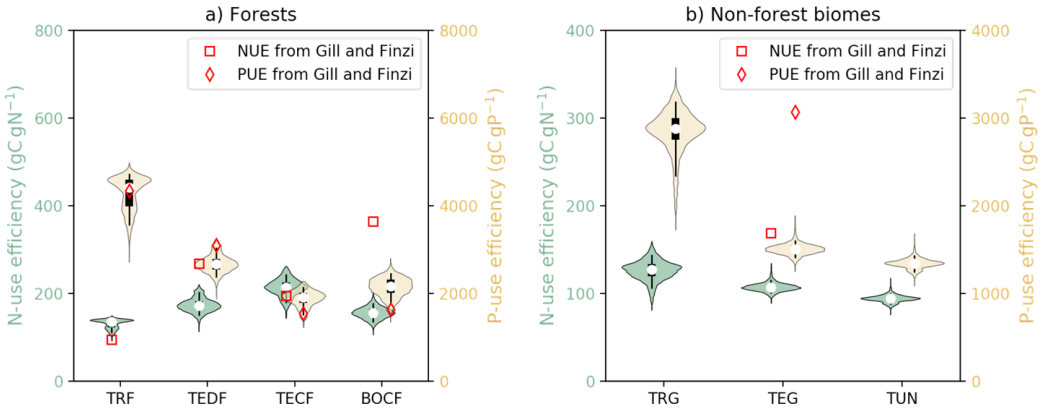

Figure 9 Violin plots of the nutrient-use efficiencies of the seven biomes from the experiment in which the allocation fraction of NPP to woody biomass and to leaves in coniferous forests is reduced. Open circles are the medians of all grid cells within each biome, with balloons representing the probability density distribution of each value. Black whiskers indicate interquartile (thick) and 95% confidence intervals (thin). The biomes are tropical rainforests (TRF), temperate deciduous forests (TEDF), temperate coniferous forests (TECF), boreal coniferous forests (BOCF), tropical/C4 grasslands (TRG), temperate/C3 grasslands (TEG) and tundra (TUN). The red squares (NUE) and diamonds (PUE) are the independent estimates from site observations and other generic data sets compiled and harmonized by Gill and Finzi (2016) based on site measurements of GPP and net N/P mineralization.